

NON-PARAMETRIC EDGE DETECTION IN SPECKLED IMAGERY

EDWIN GIOVANNY GIRÓN AMAYA

Primary advisor: Prof. Dr Alejandro C. Frery

Secondary advisor: Prof. Dr Francisco Cribari-Neto

Concentration area: Computational Statistics

Dissertation submitted to the Department of Statistics of the Federal
University of Pernambuco, in partial fulfillment of the requirements
for the degree of MSc in Statistics.

Recife, February 2008

Livros Grátis

<http://www.livrosgratis.com.br>

Milhares de livros grátis para download.

Amaya, Edwin Giovanny Girón

**Non-parametric edge detection in speckled
imagery / Edwin Giovanny Girón Amaya. – Recife:
O Autor, 2008.**

v, 121 folhas: il., fig., tab.

**Dissertação (mestrado) – Universidade Federal
de Pernambuco. CCEH. Depto. de Estatística.
2008.**

Inclui bibliografia e apêndices.

**1. Estatística não paramétrica. 2. Detecção de
bordas. 3. Imagens SAR. I. Título.**

519.5

CDD (22.ed.)

MEI2008-020

Universidade Federal de Pernambuco
Pós-Graduação em Estatística

15 de fevereiro de 2008

(data)

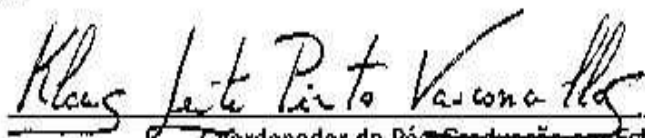
Nós recomendamos que a dissertação de mestrado de autoria de

Edwin Giovanny Girón Amaya

intitulada

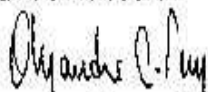
"Detecção não Paramétrica de Bordas em Imagens SAR"

seja aceita como cumprimento parcial dos requerimentos para o grau
de Mestre em Estatística.



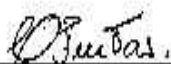
Coordenador da Pós-Graduação em Estatística

Banca Examinadora:

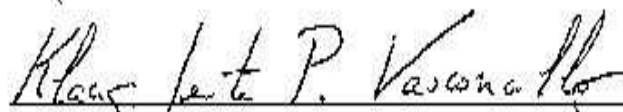


Alejandro César Frey Orgambide

orientador



Corina da Costa Freitas Yanasse (INPE)



Klaus Leite Pinto Vasconcellos

Este documento será anexado à versão final da dissertação.

To my parents, Cecilia Amaya and Ernesto Giron, my Grandparents Antonio and Cecilia, my sister Jessica. It is my tribute for so many wait and sacrifice.

I dedicate this work to Alexandra Esteban, friend, girlfriend and adviser, with whom I learned that the life is not fair, and even like that, she gave to me force not to desist. Do not stop Ale...

Acknowledgements

First thank God for fortifying me and for taking care of me and allowing me to be careful myself and to permit reach the current stage of my life.

I would like to thank my advisors, Alejandro Frery and Francisco Cribari-Neto. Throughout my career as student, combined with their careful advice, they have been invaluable in providing guidance and support. Alejandro and Francisco have been exemplary models, showing me how to choose important research topics grounded in real-world problems and how to attack them; I clearly would not be where I am without the time and effort they devoted to his mentorship.

I am very grateful to all my friends and colleagues at UFPE, in special, Hemilio Fernandes, Carlos Raphael, Valmir Rogerio, Marcelo Rodrigo, Fabio Jaques, Abraão David Costa with whom I spent many hours talking about a wide variety of academic and non-academic topics.

I would like to thank the staff at the Department of Statistics of Federal University of Pernambuco, in special Valeria Betancourt.

Most of all, I want to express my gratitude to Alexandra Johanna, my confidante and best friend. She gives me strength and helps me in countless ways. Above all, I am thankful for how she fills my life with happiness and joy.

I also thank CAPES for financial suggest of my post-graduation studies, without which this work would not be materialized.

Finally, I thank the thesis committee members for suggestions and corrections.

The most beautiful thing we can experience is the mysterious. It is the source of all true art and science. He to whom this emotion is a stranger, who can no longer pause to wonder and stand rapt in awe, is as good as dead: his eyes are closed.

Albert Einstein

Resumo

Este trabalho propõe uma técnica não-paramétrica para detecção de bordas em imagens speckle. As imagens SAR (“Synthetic aperture Radar”), sonar, B-ultrasound e laser são corrompidas por um ruído não aditivo chamado speckle. Vários modelos estatísticos foram propostos para descrever este ruído, levando ao desenvolvimento de técnicas especiais para melhoramento e análise de imagens. A distribuição \mathcal{G}^0 é um modelo estatístico que consegue descrever uma ampla gama de áreas, como, por exemplo, em dados SAR, pastos (lisos), florestas (rugosos) e áreas urbanas (muito rugosos). O objetivo deste trabalho é estudar técnicas alternativas na detecção de imagens speckled, tomando como ponto de partida Gambini et al. (2006, 2008).

Um novo detector de borda baseado no teste de **Kruskal Wallis** é proposto. Os nossos resultados numéricos mostram que esse detector é uma alternativa atraente ao detector de **M. Gambini**, que é baseado na função de verossimilhança.

Neste trabalho fornecemos evidências de que a técnica de **M. Gambini** pode ser substituída com sucesso pelo método **Kruskal Wallis**. O ganho reside em ter um algoritmo 1000 vezes mais rápido, sem comprometer a qualidade dos resultados.

Palavras-chave: estatística não-paramétrica, detecção de bordas, imagens SAR, imagens speckled, ruído speckle.

Abstract

This thesis proposes a non-parametric technique for boundary detection in speckled imagery. Synthetic Aperture Radar (SAR), sonar, B-ultrasound and laser imagery is corrupted by a signal-dependent non-additive noise called speckle. Several statistical models have been proposed to describe such a noise, thus of specialized techniques for image improvement and analysis. The \mathcal{G}^0 distribution is a statistical model that succeeds in describing a wide range of areas as, for instance in SAR data, pastures (smooth), forests (rough) and urban (extremely rough) areas. The aim of this thesis is to develop alternative techniques for edge detection in speckled imagery. Its starting point are the works by Gambini et al. (2006, 2008). We describe a new edge detector based on the **Kruskal Wallis** test and show that it is an useful alternative to the method proposed by M. Gambini, which is based on the likelihood function of the data. We provide evidence that the M. Gambini technique can be successfully replaced by the **Kruskal Wallis** method. The latter is more computationally efficient, the corresponding algorithm being up to 1000 times faster than the M. Gambini algorithm.

Keywords: non-parametrics statistics, edges detection, SAR imagery, speckled imagery, speckle noise.

Contents

1	Introduction	6
2	Methodology	15
2.1	The multiplicative model	19
2.2	\mathcal{G}_1^0 distribution: properties and estimation	23
2.3	Edge detection in SAR imagery	27
2.3.1	Gambini algorithm for edge detection	29
2.3.2	Non-parametric edge detection	31
2.3.3	The Mann-Whitney test	33
2.3.4	The Kruskal-Wallis test	34
2.3.5	The Squared Ranks test for variances	37
2.3.6	The TPE empirical statistic	39
2.4	Proposal	40
3	Results	43
3.1	Extremely heterogeneous areas, $n = 1$ and $\alpha_\ell = -3$	48
3.2	Heterogeneous areas, $n = 1$ and $\alpha_\ell = -8$	51
3.3	Homogeneous areas, $n = 1$ and $\alpha_\ell = -12$	54
3.4	Homogeneous areas, $n = 1$ and $\alpha_\ell = -18$	57
3.5	Extremely heterogeneous areas, $n = 3$ and $\alpha_\ell = -3$	60
3.6	Heterogeneous areas, $n = 3$ and $\alpha_\ell = -8$	62
3.7	Homogeneous areas, $n = 3$ and $\alpha_\ell = -12$	65

3.8	Homogeneous areas, $n = 3$ and $\alpha_\ell = -18$	68
3.9	Extremely heterogeneous areas, $n = 8$ and $\alpha_\ell = -3$	71
3.10	Heterogeneous areas, $n = 8$ and $\alpha_\ell = -8$	74
3.11	Homogeneous areas, $n = 8$ and $\alpha_\ell = -12$	77
3.12	Homogeneous areas, $n = 8$ and $\alpha_\ell = -18$	80
4	Conclusions	84
A	Simulation results for $n = 1$	88
B	Simulation results for $n = 3$	94
C	Simulation results for $n = 8$	100
D	Ox Codes	106

List of Figures

1.1	Interpretation of the roughness parameter	13
2.1	Densidade do speckle para 1, 2, 4 e 8 looks	20
2.2	Γ^{-1} densities for $\alpha = -0.5, -2, -4, -10$	22
2.3	\mathcal{G}_I^0 densities for $\alpha = -2, -4, -6, -8 - 12$	24
2.4	Radial straight lines projected	30
2.5	Values of the objective function for a segment of straight	31
2.6	Displacement of a rectangular window on a straight segment	40
2.7	Typical values of the non-parametric statistics	42
3.1	Scheme of a rectangular window on a straight segment	46
3.2	Synthetic images $\mathcal{G}_I^0(-3, 1, 1)$	48
3.3	Average execution time for $\alpha_\ell = -3$ and $n = 1$	50
3.4	Synthetic images from $\mathcal{G}_I^0(-8, 1, 1)$	51
3.5	Error rate in edge detection for $\alpha_\ell = -8$ and $n = 1$	53
3.6	Average execution time for $\alpha_\ell = -8$ and $n = 1$	53
3.7	Synthetic images from $\mathcal{G}_I^0(-12, 1, 1)$	54
3.8	Error rate in edge detection for $\alpha_\ell = -12$ and $n = 1$	56
3.9	Average execution time for $\alpha_\ell = -12$ and $n = 1$	56
3.10	Synthetic images $\mathcal{G}_I^0(-18, 1, 1)$	57
3.11	Error rate for $\alpha_\ell = -18$ and $n = 1$	59
3.12	Average execution time for $\alpha_\ell = -18$ and $n = 1$	59
3.13	Synthetic images $\mathcal{G}_I^0(-3, 1, 3)$	60

3.14	Average execution time for $\alpha_\ell = -3$ and $n = 3$	61
3.15	Synthetic images $\mathcal{G}_I^0(-8, 1, 3)$	62
3.16	Error rate in edge detection for $\alpha_\ell = -8$ and $n = 3$	64
3.17	Average execution time for $\alpha_\ell = -8$ and $n = 3$	64
3.18	Synthetic images $\mathcal{G}_I^0(-12, 1, 3)$	65
3.19	Error rate in edge detection for $\alpha_\ell = -12$ and $n = 3$	67
3.20	Average execution time for $\alpha_\ell = -12$ and $n = 3$	67
3.21	Synthetic images $\mathcal{G}_I^0(-18, 1, 3)$	68
3.22	Error rate in edge detection for $\alpha_\ell = -18$ and $n = 3$	70
3.23	Average execution time for $\alpha_\ell = -18$ and $n = 3$	70
3.24	Synthetic images $\mathcal{G}_I^0(-3, 1, 8)$	71
3.25	Average execution time for $\alpha_\ell = -3$ and $n = 8$	73
3.26	Synthetic images $\mathcal{G}_I^0(-8, 1, 8)$	74
3.27	Error rate in edge detection for $\alpha_\ell = -8$ and $n = 8$	76
3.28	Average execution time for $\alpha_\ell = -8$ and $n = 8$	76
3.29	Synthetic images $\mathcal{G}_I^0(-12, 1, 8)$	77
3.30	Error rate in edge detection for $\alpha_\ell = -12$ and $n = 8$	79
3.31	Average execution time for $\alpha_\ell = -12$ and $n = 8$	79
3.32	Synthetic images $\mathcal{G}_I^0(-18, 1, 8)$	80
3.33	Error rate in edge detection for $\alpha_\ell = -18$ and $n = 8$	82
3.34	Average execution time for $\alpha_\ell = -18$ and $n = 8$	82

List of Tables

3.1	Error rate and average time for $\alpha_\ell = -3$ and $n = 1$	50
3.2	Error rate and average time for $\alpha_\ell = -8$ and $n = 1$	52
3.3	Error rate and average time for $\alpha_\ell = -12$ and $n = 1$	55
3.4	Error rate and average time for $\alpha_\ell = -18$ and $n = 1$	58
3.5	Error rate and average time for $\alpha_\ell = -3$ and $n = 3$	61
3.6	Error rate and average time for $\alpha_\ell = -8$ and $n = 3$	63
3.7	Error rate and average time for $\alpha_\ell = -12$ and $n = 3$	66
3.8	Error rate and average time for $\alpha_\ell = -18$ and $n = 3$	69
3.9	Error rate and average time for $\alpha_\ell = -3$ and $n = 8$	72
3.10	Error rate and average time for $\alpha_\ell = -8$ and $n = 8$	75
3.11	Error rate and average time for $\alpha_\ell = -12$ and $n = 8$	78
3.12	Error rate and average time for $\alpha_\ell = -18$ and $n = 8$	81

Chapter 1

Introduction

Resumo

Nos últimos anos, o desenvolvimento de novas tecnologias de observação da terra a partir do espaço tem estimulado o interesse da sociedade em suas aplicações. Estas tecnologias permitiram que alguns dos países desenvolvidos começassem a corrida espacial, induzindo o desenvolvimento de novas técnicas que, com o tempo, foram denominadas “espaço de sensoriamento remoto”.

As imagens de radar SAR (“Synthetic aperture Radar”) oferecem uma perspectiva única da terra, seus recursos e o impacto que sobre ela exercem os seres humanos. Imagens SAR têm demonstrado ser uma fonte de informação valiosa para várias aplicações, entre as quais é possível citar o planejamento urbano, o monitorização ambiental, a gestão dos cultivos, a prospecção de petróleo, a exploração mineral, a detecção de vida animal e muitas outras.

SAR é um radar de iluminação coerente de alta resolução que funciona utilizando uma antena sintética a bordo de uma plataforma aérea móvel, como um avião ou um satélite, cobrindo grandes superfícies e produzindo imagens de alta resolução. Ao contrário de um radar convencional, SAR utiliza o movimento da plataforma para obter uma antena sintética de maior dimensão e, por conseguinte, maior resolução do que a obtida a través antena real.

Um sensor SAR emite e recebe sinais eletromagnéticos de natureza complexa, o sinal recebido podendo ser armazenado em diferentes formatos: complexo, intensidade e fase (Oliver and Quegan, 1998).

O radar ilumina uma cena com uma sucessão de pulsos e uma determinada frequência. A energia é propagada em todas as direções e uma parte retorna à antena (este retorno é chamado eco). O sensor mede a intensidade e o atraso dos sinais emitidos e devolvidos à antena. A interpretação desses ecos permite a formação de imagens em termos de distâncias ao radar, ou seja, a imagem é formada em função da energia devolvida por qualquer ponto da superfície.

Algumas das características mais importantes que o sensor SAR apresenta são:

- O caráter ativo do instrumento o torna independente da iluminação solar, sendo capaz de recolher imagens a qualquer momento.
- As microondas são pouco afetadas pela presença de nuvens, o que torna possível a aquisição de imagens independentemente das condições meteorológicas e em regiões com cobertura freqüente.
- O sensor SAR permite obter imagens com resoluções de dezenas de centímetros a quilômetros de altura.
- As imagens SAR fornecem informações complementares às proporcionadas pelas imagens ópticas. A seleção da frequência, da polarização e do ângulo de incidência do SAR permite discriminar diferentes propriedades da superfície.

Em uma imagem SAR é possível distinguir vários tipos de rugosidade ou textura:

Áreas homogêneas: Superfícies de pouca textura, por exemplo, zonas de cultivos, zonas com desmatamento, neve, água ou gelo, etc.

Áreas heterogêneas: Superfícies que apresentam certo grau de textura, por exemplo, florestas.

Áreas extremamente heterogêneas: Superfícies onde a textura é intensa, por exemplo, zonas urbanas, industriais, entre outros.

Um fator importante que degrada a qualidade da imagem SAR é o ruído speckle, que aparece quando se usa iluminação coerente como é o caso de todas as tecnologias que utilizam microondas, Sonar, laser e ultra-som. Para reduzir o nível de ruído speckle em imagens SAR, uma técnica chamada “multilook” pode ser usada. Esta técnica consiste em subdividir o pulso emitido pela antena em vários setores independentes e combinar os dados obtidos em uma imagem final, de modo que esta imagem seja menos afetada pelo speckle.

Para encontrar os pontos de borda entre as diferentes regiões da imagem, os dados SAR são modelados com a distribuição \mathcal{G}_1^0 sob o modelo multiplicativo. As regiões da imagem com diferentes graus de homogeneidade ficam caracterizadas pelos parâmetros da distribuição. Se um ponto pertence à borda, então numa vizinhança desse ponto existe uma mudança brusca nos parâmetros da distribuição.

O modelo multiplicativo afirma que a variável aleatória Z que descreve as observações, é o resultado do produto de duas variáveis aleatórias independentes, que não são observadas diretamente: X e Y , a variável aleatória X modela área de estudo (backscatter), enquanto que a variável aleatória Y modela o ruído speckle.

O objetivo deste trabalho é estudar técnicas alternativas na detecção de imagens speckled, tomando como ponto de partida o trabalho de *Gambini et al. (2006, 2008)*. Neste trabalho fornecemos evidências de que a técnica de M. Gambini pode ser substituída com sucesso pelo método **Kruskal Wallis**. O ganho reside em ter um algoritmo 1000 vezes mais rápido, sem compromisso da qualidade dos resultados.

Esta tese é composta pelos seguintes capítulos: o presente capítulo 1; o capítulo 2 apresenta o modelo multiplicativo que descreve as imagens SAR, a distribuição \mathcal{G}_1^0 e suas propriedades, e apresenta uma revisão de detecção de bordas em imagens SAR incluindo técnicas não-paramétrica e nossa proposta. Capítulo 3 apresenta resultados que permitem a comparação dos métodos sob avaliação. Capítulo 4 discute as conclusões extraídas dos resultados apresentados.

Introduction

In the last years, the development of new technologies for Earth observation from space has stimulated the interest of the society on their applications. These technologies allowed some of the most powerful countries to begin the space race, inducing the development of new techniques that, with time, were denominated “space remote sensing”.

SAR (“Synthetic Aperture Radar”) imagery offers an unique Earth perspective, its resources and the impact that on its humans exert. SAR images have demonstrated to be a source of valuable information for numerous applications, among which it is possible to mention urban planning, monitoring of environment, management of crops, oil prospection, mining exploration, wind detection, detection of animal life and many others.

SAR is a coherent radar of high resolution that works on board using a synthetic antenna of a movable platform, like an airplane or a satellite, covering extended surfaces and producing images. Unlike a conventional radar, SAR uses the movement of the platform to obtain a synthetic antenna and, therefore, higher resolutions than the real antenna.

During the process of data acquisition, the target remains illuminated under the antenna beam during several instants, being observed by the radar from numerous positions caused by movement throughout the platform trajectory, prolonging in this way the real length of the antenna. The radar illuminates a scene with a succession of pulses in a certain frequency. The energy is propagated in all directions and returns partially to the antenna (this return is called echo). The sensor measures both the intensity and the delay of the emitted and returned signals to the antenna. The interpretation of these echoes allows the formation of images in terms of distances to the radar, the image being formed as function of the energy returned by every point of the surface.

Some of the most important characteristics that the SAR sensor presents for remote sensing are:

- The active nature of the instrument makes it independent of other illumination sources, being able to gather images at any time.
- Microwaves are little affected by the presence of clouds, so image acquisition is possible regardless of the meteorological conditions and in regions with permanent cloud coverage.
- SAR images can have high spatial resolution, e.g. of less than one meter, allowing, thus, the study of small scale phenomena.
- SAR images contain complementary information to that provided by optical images. The selection of the frequency band, polarization and angle of incidence in SAR imagery allows discrimination of different surface properties.

A SAR sensor emits and receives electromagnetic waves of complex nature and, therefore, the received signal can be stored in different formats: complex, intensity, amplitude and phase (Oliver & Quegan 1998).

In a SAR image it is possible to distinguish several types of roughness or texture, according to which it is possible to classify the different types of covers in:

Homogenous areas: Surfaces of very little texture, for example, zones of crops, zones with deforestation, snow, water or ice, etc.

Heterogeneous areas: Surfaces that present certain degree of texture, for example forest on not very pronounced relief, among others.

Extremely heterogeneous areas: Surfaces where the texture is intense, for example urban and industrial zones and of pronounced reliefs, among others.

“Texture”, in the context of SAR imagery, should be understood as a measure of the number of objects in a cell of the size of the wavelength employed by the sensor. A fine texture is associated to a large number of objects per cell, while a coarse or extremely heterogeneous textures are those for which only a few objects are counted per cell. The Japanese Earth Resources Satellite JERS-1, for instance, operates on

L-Band (1.3 GHz, 23.5 cm wavelength) and the European Remote Sensing Satellites ERS-1 and ERS-2 use C-Band (5.3 GHz, 5.6 cm wavelength). The ERS1 is not ideal for forest discrimination, with less than 50% of the nonforest areas being correctly detected. This reflects the fact that even low vegetation canopies can have a backscattering coefficient similar to that of primary forest at C-band. Longer wavelengths are more appropriate to this application, such as the L-band data provided by JERS-1. A more complete temporal coverage of the region may have given better performance. Long time sequences of ERS images gathered over temperate forest, which also show very stable behavior, allow good forest discrimination using change-detection techniques. C-band systems are capable of good forest discrimination in the tropics if they have sufficient resolution (Oliver & Quegan 1998).

A problem of fundamental importance in the analysis of images is the detection of edges. Edges characterize the limits of objects and, therefore, they are useful for segmentation, registration and identification of objects. Edge points can be thought as the locations of pixels where abrupt changes of intensity or other relevant property occur.

Segmentation is the process that divides an image in its constituent parts or objects. It is one of the most important steps in the whole process of image analysis. Its objective is to group image areas that have similar characteristics within different groups that represent parts of the image.

One of the basic principles in the segmentation process is the detection of discontinuities. The edges characterize the borders of the objects, and therefore they are very useful for the segmentation and identification of objects in scenes.

An important factor that degrades the quality of the SAR images is the speckle noise, that appears when coherent illumination is used. It is the case of all technologies that employ microwaves, sonar, laser and ultrasound; it is inherent to the coherent illumination, i.e., image formation where phase is recorded.

The noise is the main difficulty for the edge detection algorithms, because many of them find regions using local characteristics. In the case of detection of edges of objects in images with speckle noise, it is not possible in general to use pointwise

information; it is necessary to analyze the image using sets of pixels that provide local information (Gambini et al. 2006).

To reduce the level of speckle noise in SAR images, a technology called “multi-look” can be used. It consists of subdividing the antenna beam in several independent sectors and combining the resulting data in a final image, so that this image is less affected by speckle. Meanwhile, this type of processing reduces the spatial resolution proportionally to the number of looks.

Different approaches can be used in order to find edges of different regions, among them a statistical approach has been shown to be one of the most suited for speckled imagery (Gambini et al. 2008). In order to do this, the family of \mathcal{G} distributions can be used to model data. This choice is based on the fact that this distribution presents the best results when used to describe areas with different degree of homogeneity (Frery et al. 1997, Mejail et al. 2001, 2003, Freitas et al. 2005).

The multiplicative model states that the random field Z that describes the observations is the result of the product of two independent random fields, which are not observed directly: X and Y .

The random field X models the properties of the studied area (backscatter), whereas the random field Y models the speckle noise associated to the mechanism of image formation inherent to coherent illumination. We shall only consider the intensity format in this thesis.

The phenomenon of speckle noise generation allows us to assume that each component of the field Y follows a Γ law (Goodman 1985). Several models can be used for the random field X , among them the Γ distribution, which leads to \mathcal{K}_I distribution for the return Z (Jakeman & Pusey 1976, Jao 1984, Oliver & Quegan 1998). Nevertheless, this model fails in situations where the return represents extremely heterogeneous areas, like urban areas, the distribution being in addition difficult to deal with from the computational viewpoint.

Frery et al. (1997) propose a new class of distributions, \mathcal{G} , which has the \mathcal{K}_I distribution as a special case. Another special case is the \mathcal{G}_I^0 distribution, which has as many parameters as the \mathcal{K}_I law, and allows modeling successfully extremely

heterogeneous areas, such as urban zones, which cannot be adequately modeled by the \mathcal{K}_I distribution (Picco et al. (2007)).

The \mathcal{G}_I^0 distribution is characterized by as many parameters as the \mathcal{K}_I distribution, namely: the number of looks (n), the (γ) parameter of scale and the parameter (α). Both \mathcal{K}_I and \mathcal{G}_I^0 distributions allow the interpretation of their parameters. The roughness parameter is of interest in many applications, since it can be used as an indicator of are land type. The scale parameter (γ) makes reference to the relative power between the reflected and incident signals (Frery et al. 1997).

Figure 1.1 presents the interpretation of the roughness parameter α . Small values of α ($\alpha < -10$, for instance) are associated with homogeneous areas, e.g. pastures. Values of $\alpha \in [-10, -4]$ characterize heterogeneous regions, for example forests, whereas bigger values of α (say $-4 < \alpha < 0$) are observed in extremely heterogeneous areas as is the case of cities (Bustos et al. 2002, Mejail et al. 2003, Pizarro 2003).

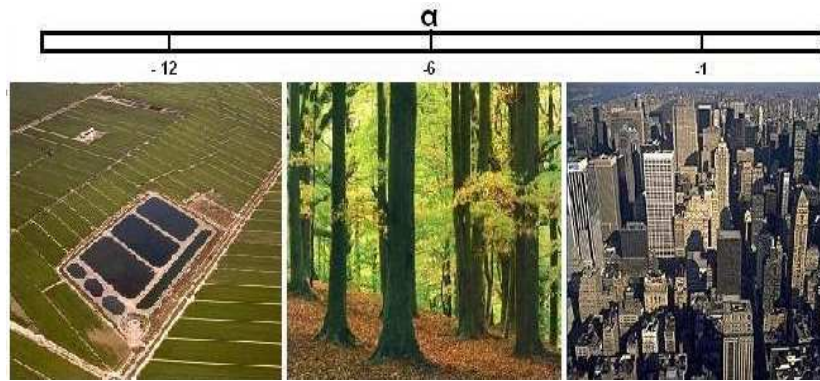


Figure 1.1: Interpretation of the roughness parameter

This thesis does not aim at combating speckle, but at taking advantage of its statistical properties for edge detection.

In this work we propose non-parametric methods for the detection of edges, and we compare them with existing ones to determine their advantages and disadvantages.

After proposing and analyzing different methods of edge detection, we evaluate and compare them using a Monte Carlo experiment. The function under assessment

is a measure of error in fitting (estimating) an edge to known situations.

This thesis is composed of the following chapters: the present Chapter 1; Chapter 2 presents the multiplicative model for SAR image description, the \mathcal{G}_1^0 distribution and its properties, and a review of edge detection in SAR imagery including non-parametric techniques and our proposal. Chapter 3 presents the results that allow the comparison of the methods under assessment. Chapter 4 discusses the conclusions drawn from this approach.

Chapter 2

Methodology

Resumo

O modelo multiplicativo é uma excelente ferramenta para explicar as características estatísticas dos dados provenientes de um sistema que emprega iluminação por radiação coerente como as imagens SAR.

Este modelo considera que o retorno, denotado como Z , pode ser modelado como o produto de duas variáveis aleatórias independentes, uma correspondente ao terreno X , também conhecida como *backscatter*, que descreve as propriedades intrínsecas da área, e outra correspondente ao ruído speckle Y , que degrada a qualidade da imagem e dificulta a sua visualização e interpretação.

O modelo multiplicativo “clássico” introduzido por Tur et al. (1982), afirma que o retorno de áreas não homogêneas segue uma distribuição \mathcal{K} . Quando a área é homogênea, a distribuição Γ modela muito bem os dados por ser um caso particular da distribuição \mathcal{K} ; no entanto, a distribuição \mathcal{K} não modela adequadamente os dados provenientes de áreas extremamente heterogêneas.

Frery et al. (1997) propuseram uma nova classe de distribuições, \mathcal{G} , que tem a distribuição \mathcal{K} como um caso particular. Outro caso especial desta família é a distribuição \mathcal{G}^0 , que tem o mesmo número de parâmetros que a distribuição \mathcal{K} e permite a modelagem de áreas extremamente heterogêneas, tais como as zonas urbanas que

não são modeladas adequadamente pela distribuição \mathcal{K} .

Sob o modelo em formato intensidade n -look (Frery et al. 1997), o ruído speckle segue uma distribuição gamma, denotada por $Y_I^{(n)} \sim \Gamma(n, n)$, cuja densidade é dada por

$$f_{Y_I}(y) = \frac{n^n}{\Gamma(n)} y^{n-1} \exp(-ny), \quad n \geq 1, y > 0,$$

onde o número de looks (n) indica a quantidade de imagens independentes que foram registradas na área.

A partir dos resultados apresentados em Frery et al. (1997) e Mejail (1999), o backscatter é considerado como uma variável aleatória com distribuição gaussiana inversa generalizada. Esta distribuição está caracterizada pela densidade

$$f_X(x) = \frac{(\lambda/\gamma)^{\frac{\alpha}{2}}}{2K_\alpha(\sqrt{\lambda\gamma})} x^{\alpha-1} \exp\left\{\frac{-1}{2}\left(\lambda x + \frac{\gamma}{x}\right)\right\}, \quad x > 0,$$

onde K_α denota a função de Bessel modificada do terceiro tipo e ordem α .

Se $X_I \sim N^{-1}(\alpha, \gamma, \lambda)$ e $Y_I \sim \Gamma(n, n)$ são variáveis aleatórias independentes, então o produto $Z_I = X_I Y_I$ tem distribuição $\mathcal{G}_J(\alpha, \gamma, \lambda, n)$ e sua densidade é dada por Frery et al. (1997):

$$f_{Z_I}(z) = \frac{n^n (\lambda/\gamma)^{\alpha/2}}{\Gamma(n) K_\alpha(2\sqrt{\lambda\gamma})} z^{n-1} \left(\frac{\gamma + nz}{\lambda}\right)^{(\alpha-n)/2} K_{\alpha-n}\left(2\sqrt{\lambda(\gamma + nz)}\right),$$

onde $n \geq 1, z > 0$.

A distribuição \mathcal{G}_I^0 é muito atraente para modelagem de dados com ruído speckle, devido a seu fácil manejo matemático e porque ela é capaz de modelar muito bem dados provenientes de qualquer tipo de área. Sua densidade é dada por Frery et al. (1997):

$$f_{Z_I}(z) = \frac{n^n \Gamma(n - \alpha)}{\gamma^\alpha \Gamma(n) \Gamma(-\alpha)} \frac{z^{n-1}}{(\gamma + nz)^{n-\alpha}}, \quad z > 0, \quad (2.1)$$

onde $-\alpha > 0$ é o parâmetro de rugosidade, $\gamma > 0$ é o parâmetro de escala e $n \geq 1$ é o número de looks.

Detectores de bordas de imagens ruidosas baseados na teoria estatística foram

descritos por diversos autores, como, por exemplo, Bovik et al. (1986). Os autores introduziram o uso da estatística não-paramétrica para a detecção de bordas com ruído gaussiano aditivo.

A detecção de bordas em imagens com ruído speckle tem sido estudada por diversos autores e uma variedade de técnicas é apresentada em Gambini et al. (2006, 2008). O algoritmo utilizado por Gambini et al. (2006, 2008) considera a imagem por regiões, em vez de considerar a imagem total, economizando tempo computacional. Se um ponto pertence à borda do objeto, então uma amostra retirada da sua vizinhança deverá exibir uma mudança nos parâmetros e, portanto, é considerado como ponto de transição.

Este capítulo apresenta uma introdução elementar a imagens SAR, o básico do modelo multiplicativo para speckled imagens, a distribuição G_1^0 e os quatro testes estatísticos. Faremos mais adiante uma avaliação dos desempenhos destas quatro técnicas, comparativamente ao método apresentado por Gambini et al. (2006, 2008).

Methodology

The multiplicative model is an excellent tool for explaining the statistical characteristics of data obtained by systems which employ coherent illumination; such as sonar, laser, ultrasound-B and SAR imagery. This model considers that the intensity return, denoted Z , in every pixel, can be viewed as the product of two independent random variables, one corresponding to the terrain, X , also known as *backscatter*, that describes the intrinsic properties of the area, and another corresponding to the speckle noise Y , that degrades the quality of the image and hampers its visualization and interpretation. The distribution of $Z = XY$ is determined by the distributions of X and of Y .

The image format (complex, intensity or amplitude) determines the distribution of the variable Y , whereas the heterogeneity of the target determines the X distribution. It is, therefore, possible to obtain different distributions to model the return Z , depending on the degree of target homogeneity.

The “classical” multiplicative model, introduced by Tur et al. (1982), states that the return from non-homogeneous areas follows the \mathcal{K} distribution. When the area is homogeneous the Γ distribution models the return data well and, being a particular case of the previous one, the validity of the \mathcal{K} model is preserved. Nevertheless, the \mathcal{K} distribution does not model adequately data from extremely heterogeneous areas.

Frery et al. (1997) proposed a new class of distributions, \mathcal{G} , which has the \mathcal{K} distribution as a particular case. Another special case of this family is the \mathcal{G}^0 distribution, that has as many parameters as the \mathcal{K} law, and allows the modeling of extremely heterogeneous areas, such as urban zones, which cannot be appropriately modeled by the \mathcal{K} distribution.

In the following section, we will present a review of the multiplicative model, with emphasis on the information required for our proposal.

2.1 The multiplicative model

Under the n -looks format model of intensity (Frery et al. 1997), the speckle noise follows a gamma distribution, denoted by $Y_I^{(n)} \sim \Gamma(n, n)$, whose density is given by:

$$f_{Y_I}(y) = \frac{n^n}{\Gamma(n)} y^{n-1} \exp(-ny), \quad n \geq 1, y > 0,$$

where the number of looks (n) denotes the quantity of independent images that were registered on the area. The moments of this distribution are given by

$$E[Y_I^r] = \frac{1}{n^r} \frac{\Gamma(n+r)}{\Gamma(n)},$$

where r is the order of the moment.

In the modeling of SAR images, the minimum value of n is 1, which corresponds to images generated without multi-look processing. Such images are, thus, noisier, but they carry more information with respect to resolution. The number n can be assumed to be known or estimated beforehand from the whole image. In this work we assume it is known.

Figure 2.1 shows four gamma densities corresponding to 1, 2, 4 and 8 looks. It is noticeable that the bigger n the more symmetric the density. In fact, it is easy to show that the variance, the skewness and the kurtosis of this distribution converge to zero when $n \rightarrow \infty$ (see, for instance, Yanasse et al. 1995).

The backscatter may exhibit different degrees of homogeneity, and different models could be used to encompass this characteristic. Two main models have proved useful for modelling intensity backscatter: a gamma distributed random variable (for heterogeneous areas) and, more recently, a reciprocal of a gamma distributed random variable (for extremely heterogeneous areas). From the results presented in Frery et al. (1997) these two situations are unified by the generalized inverse Gaussian distribution, whose density function is given by

$$f_X(x) = \frac{(\lambda/\gamma)^{\frac{\alpha}{2}}}{2K_{\alpha}(\sqrt{\lambda\gamma})} x^{\alpha-1} \exp\left\{\frac{-1}{2}\left(\lambda x + \frac{\gamma}{x}\right)\right\}, \quad x > 0, \quad (2.2)$$

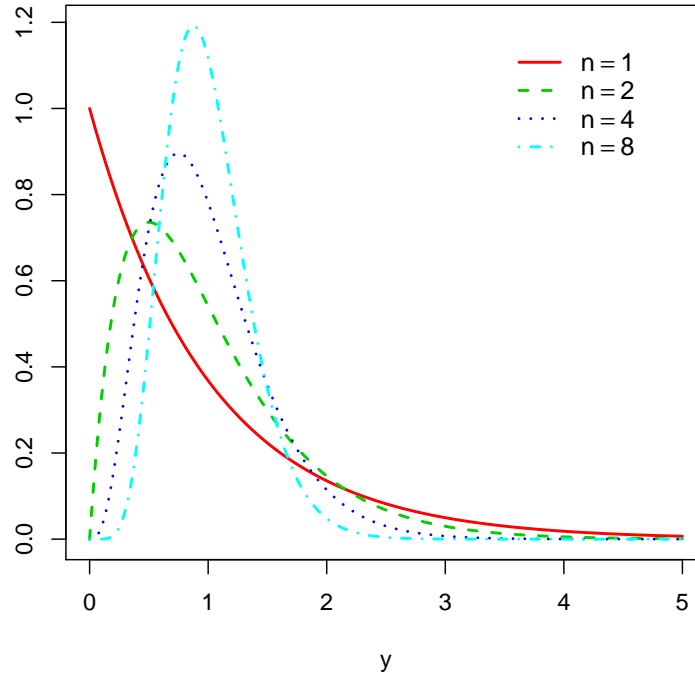


Figure 2.1: Densidade do speckle para 1, 2, 4 e 8 looks (Sólido, traços, pontos e pontos de traços respectivamente)

where K_α denotes the modified Bessel function of the third kind and order α (Gradshteyn & Ryzhik 1998) given by

$$K_\alpha(\sqrt{\lambda\gamma}) = \frac{1}{2} \left(\frac{\lambda}{\gamma} \right)^{\frac{\alpha}{2}} \int_0^\infty t^{\alpha-1} \exp\left\{-\frac{\gamma}{t} - \lambda t\right\} dt.$$

The parameter space is

$$\begin{cases} \gamma > 0, \lambda \geq 0, & \text{if } \alpha < 0 \\ \gamma > 0, \lambda > 0, & \text{if } \alpha = 0 \\ \gamma \geq 0, \lambda > 0, & \text{if } \alpha > 0. \end{cases} \quad (2.3)$$

The distribution induced by the density given in equation (2.2) is denoted as $X \sim N^{-1}(\alpha, \gamma, \lambda)$. This distribution can be reduced to several important particular

cases, but the following two are of special interest in applications:

- the gamma distribution, when $\gamma = 0$, denoted as $\Gamma(\alpha, \lambda)$;
- the distribution of the reciprocal of a gamma distributed random variable, when $\lambda = 0$, denoted as $\Gamma^{-1}(\alpha, \gamma)$.

The aforementioned particular cases, i.e., the gamma and reciprocal of gamma laws, are obtained imposing restrictions on the parameter space. In order to make these derivations, two properties of that Bessel function have to be recalled:

1. for every $x > 0$, $K_{-v}(x) = K_v(x)$, and
2. every $K_v(x)$ can be approximated by $\Gamma(v)2^{v-1}x^{-v}$ when $x \downarrow 0$ and $v > 0$.

The first distribution provides a model for studying surfaces which are fairly homogeneous and heterogeneous. The second, in addition to maintaining the skills of the first law, allows

A random variable X is distributed as the reciprocal of a gamma, $X \sim \Gamma^{-1}(\alpha, \gamma)$, if its density function is

$$f_x(x) = \frac{1}{\gamma^\alpha \Gamma(-\alpha)} x^{-\alpha-1} \exp\left\{-\frac{\gamma}{x}\right\}, \quad -\alpha, \gamma, x > 0.$$

Figure 2.2 shows several Γ^{-1} densities, according to the following parameters: $\gamma = 1$ and $\alpha = (-0.5, -2, -4, -10)$. It is noteworthy that as the values of α are close to zero, the curve becomes flat, thus indicating that the variance increases with α . Hence, this distribution is useful for modeling dispersed data, as is the case of very heterogeneous areas in SAR images, such as, for example, images from urban areas.

Under the multiplicative model, the return of intensity data Z_I is the product of two independent variables: the intensity backscatter X_I and the intensity speckle Y_I . Therefore, the return has a distribution that depends on the model chosen for the backscattering and noise speckle.

If $X_I \sim N^{-1}(\alpha, \gamma, \lambda)$ and $Y_I \sim \Gamma(n, n)$ are independent random variables, then the product $Z_I = X_I Y_I$ has a distribution which is called intensity $\mathcal{G}_I(\alpha, \gamma, \lambda, n)$ and its

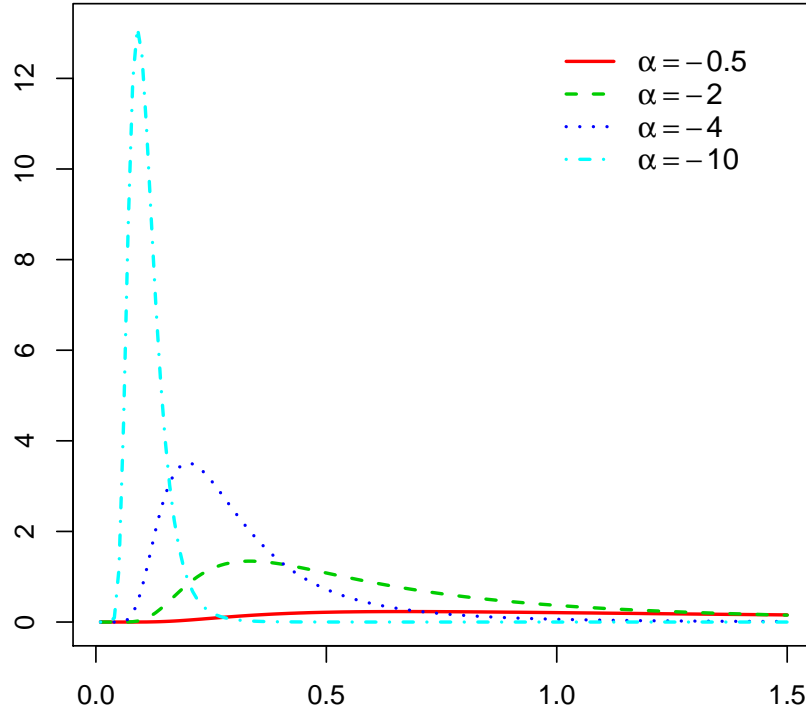


Figure 2.2: Γ^{-1} densities for $\alpha = -0.5, -2, -4, -10$ (solid, dashes, dots and dots-dashes respectively)

density is given by Frery et al. (1997):

$$f_{z_I}(z) = \frac{n^n (\lambda/\gamma)^{\alpha/2}}{\Gamma(n) K_\alpha(2\sqrt{\lambda\gamma})} z^{n-1} \left(\frac{\gamma + nz}{\lambda} \right)^{(\alpha-n)/2} K_{\alpha-n}(2\sqrt{\lambda(\gamma + nz)}),$$

where $n \geq 1$, $z > 0$. The space parameter of $(\alpha, \gamma, \lambda)$ is the same as in (2.3).

With this model for the return, it is possible to obtain closed form expressions for the densities of the return under the multiplicative model in, among others, the following cases:

- If $\alpha, \lambda > 0$ and $\gamma \downarrow 0$, the $\mathcal{G}_I(\alpha, \gamma, \lambda, n)$ distribution converges in distribution to distribution denoted as $\mathcal{K}_I(\alpha, \lambda, n)$;
- If $-\alpha, \gamma > 0$ and $\lambda \downarrow 0$, the $\mathcal{G}_I(\alpha, \gamma, \lambda, n)$ distribution converges in distribution to distribution denoted as $\mathcal{G}_I^0(\alpha, \gamma, n)$.

The parameters of the \mathcal{G}_I^0 distribution have the same interpretation as those of the \mathcal{K}_I distribution, but the first law has greater flexibility for modeling surfaces with different degrees of homogeneity. The \mathcal{G}_I^0 law is numerically and computationally more manageable than the \mathcal{K}_I law, which makes it very attractive as an alternative for the analysis of SAR data. This distribution was developed for describing areas with extremely heterogeneous clutter by Frery et al. (1997), and was later proposed and evaluated as an universal model for data with speckle noise by Mejail et al. (2001). An extension for the polarimetric case is presented in Freitas et al. (2005), and its application to polarimetric SAR image classification is demonstrated in Frery et al. (2007).

Next section presents some useful properties of the distribution that will be used to describe the return in those images where we will look for edges.

2.2 \mathcal{G}_I^0 distribution: properties and estimation

The \mathcal{G}_I^0 distribution is very attractive for modeling data with speckle noise, due to its mathematical tractability and because it is able to model very well information from most types of area.

Let X_I and Y_I be two independent random variables such that $X_I \sim \Gamma^{-1}(\alpha, \gamma)$ and $Y_I \sim \Gamma(n, n)$ with $-\alpha, \gamma > 0, n \geq 1$. Then, the random variable $Z_I = X_I Y_I$ follows a \mathcal{G}_I^0 distribution: $Z_I \sim \mathcal{G}_I^0(\alpha, \gamma, n)$ (Frery et al. 1997), characterized by the density

$$f_{Z_I}(z) = \frac{n^n \Gamma(n - \alpha)}{\gamma^\alpha \Gamma(n) \Gamma(-\alpha)} \frac{z^{n-1}}{(\gamma + nz)^{n-\alpha}}, \quad z > 0, \quad (2.4)$$

where $-\alpha > 0$ is the roughness parameter, $\gamma > 0$ is the scale parameter and $n \geq 1$ is the number of looks.

The moments of order r , are given by

$$E[Z_I^r] = \left(\frac{\gamma}{n}\right)^r \frac{\Gamma(-\alpha - r) \Gamma(n + r)}{\Gamma(-\alpha) \Gamma(n)}, \quad -\alpha > r/2. \quad (2.5)$$

Using equation (2.5), the variance of the \mathcal{G}_1^0 distribution can be computed as

$$\text{Var}[Z_1] = \begin{cases} \left(\frac{\gamma}{n}\right)^2 \left[\frac{\Gamma(-\alpha)\Gamma(n)\Gamma(-\alpha-2)\Gamma(n+2) - \Gamma^2(-\alpha-1)\Gamma^2(n+1)}{\Gamma^2(n)\Gamma^2(-\alpha)} \right] & -\alpha > 1, \\ \infty & 0 < -\alpha \leq 1. \end{cases}$$

Figure 2.3 shows different $\mathcal{G}_1^0(\alpha, \gamma, n)$ densities for different values of α ; the parameters $\gamma = 5$ and $n = 3$ are fixed. It is noted that the variance increases when α approaches zero.

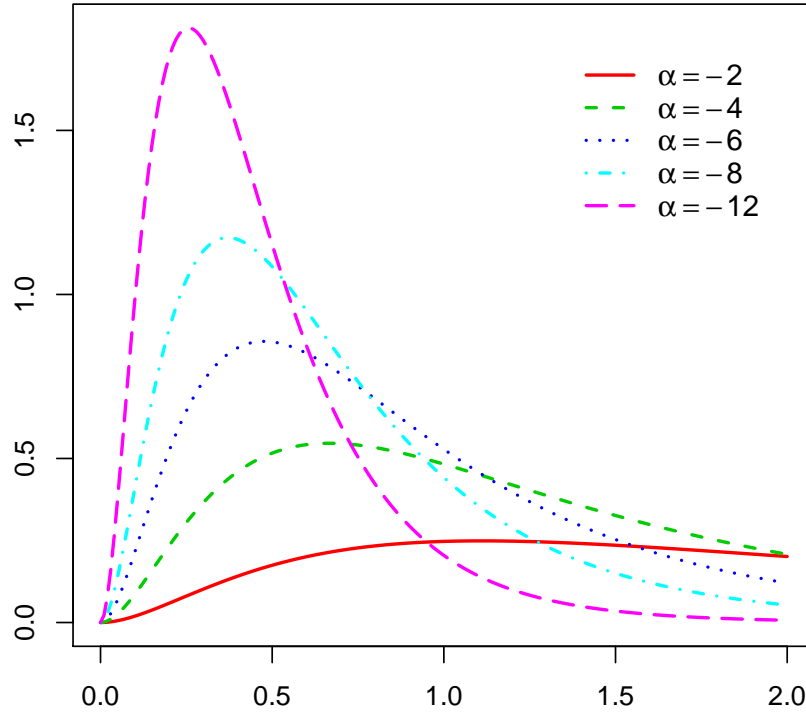


Figure 2.3: \mathcal{G}_1^0 densities for $\alpha = -2, -4, -6, -8, -12$ (solid, dashes, dots, dots-dashes respectively, solid-solid)

The proposed model for the return in SAR images depends on three parameters: roughness (α), scale (γ) and number of looks (n). There are a number of techniques for estimating such parameters, the most commonly used being those based on the substitution method (Manski 1988), maximum likelihood methods (Casella & Lehman 1998) and robust methods (Hampel et al. 1986). Besides those approaches,

there are also proposals of improvement techniques based either on analytic correction or on re-sampling.

Cribari-Neto et al. (2002) evaluate the effectiveness of bootstrap methods in improving estimation of clutter properties in speckled imagery. The estimation is performed by maximum likelihood methods. They show that the estimators obtained in this way can be quite biased in finite samples, and develop bias correction schemes using bootstrap re-sampling. They propose, for numerically bias correcting the maximum likelihood point estimates, alternative estimators that can deliver substantial finite-sample improvement over the original maximum likelihood parameter estimates and over other bootstrap-based bias-corrected estimation procedures.

Vasconcellos et al. (2005) propose an analytical bias correction for the maximum likelihood estimators of the \mathcal{G}_I^0 distribution. Comparing the performance of the corrected estimators with the corresponding original version, they observe that the maximum likelihood estimator and its corrected version are the preferred inference procedures with respect to bias. Also, they have verified that there is a wide range of practical situations for which the corrected estimator effectively reduces both bias and mean square error of the original maximum likelihood estimator.

Bustos et al. (2002) derive M-estimators for the parameters of the \mathcal{G}_A^0 distribution, and compare them with maximum likelihood estimators. They show that this robust technique is superior to the classical approach under the presence of corner reflectors, a common source of contamination in SAR images.

Allende et al. (2006) present the derivation of M-estimators with asymmetric influence functions, motivated by the \mathcal{G}_A^0 distribution. They propose the asymmetric M-estimator (AM-estimator), an M-estimator with asymmetric redescending functions. The performance of AM estimators is assessed, and it is shown that they either compete with or outperform both maximum likelihood and Huber-type M-estimators.

In this section we present estimators for parameters of the \mathcal{G}_I^0 distribution, assuming known number of looks and using the method of moments of orders $\frac{1}{2}$ and 1. This was the approach used by Gambini et al. (2006, 2008), and since we aim at

extending their work and comparing our proposal with theirs, we implemented the same approach they used.

Let (Z_1, \dots, Z_n) be a vector of independent and identically distributed random variables, with common $\mathcal{G}_I^0(\alpha, \gamma, n)$ distribution, $\alpha < -1$, $\gamma > 0$ and n known. Define the r -th sample moment as:

$$\hat{m}_r = \frac{1}{n} \sum_{i=1}^n Z_i^r,$$

with $r = \frac{1}{2}, 1$ (that is the reason why we assume $\alpha < -1$ rather than $\alpha < 0$).

From equation (2.5) it is immediate that

$$E(Z) = \left(\frac{\gamma}{n}\right) \frac{\Gamma(-\alpha - 1)\Gamma(n + 1)}{\Gamma(-\alpha)\Gamma(n)}, \quad -\alpha > 1/2.$$

and that

$$E(Z^{\frac{1}{2}}) = \left(\frac{\gamma}{n}\right)^{\frac{1}{2}} \frac{\Gamma(-\alpha - \frac{1}{2})\Gamma(n + \frac{1}{2})}{\Gamma(-\alpha)\Gamma(n)}, \quad -\alpha > 1/4.$$

Replacing the theoretical moments by the sample expressions, and the parameters by their estimators, we build a system of two equations:

$$m_1 = \left(\frac{\hat{\gamma}}{n}\right) \frac{\Gamma(-\hat{\alpha} - 1)\Gamma(n + 1)}{\Gamma(-\hat{\alpha})\Gamma(n)}, \quad -\hat{\alpha} > 1/2. \quad (2.6)$$

and

$$m_{\frac{1}{2}} = \left(\frac{\hat{\gamma}}{n}\right)^{\frac{1}{2}} \frac{\Gamma(-\hat{\alpha} - \frac{1}{2})\Gamma(n + \frac{1}{2})}{\Gamma(-\hat{\alpha})\Gamma(n)}, \quad -\hat{\alpha} > 1/4.$$

clearing $\hat{\gamma}$ of both equations, we obtain

$$\hat{\gamma} = \frac{m_1 \Gamma(-\hat{\alpha}) \Gamma(n) n}{\Gamma(-\hat{\alpha} - 1) \Gamma(n + 1)}, \quad (2.7)$$

and

$$\hat{\gamma} = \frac{m_{\frac{1}{2}}^2 \Gamma^2(-\hat{\alpha}) \Gamma^2(n) n}{\Gamma^2(-\hat{\alpha} - \frac{1}{2}) \Gamma^2(n + \frac{1}{2})}. \quad (2.8)$$

From equations (2.7) and (2.8) we then obtain

$$\frac{m_1 \Gamma(-\hat{\alpha}) \Gamma(n) n}{\Gamma(-\hat{\alpha} - 1) \Gamma(n + 1)} = \frac{m_{\frac{1}{2}}^2 \Gamma^2(-\hat{\alpha}) \Gamma^2(n) n}{\Gamma^2(-\hat{\alpha} - \frac{1}{2}) \Gamma^2(n + \frac{1}{2})}$$

The estimator of α is obtained by solving numerically the following equation

$$g(\hat{\alpha}) - \zeta = 0,$$

where

$$g(\hat{\alpha}) = \frac{\Gamma^2(-\hat{\alpha} - \frac{1}{2})}{\Gamma(-\hat{\alpha}) \Gamma(-\hat{\alpha} - 1)},$$

and

$$\zeta = \frac{m_{\frac{1}{2}}^2}{m_1} \frac{\Gamma(n + 1) \Gamma(n)}{\Gamma^2(n + \frac{1}{2})}.$$

By plugging the value of $\hat{\alpha}$ into equation (2.6) one finds the value of $\hat{\gamma}$.

Next section presents a summary of the main techniques for edge detection in SAR imagery, with special emphasis on those that explicitly employ statistical models and techniques.

2.3 Edge detection in SAR imagery

Edge detectors based on the statistical theory of edges detection in noisy images have been described by, for example, Bovik et al. (1986). Those authors introduced nonparametric statistics for edge detection in Gaussian additive noise. They demonstrated the usefulness of the median and the Wilcoxon-Mann-Whitney tests for edge detection with the help of a sample image interpreted visually.

Fesharaki & Hellestrand (1994) proposed an algorithm for detecting edges by using a t-test. Beauchemin et al. (1998) described an edge detection method which uses a nonparametric alternative based on the Wilcoxon-Mann-Whitney statistics for detecting changes in adjacent pixel neighborhoods with relatively distinct grey level values. They assumed that the neighborhoods are sufficiently homogeneous and

changes in adjacent neighborhoods are detected by testing differences in location parameters such as means or medians. Although these tests may be appropriate for specific types of images, they may not detect changes in local grey level values in images with low signal-to-noise ratios, as is the case of SAR imagery.

Recently, Hoon Lim & Ju Jang (2002) compared two-sample tests for edge detection in noisy images. Later, Lim (2006) describes a new edge detector based on the robust rank-order test which is a useful alternative to the Wilcoxon test, using $\ell \times \ell$ windows for detecting edges of all possible orientations in noisy images. This method is based on testing whether an $\ell \times \ell$ window is partitioned into two sub-regions having significant differences in local gray-level values between neighborhoods of a given pixel, using an edge-height model to extract edges of some sufficient brightness from images corrupted with noises.

The two main advantages of nonparametric tests are:

1. their statistical significance is independent of the distribution form, and
2. they are robust against the presence of extreme observations.

These features are of particular interest in the case at hand, namely, speckled imagery.

The detection of edges in images with speckle noise has been studied by many authors and a variety of techniques are presented in the work of Gambini et al. (2006, 2008).

This study is based on Juliana Gambini's doctoral thesis, who proposed a method of curve fitting with contours of objects and regions in images with speckle noise which displays excellent results, with an acceptable computational cost. The algorithms used by Gambini et al. (2006, 2008) consider the image region by region, instead of considering the whole image, saving computational time. In addition, this approach employs B-splines as the mathematical model for the contours; such curves depend on few parameters and are easily computed (Brigger et al. 2000).

In order to find edge points between different regions of the image, Gambini et al. (2006, 2008) used the assumption that the squared SAR data can be modeled by the

\mathcal{G}_I^0 distribution, i.e., the so-called \mathcal{G}_A^0 distribution. Under this model, the regions of the image with different degrees of homogeneity are characterized by the parameters of the distribution. Hence, the relevant parameters are estimated, along straight segments arranged in an adequate surrounding of an initial curve. If a point belongs to the edge of the object, then in a neighborhood of this point there should be a sudden change in the estimated parameters of the distribution.

In this Chapter we describe five techniques for detecting edges in SAR images. One is the method of Gambini and four similar methods based on linear rank sums are described; specifically, the Wilcoxon-Mann-Whitney, Kruskal-Wallis, Variance test and a new statistical propose.

2.3.1 Gambini algorithm for edge detection

If a point belongs to an object edge, then a sample taken from its neighbourhood should exhibit a changes in the statistical parameters and, therefore, should be considered a transition point.

Consider N segments of the image, $s^{(i)}, i \in \{1, \dots, N\}$, of the form $s^{(i)} = \overline{CP_i}$ where C is the centroid of the initial region, the extreme P_i is a point outside the region and $\theta_i = \angle(s^{(i)}, s^{(i+1)})$ is the angle between two successive segments, as shown in Figure 2.4.

The segment $s^{(i)}$ is an array of m elements coming from a discretization of the straight line on the image and is given by

$$s^{(i)} = (z_1^{(i)}, \dots, z_m^{(i)}).$$

For each segment $s^{(i)}, 1 \leq i \leq N$, the following partition is considered:

$$\begin{aligned} Z_k^{(i)} &\sim \mathcal{G}_I^0(\alpha_\ell, \gamma_\ell), & k &= 1, \dots, j_i, \\ Z_k^{(i)} &\sim \mathcal{G}_I^0(\alpha_r, \gamma_r), & k &= j_i, \dots, m, \end{aligned}$$

where, for each k , with $1 \leq k \leq m$, $z_k^{(i)}$ is the realization of the random variable

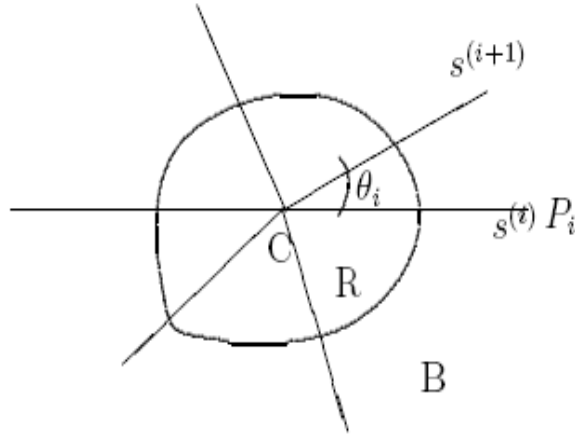


Figure 2.4: Radial straight lines projected from the centroid of R to the exterior of the region, with a separation of θ_i

$Z_k^{(i)}$. The parameters $(\alpha_\ell, \gamma_\ell)$ and (α_r, γ_r) characterize the region and its background, respectively, and they are estimated as explained in section 2.2.

In order to find the transition point on each segment, $s^{(i)}$, an objective function is considered: the likelihood of the sample, which is given by

$$l = \prod_{i=1}^j \Pr(z_i; \hat{\alpha}_\ell, \hat{\gamma}_\ell) \prod_{i=j+1}^m \Pr(z_i; \hat{\alpha}_r, \hat{\gamma}_r).$$

To find the transition point, we maximize $L = \ln(l)$

$$L = \ln(l) = \sum_{i=1}^j \ln\left(f_{\mathcal{G}_I^0}(z_i; \hat{\alpha}_\ell, \hat{\gamma}_\ell)\right) + \sum_{i=j+1}^m \ln\left(f_{\mathcal{G}_I^0}(z_i; \hat{\alpha}_r, \hat{\gamma}_r)\right).$$

Then, using equations (2.4),

$$L = \sum_{i=1}^j \ln\left(\frac{n^n \Gamma(n - \hat{\alpha}_\ell) z_i^{n-1}}{\hat{\gamma}_\ell^{\hat{\alpha}_\ell} \Gamma(n) \Gamma(-\hat{\alpha}_\ell) (\hat{\gamma}_\ell + n z_i)^{n - \hat{\alpha}_\ell}}\right) + \sum_{i=j+1}^m \ln\left(\frac{n^n \Gamma(n - \hat{\alpha}_r) z_i^{n-1}}{\hat{\gamma}_r^{\hat{\alpha}_r} \Gamma(n) \Gamma(-\hat{\alpha}_r) (\hat{\gamma}_r + n z_i)^{n - \hat{\alpha}_r}}\right).$$

Finally, the estimated index on the segment that corresponds to the transition point, \hat{j} , is

$$\hat{j} = \arg \max_j L. \quad (2.9)$$

Figure 2.5 shows typical values of the objective function, taken along a straight line segment. The corresponding position of the maximum is considered to be the point of transition between both regions, according to formula (2.9).

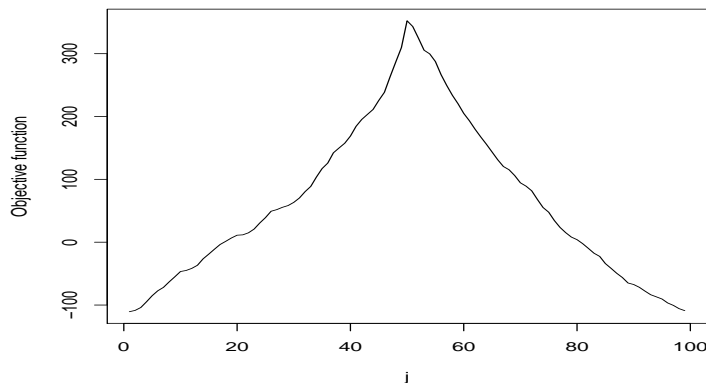


Figure 2.5: Values of the objective function for a segment of straight

The relevant parameters are estimated within a rectangular window, such that the direction of its major axis coincides with the segment being processed and such that it includes a sample from the region and a sample from the background. These samples are used to estimate the $(\alpha_\ell, \gamma_\ell)$ and (α_r, γ_r) parameters, respectively.

Estimation of the parameters that index the \mathcal{G}_1^0 distribution was discussed in Section 2.2. Next section will present non-parametric alternatives to edge detection, that will lead to the main proposal of this work.

2.3.2 Non-parametric edge detection

The usual two-sample situation is that one for which the experimenter has obtained two samples from possibly different populations and wishes to use a statistical test to check if the null hypothesis that the two populations are identical can be rejected.

That is, the experimenter wishes to detect differences between the two populations on the basis of random samples from those populations. If the samples consist of ordinal-type data, the most interesting difference is a difference in the locations of the two populations.

An intuitive approach to the two-sample problem is to combine both samples into a single ordered sample and assign ranks to the sample values from the smallest value to the largest, regardless the population each value came from. Then, the test statistic can be computed as the sum of the ranks assigned to those values from one of the populations. If the sum is too small (or too large), there is indication that the values from that population tend to be smaller (or larger, as the case may be) than the values from the other population. Hence, the null hypothesis of no differences between populations may be rejected if the ranks associated with one sample tend to be larger than those of the other sample.

Ranks may be preferable to the actual data for several reasons. First, if the numbers assigned to the observations have no meaning by themselves but attain meaning only in an ordinal comparison with the other observations, the numbers contain no more information than the ranks contain. Such is the nature of ordinal data. Second, even if the numbers have meaning but the distribution is not a Gaussian distribution function, the theory is usually beyond our reach when the test statistic is based on the actual data. The probability theory of statistics based on ranks is relatively simple and, in many cases, it does not depend on the underlying distribution. A third reason for preferring ranks is that the asymptotic relative efficiency of the Mann-Whitney test below is never low when compared with the two-sample t test, the usual parametric counterpart. And yet the contrary is not true; the asymptotic relative efficiency of the t test compared to the Mann-Whitney test may be as small as zero, or “infinitely bad.” So, the Mann-Whitney test is a safer test to use (Conover 1980).

In this paper we will use test statistical for each non-parametric method, and does not take decision on the hypothesis, for that reason not to follow rules of decision.

2.3.3 The Mann-Whitney test

The data consist of samples from two different populations. Let X_1, X_2, \dots, X_n denote the random variables representing a sample of size n from population A and let Y_1, Y_2, \dots, Y_m denote the random variables representing a sample of size m from population B. Assign ranks 1 to $n + m$. Let $R(X_i)$ and $R(Y_j)$ denote the ranks assigned to X_i and Y_j for all i and j . For convenience, let $N = n + m$.

If several sample values are exactly equal to each other (tied), assign to each the average of the ranks that would have been assigned to them had there been no ties.

Assumptions

- Both samples are random samples from the respective populations.
- In addition to independence within each sample, there is mutual independence between the two samples.
- The measurement scale is at least ordinal.

Hypotheses

Let $F(x)$ and $G(x)$ be the distribution functions of X and Y corresponding to populations A and B, respectively. Then, the hypotheses may be stated as follows:

$$H_0 : F(x) = G(x)$$

$$H_1 : F(x) \neq G(x)$$

In many real situations, as is our case in edge detection, differences between distributions imply that $\Pr(X < Y)$ is no longer equal to $1/2$. Therefore, the following

set of hypotheses is often used instead of the above.

$$\begin{aligned} H_0 : \Pr(X < Y) &= \frac{1}{2} \\ H_1 : \Pr(X < Y) &\neq \frac{1}{2} \end{aligned}$$

The Mann-Whitney test is unbiased and consistent when testing the preceding hypotheses involving $\Pr(X < Y)$.

Test Statistic

If there are no or just a few ties, the sum of the ranks assigned to the sample from population A can be used as a test statistic:

$$T = \sum_{i=1}^n R(X_i).$$

If there are many ties, subtract the mean from T and divide by the standard deviation to get

$$T_1 = \left| \frac{T - n \frac{N+1}{2}}{\sqrt{\frac{nm}{N(N-1)} \sum_{i=1}^N R_i^2 - \frac{nm(N+1)^2}{4(N-1)}}} \right|.$$

where $\sum_{i=1}^N R_i^2$ refers to the sum of the squares of all N of the ranks or average ranks actually used in both samples.

2.3.4 The Kruskal-Wallis test

The Mann-Whitney test for two independent samples was extended to the problem of analyzing k independent samples, for $k \geq 2$, by Kruskal & Wallis (1952). The experimental situation is one where k random samples have been obtained, one from each of k possible different populations, and we want to test the null hypothesis that all populations are identical against the alternative that some of the populations tend to yield greater observed values than others. The term “greater” applies to observations from random variables, but actually any observations that may be

arranged in increasing order according to some property such as quality, value, and the like may be analyzed using the Kruskal-Wallis test in a manner analogous to the analysis of nonnumeric data using the Mann-Whitney test.

The Kruskal-Wallis test statistic is a function of the ranks of the observations in the combined sample, in a similar fashion to the Mann-Whitney test.

Data

The data consist of k random samples of possibly different sizes. Denote the i -th random sample of size n_i by $X_{i1}, X_{i2}, \dots, X_{in_i}$. Then, the data may be arranged into columns:

Sample 1	Sample 2	\dots	Sample k
$X_{1,1}$	$X_{2,1}$		$X_{k,1}$
$X_{1,2}$	$X_{2,2}$		$X_{k,2}$
\vdots	\vdots	\ddots	\vdots
X_{1,n_1}	X_{2,n_2}		X_{k,n_k}

Let N denote the total number of observations:

$$N = \sum_{i=1}^k n_i. \quad (2.10)$$

Assign rank 1 to the smallest of the total of N observations, rank 2 to the second smallest, and so on until the largest of the all N observations, which receives rank assigned to X_{ij} . Let R_i be the sum of the ranks assigned to the i th sample:

$$R_i = \sum_{j=1}^{n_i} R(X_{ij}) \quad i = 1, 2, \dots, k \quad (2.11)$$

Compute R_i for each sample. When the ranks can be assigned in several different ways because several observations are tied, assign the average rank to each of the tied observations, as in the previous test.

Assumptions

- All samples are random samples from the respective populations.
- In addition to independence within each sample, there is mutual independence among the various samples.
- The measurement scale is at least ordinal.
- Either the k population distribution functions are identical, or some of the populations tend to yield larger values than other populations do.

Hypotheses

The following hypotheses are covered by this test:

H_0 : All k population distribution functions are identical

H_1 : At least one population tends to yield larger observations than
at least one of the other populations

Because the Kruskal-Wallis test is designed to be sensitive against differences among means in the k populations, the alternative hypothesis is sometimes stated as follows.

H_1 : k populations do not have identical means.

Test Statistic

The test statistic T is defined as

$$T = \frac{1}{S^2} \left(\sum_{i=1}^k \frac{R_i^2}{n_i} - \frac{N(N+1)^2}{4} \right), \quad (2.12)$$

where N and R_i are defined by equations (2.10) and (2.11), respectively, and where

$$S^2 = \frac{1}{N-1} \left(\sum_{\text{all ranks}} R(x_{ij})^2 - \frac{N(N+1)^2}{4} \right).$$

If there are no ties, S^2 simplifies to $N(N+1)/12$, and the test statistic reduces to

$$T_k = \frac{12}{N(N+1)} \sum_{i=1}^k \frac{R_i^2}{n_i} - 3(N+1). \quad (2.13)$$

If the number of ties is moderate there will be very little difference between equations (2.12) and (2.13), so the simpler equations (2.13) may be preferred in practice.

2.3.5 The Squared Ranks test for variances

The usual standard of comparison for several populations is based on the means or others measures of location of the population. However, in some situations the variances of the populations may be the quantity of interest. The squared ranks test can be used to assess equality of variance across two or more independent random samples which have been measured using a scale that is at least interval (Conover 1980).

Interval measurement assigned to objects have all the features of ordinal measurements, and in addition equal differences between measurements represent equivalent intervals. That is, differences between arbitrary pairs of measurements can be meaningfully compared. Operations such as addition and subtraction are therefore meaningful. The zero point on the scale is arbitrary; negative values can be used.

Data

The data consist of the two random samples. Let X_1, X_2, \dots, X_n denote the random sample of size n from population A and let Y_1, Y_2, \dots, Y_m denote the random sample of size m from population B. Convert each X_i and Y_j to its absolute deviation from

the mean using

$$U_i = |X_i - \bar{X}_1|, \quad i = 1, \dots, n,$$

and

$$V_j = |Y_j - \bar{X}_2|, \quad j = 1, \dots, m,$$

where \bar{X}_1 and \bar{X}_2 are the sample means for populations A and B.

Assign ranks 1 to $n + m$ to the combined sample for U s and V s in the usual way. If several values of U and/or V are exactly equal to each other (ties), assign to each the average of the ranks that would have been assigned to them had there been no ties.

Assumptions

- Both samples are random samples from their respective populations.
- In addition to independence within each sample there is mutual independence between the two samples.
- The measurement scale is at least interval.

Hypotheses

H_0 : X and Y are identically distributed, except for possibly different means.

H_1 :

$$\text{Var}(X) \neq \text{Var}(Y) \quad \text{or}$$

$$\text{Var}(X) < \text{Var}(Y) \quad \text{or}$$

$$\text{Var}(X) > \text{Var}(Y)$$

Test Statistic

If there are no values of U tied with values of V , the sum of the squares of the ranks assigned to population A can be used as the test statistic

$$T = \sum_{i=1}^n [R(U_i)]^2.$$

If there are ties, subtract the mean from T and divide by the standard deviation to get

$$T_v = \frac{T - n\overline{R^2}}{\left[\frac{nm}{N(N-1)} \sum_{i=1}^N R_i^4 - \frac{nm}{N-1} (\overline{R^2})^2 \right]^{\frac{1}{2}}},$$

where $N = n + m$, and $\overline{R^2}$ represents the average of the squared ranks of both samples combined, i.e.,

$$\overline{R^2} = \frac{1}{N} \left\{ \sum_{i=1}^n [R(U_i)]^2 + \sum_{j=1}^m [R(V_j)]^2 \right\},$$

and $\sum_{i=1}^N R_i^4$ represents the sum of the ranks raised to the fourth power:

$$\sum_{i=1}^N R_i^4 = \sum_{i=1}^n [R(U_i)]^4 + \sum_{j=1}^m [R(V_j)]^4.$$

2.3.6 The TPE empirical statistic

The empirical statistic **TPE** was designed based on non-parametric statistics based on ranges, which have good performance in situations where one wants to test whether two samples have means and/or different variances, as is the case with Kruskal-Wallis and Mann-Whitney statistics and the Squared Rank test for variances.

The data consist of the two random samples. Let X_1, X_2, \dots, X_n denote the random sample of size n from population A and let Y_1, Y_2, \dots, Y_m denote the random sample of size m from population B . Assign ranks 1 to $N = n + m$.

Taking as the main idea the use of the ranges of the combined sample, the em-

empirical statistic **TPE** compares the average of overall ranks of the combined sample $\mu = (N + 1)/2$ with the difference between the average ranks of the two populations $D_E = |\bar{x} - \bar{y}|$, obtaining in this way the empirical statistics E :

$$E = |D_E - \mu|.$$

2.4 Proposal

We have presented three classical and an empirical non-parametrical test that may be used for edge detection in speckled imagery. In this section we will discuss how to use them in practice.

In order to find the transition point on each segment, $s^{(i)}$, take a number of elements j_1, \dots, j_k on the segment, separated by an arbitrary length. For each element, form two rectangular windows whose division is in this point, as shown in Figure 2.6. The window to the left of j_i contains information on the ranks of population A, and, to the right of j_i , the window contains the ranks of population B. The candidate edge, namely j_i , will be displaced and at each location objective functions will be calculated.

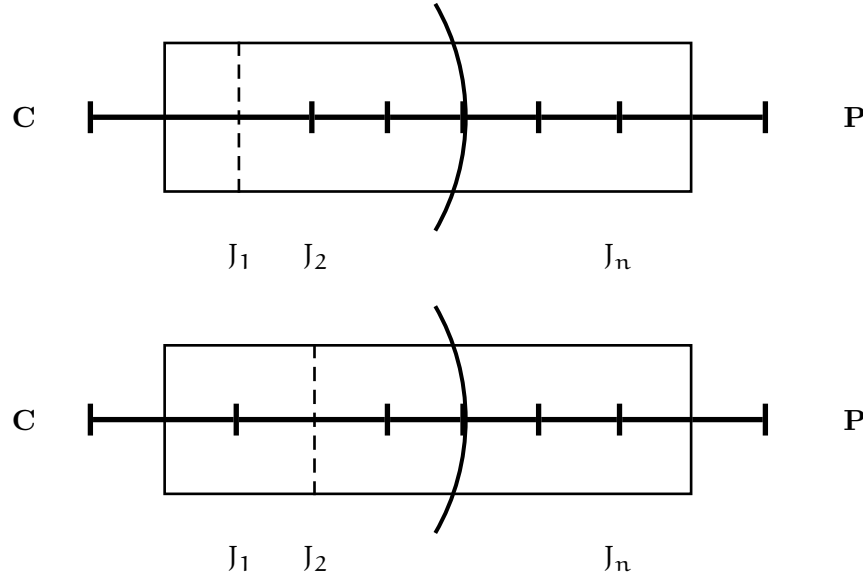


Figure 2.6: Displacement of a rectangular window on a straight segment

Finally, the estimate of the index \hat{j} corresponding to point edge b_i on the segment $s^{(i)}$ is given by:

- The Mann-Whitney Test:

$$\hat{j} = \arg \max_j T_1;$$

- The Kruskal-Wallis Test:

$$\hat{j} = \arg \max_j T_k;$$

- The squared Ranks Test for Variances:

$$\hat{j} = \arg \max_j T_v;$$

- The TPE Empirical statistic:

$$\hat{j} = \arg \min_j E.$$

Figure 2.7 shows typical values of the statistics of the Mann-Whitney test, Kruskal-Wallis test, squared ranks test for variances and the TPE empirical statistic taken along a straight line segment. The corresponding position of the maximum (Mann-Whitney, Kruskal, T. Variance) or the minimum (TPE) is considered to be the point of transition between both regions. In this figure, the true edge is at position 50 along the abscissas; it is noted that the maximum value that the Mann-Whitney, Kruskal-Wallis, squared Ranks for Variances test statistics, and TPE's minimum coincides with the point of edge, suggesting, thus, that our proposal is sensible.

This Chapter presented an elementary introduction to SAR imagery, the basics of the Multiplicative Model for speckled imagery, the G_1^0 distribution and the four test statistics. In order to make a quantitative assessment of the performance of these four techniques, and to compare them with the one claimed by Gambini et al. (2006, 2008), a Monte Carlo experience is described in the next Chapter.

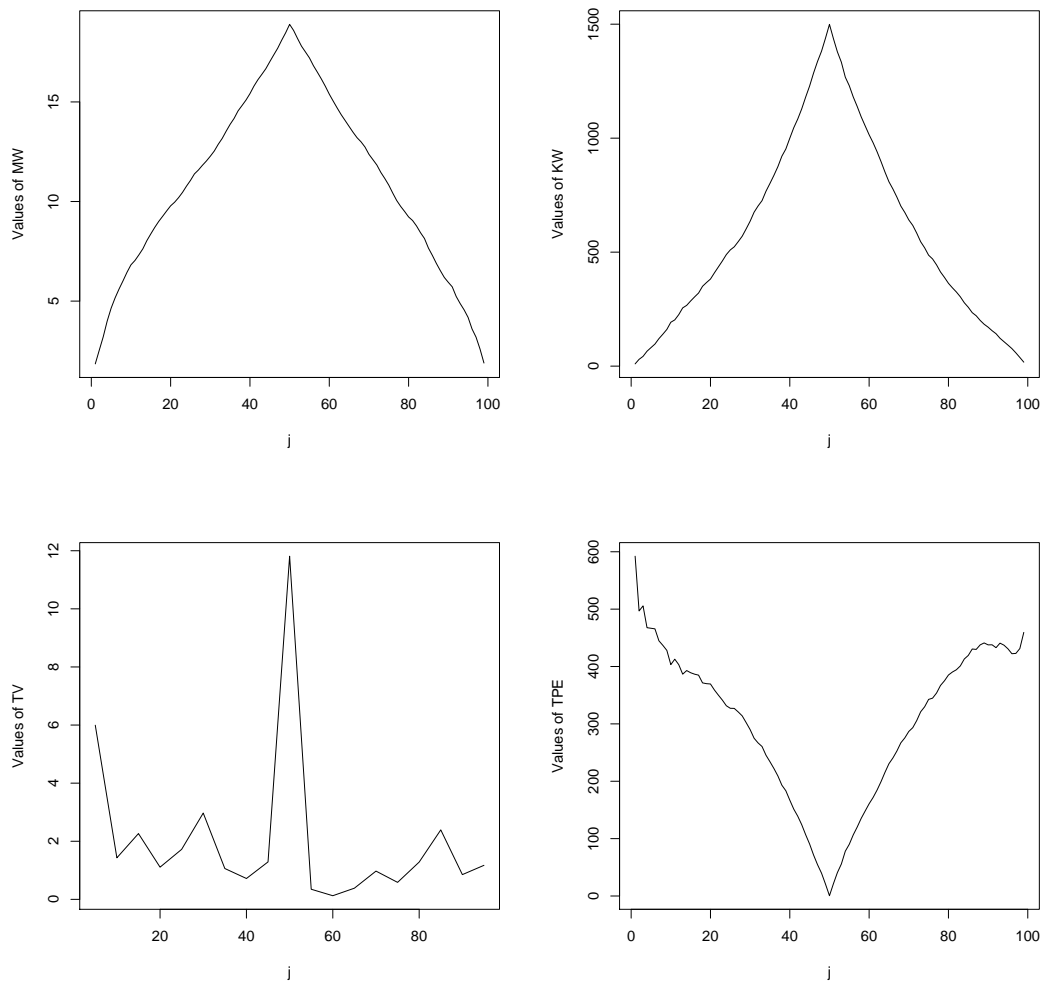


Figure 2.7: Typical values of the Mann-Whitney, Kruskal-Wallis Test, T. Variances statistics and TPE for a straight segment

Chapter 3

Results

Resumo

Este capítulo descreve as simulações realizadas com o intuito de avaliar os desempenhos das diferentes técnicas de detecção de bordas, o capítulo inclui ainda uma análise dos resultados obtidos por meio de um experimento Monte Carlo.

Todas as simulações foram realizadas em computadores Intel © Pentium© IV CPUs de 3.20 GHz sob o sistema operacional Windows XP, usando a linguagem matricial Ox versão 4.10 (Doornik 2002), os gráficos tendo sido produzidos com o programa R versão 2.6.1

Os métodos estatísticos considerados nesta tese são projetados para avaliar a precisão na procura de uma borda conhecida num vetor com dados speckled. Neste capítulo nós avaliamos o erro cometido ao estimar o ponto borda (erro local), para cada um dos métodos descritos no capítulo 2.

Nós calculamos o erro que se comete ao encontrar o ponto de transição num segmento de reta. Varias situações são consideradas, e para cada situação são simuladas 1000 janelas retangulares de tamanho 20×100 geradas com a distribuição $\mathcal{G}_I^0(\alpha, \gamma, n)$.

Cada janela é composta de duas partes e cada situação corresponde a considerar $-\alpha_\ell \in \{3, 4, 6, 8, 10, 12, 14, 16, 18, 20\}$, e $-\alpha_r \in \{2, 3, 4, 5, 6, 7, 8, 9, 10,$

11, 12, 13, 14, 15, 16, 17, 18, 19, 20}.

O número de looks em nosso experimento, para cada situação, é $n \in \{1, 3, 8\}$; esses valores abrangem uma variedade de imagens freqüentemente encontradas na prática, a partir de apenas um look até suavizados multi-looks.

Results

This Chapter describes the simulations performed to obtain a quantitative assessment of the performance of the techniques under evaluation, in addition to the analysis of results obtained by such Monte Carlo experiment. All simulations were performed on personal computers with Intel© Pentium© IV CPUs of 3.20 GHz running Windows XP operating system, and using the matrix language program Ox version 4.10 (for details, see Doornik 2002). Graphical outputs were obtained in R version 2.6.1 (Venables & Ripley 2002).

A widely used tool in statistics is Monte-Carlo simulation. Monte-Carlo techniques are based on the generation of a large number of samples from random variables with specific distributions of interest and then using them to make inferences and draw conclusions.

The statistical methods considered in this thesis are designed to assess the accuracy in finding an edge known to be present on an array of speckled data. In this chapter we evaluate the error when estimating the point edge (local error), for each of the methods described in Chapter 2.

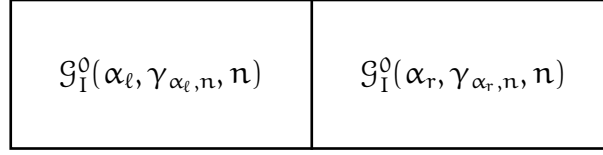
We estimate the error in finding the transition point on a straight segment, according to the process described below. Several parametric situations are considered and for each situation 1000 simulated rectangular windows of size 20×100 (20 rows, 100 columns) are filled with samples from the $\mathcal{G}_1^0(\alpha, \gamma, n)$ distribution.

Each window is composed of two halves, and each situation corresponds to considering $-\alpha_\ell \in \{3, 4, 6, 8, 10, 12, 14, 16, 18, 20\}$, and $-\alpha_r \in \{2, 3, 4, 5, 6, 7, 8, 9, 10, 11, 12, 13, 14, 15, 16, 17, 18, 19, 20\}$. The number of looks in our experience, for each situation, is $n \in \{1, 3, 8\}$; these values span a variety of images often encountered in practice, from single-look to smoothed multi-look. The scale parameter γ assumes the values resulting from replacing n and α in the expression

$$\gamma_{\alpha, n} = \frac{\Gamma(-\alpha)\Gamma(n)n}{\Gamma(-\alpha-1)\Gamma(n+1)}, \quad (3.1)$$

in order to guarantee unitary mean. It is noteworthy that we opted for testing

the edge detection algorithms in a difficult situation, namely, in a case where the areas have the same mean value (granted by $\gamma_{\alpha,n}$) and differ only by the texture. Figure 3.1 shows a scheme of the form that has each of the rectangular samples.



$$J = 50$$

Figure 3.1: Scheme of a rectangular window on a straight segment

Situations for which $\alpha_\ell = \alpha_r$ are not considered, since in those 10 cases there is no edge. In this manner, we consider $((10 \times 19) - 10) \times 3 = 540$ (α_ℓ , α_r and n) situations, and 1000 windows are simulated for each of them. In each of these 540,000 windows, the edge is detected by the five techniques already described, and the error is calculated as the absolute difference between the detected edge and the true edge, located at position 50.

The errors are stored in an 1000-dimensional array $D_M(j)$, with $N = 1000$, defined in the following way:

$$D_M(j) = |P_V - P_T(j)| \quad j = 1, 2, \dots, 1000,$$

where $P_V = 50$ is the true edge or transition point and $P_T(j)$, $j = 1, \dots, 1000$ is the transition point found by the method under evaluation assessment, correspondent to the j - th sample. Note that M ranges in the set $\{M. Gambini, T. Kruskal, T. Mann-Whitney, T. Variance, TPE\}$, where $M. Gambini$ denotes the method that maximizes a likelihood function of Gambini et al. (2006), $T. Kruskal$ the method Kruskal Wallis, $T. Mann-Whitney$ denotes the Mann-Whitney Test, $T. Variance$ the Squared Ranks Test for Variances and TPE the Empirical Statistics TPE.

Here, $f(M)$ is the proportion of times that the difference between the estimated

point and the true point is greater than 5 pixels, using method M :

$$f(M) = \frac{\#\{j \in \{1, \dots, 1000\} : D_M(j) > 5\}}{1000}.$$

Method M_i is more efficient than method M_j ($i \neq j$) whenever $f(M_i) < f(M_j)$, i.e., if the proportion of errors of method M_i is smaller than that of method M_j .

Instead of showing the results of all 540 situations, only the ones we identified as the most relevant are discussed in detail. This chapter presents a detailed analysis of $((4 \times 19) - 4) \times 3 = 216$ situations, namely for each of the 3 looks and each of the 19 values of α_r , but only for 4 values of α_ℓ : extremely heterogeneous areas ($\alpha_\ell = -3$), heterogeneous areas ($\alpha_\ell = -8$) and two completely homogeneous areas ($\alpha_\ell = -12, -18$). Four situations for which $\alpha_r = \alpha_\ell$ were not considered. The data from the remaining $540 - 216 = 324$ situations, though not analyzed in detail, are presented in Appendices A, B and C.

It is shown that the **M. Gambini** method and the Kruskal-Wallis and Mann-Whitney statistics are the best choices in our case studies.

The execution time of each method is also computed and assessed, and the Monte Carlo experience provides strong evidence that the Kruskal-Wallis approach is approximately three orders of magnitude faster than the **M. Gambini** method.

3.1 Extremely heterogeneous areas with $n = 1$ and $\alpha_\ell = -3$

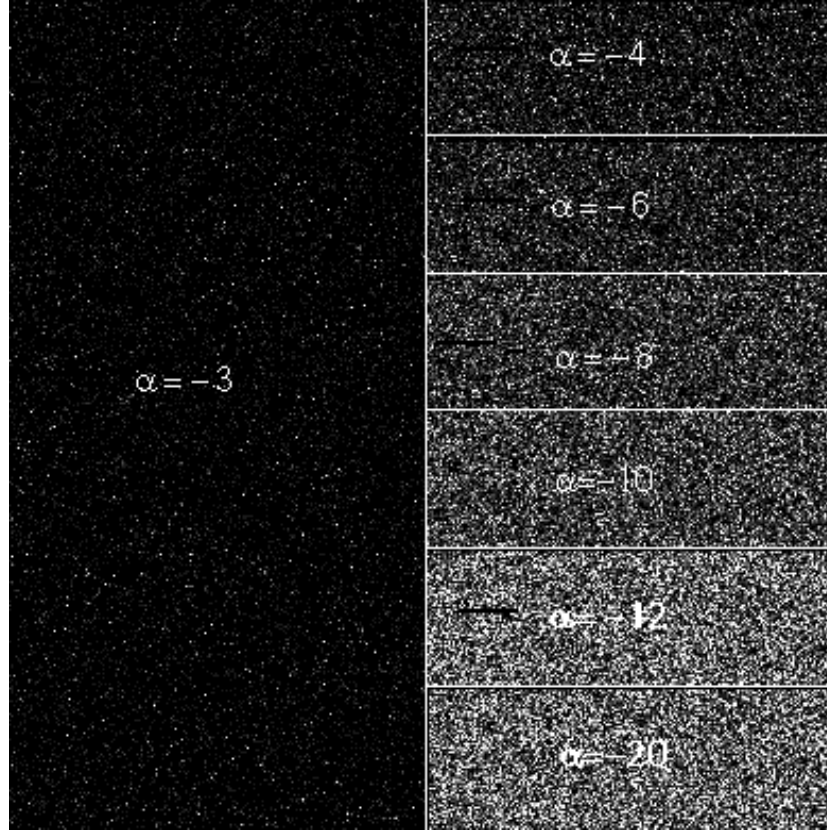


Figure 3.2: Synthetic images $\mathcal{G}_I^0(\alpha, 1, 1)$, $\gamma = 1$ and $\alpha_\ell = -3$ to the left against $\alpha_r = \{-4, -6, -8, -10, -12, -20\}$ to the right

Figure 3.2 presents samples generated from the $\mathcal{G}_I^0(\alpha, 1, 1)$ distribution using different values of α and $\gamma = 1$. These samples correspond to different degrees of homogeneity. It can be noted that when the parameter α is close to zero, the variance increases and, therefore, a higher degree of heterogeneity is observed. To the left side of this figure there is an image generated from $\mathcal{G}_I^0(-3, 1, 1)$, which represents extremely heterogeneous areas, and to the right there are images generated with the $\mathcal{G}_I^0(\alpha, 1, 1)$ with $\alpha = -4$ up to $\alpha = -20$, that represent areas with different degrees of roughness.

In this and in all subsequent figures, each patch of data with same distribution was scaled independently of the others, in order to provide an acceptable contrast of the whole compound image, these images are generated with γ fixed equal to 1. These images are a graphic representation of changes in texture when varies α , are not generated with the data used to detect edges, since the data generated dependent the α and γ , and the latter depends of the first.

Table 3.1 presents the error rate and average time for $\alpha_\ell = -3$ versus $\alpha_r \in \{-2, -4, \dots, -20\}$. It is noted that from $\alpha_r = -6$ up to $\alpha_r = -20$ all methods display an error rate of 0%, and that as α_r becomes closer to α_ℓ the error rate increases considerably for the methods **TPE** and **T. Variance**. The error rate of the **M. Gambini** is only 0.1% with $\alpha_r = -4$. **T. Kruskal** and **T. Mann-Whitney** have the best performance since the percentage of error is 0% for all different values of α_r . The different execution times between the non-parametric and the **M. Gambini** methods are noticeable, the latter being approximately 74 times slower than **T. Variance**, which presents the slowest times among the non-parametric methods.

Figure 3.3, left, shows that the average execution time of **M. Gambini** diminishes as the value of α_r increases. Figure 3.3, right, shows the behavior of the average times of the non-parametric methods, which were always less than a second, being **T. Kruskal** the one exhibiting the shortest execution times followed by **T. Mann-Whitney**.

	M. Gambini		TPE		T. Kruskal		T. Variance		T. M-Whitney	
α_r	Error rate	Time	Error rate	Time	Error rate	Time	Error rate	Time	Error rate	Time
-20	0.00%	1.415	0.00%	0.012	0.00%	0.002	0.00%	0.015	0.00%	0.003
-19	0.00%	1.401	0.00%	0.012	0.00%	0.002	0.00%	0.015	0.00%	0.003
-18	0.00%	1.376	0.00%	0.012	0.00%	0.002	0.00%	0.015	0.00%	0.003
-17	0.00%	1.362	0.00%	0.012	0.00%	0.002	0.00%	0.015	0.00%	0.003
-16	0.00%	1.352	0.00%	0.012	0.00%	0.002	0.00%	0.015	0.00%	0.003
-15	0.00%	1.338	0.00%	0.012	0.00%	0.002	0.00%	0.015	0.00%	0.003
-14	0.00%	1.307	0.00%	0.012	0.00%	0.002	0.00%	0.015	0.00%	0.003
-13	0.00%	1.287	0.00%	0.012	0.00%	0.002	0.00%	0.015	0.00%	0.003
-12	0.00%	1.275	0.00%	0.012	0.00%	0.002	0.00%	0.015	0.00%	0.003
-11	0.00%	1.257	0.00%	0.012	0.00%	0.002	0.00%	0.015	0.00%	0.003
-10	0.00%	1.238	0.00%	0.012	0.00%	0.002	0.00%	0.015	0.00%	0.003
-9	0.00%	1.221	0.00%	0.012	0.00%	0.002	0.00%	0.015	0.00%	0.003
-8	0.00%	1.198	0.00%	0.012	0.00%	0.002	0.00%	0.015	0.00%	0.003
-7	0.00%	1.189	0.10%	0.012	0.00%	0.002	0.00%	0.015	0.00%	0.003
-6	0.00%	1.168	0.00%	0.012	0.00%	0.002	0.00%	0.015	0.00%	0.003
-5	0.00%	1.158	0.40%	0.012	0.00%	0.002	0.60%	0.015	0.00%	0.003
-4	0.10%	1.140	15.40%	0.012	0.00%	0.002	16.90%	0.015	0.00%	0.003
-2	0.00%	1.101	2.80%	0.012	0.00%	0.002	9.30%	0.015	0.00%	0.003

Table 3.1: Error rate and average time for $\alpha_\ell = -3$ vs. $\alpha_r \in \{-2, -4, -5, \dots, -19, -20\}$ when $n = 1$

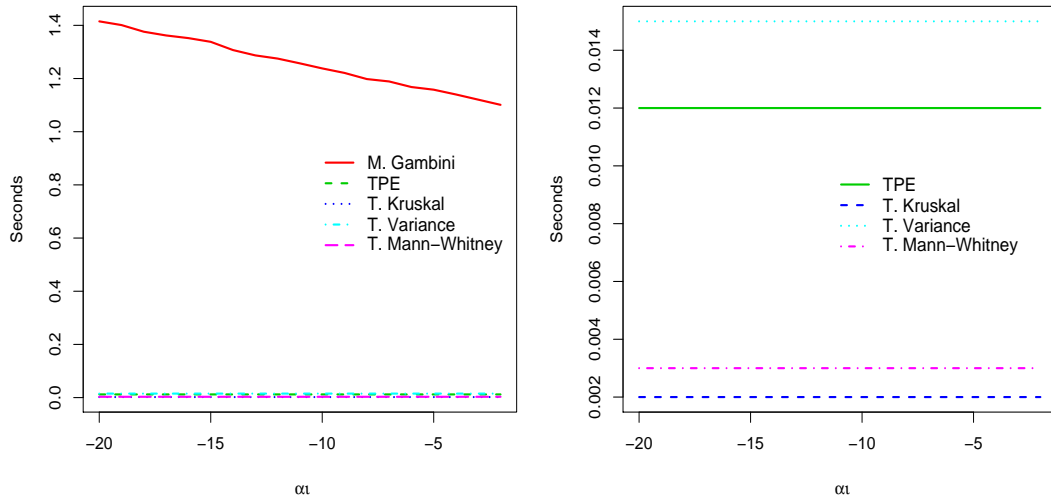


Figure 3.3: Average execution time in seconds for Gambini, Kruskal, Mann-Whitney, Variance and TPE, $\alpha_\ell = -3$ vs. $\alpha_r \in \{-2, -4, -5, \dots, -19, -20\}$ with $n = 1$

3.2 Heterogeneous areas with $n = 1$ and $\alpha_\ell = -8$

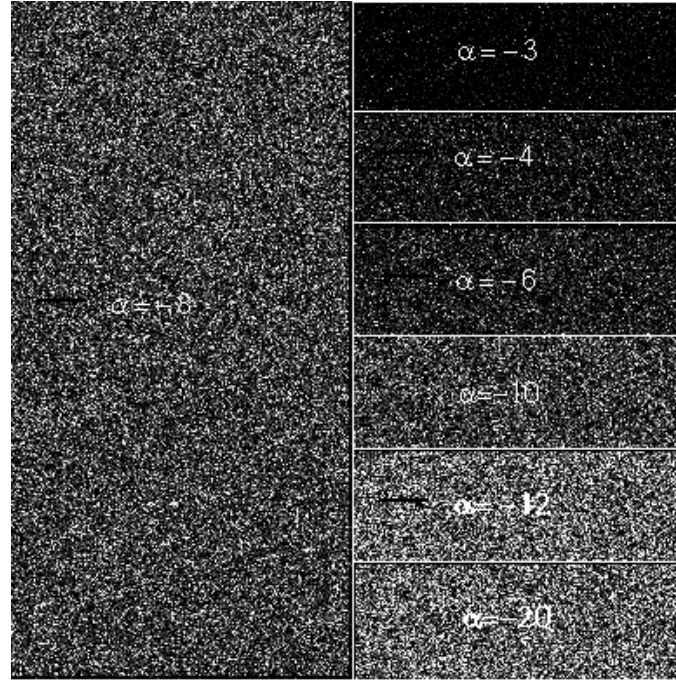


Figure 3.4: Synthetic images from $\mathcal{G}_1^0(\alpha, 1, 1)$, $\gamma = 1$ and $\alpha_\ell = -8$ to the left against $\alpha_r = \{-3, -4, -6, -10, -12, -20\}$ to the right

Figure 3.4, left, is an image formed by samples from the $\mathcal{G}_1^0(-8, 1, 1)$, representing heterogeneous areas. Figure 3.4, right, presents samples from the $\mathcal{G}_j^0(\alpha_r, 1, 1)$ distribution with $\alpha_r = -4$ up to $\alpha_r = -20$ representing areas with different degrees of roughness.

Table 3.2 presents the error rate and average time of the different methods for $n = 1$, $\alpha_\ell = -8$. Note that the percentages achieved by **TPE** and **T. Variance** are greater than zero when α_r comes closer to α_ℓ , reaching the greatest value when $\alpha_r = -9$ (81.0% **TPE** and 64.5% **T. Variance**). Regarding the Average execution time, we see that the difference between **M. Gambini** and the non-parametric methods is kept as described in Section 3.1.

	M. Gambini		TPE		T. Kruskal		T. Variance		T. M-Whitney	
α_r	Error rate	Time	Error rate	Time	Error rate	Time	Error rate	Time	Error rate	Time
-20	0.00%	1.513	0.00%	0.012	0.00%	0.002	0.00%	0.015	0.00%	0.003
-19	0.00%	1.519	0.00%	0.012	0.00%	0.002	0.00%	0.015	0.00%	0.003
-18	0.00%	1.502	0.00%	0.012	0.00%	0.002	0.00%	0.015	0.00%	0.003
-17	0.00%	1.469	0.00%	0.012	0.00%	0.002	0.00%	0.015	0.00%	0.003
-16	0.00%	1.449	0.00%	0.012	0.00%	0.002	0.00%	0.015	0.00%	0.003
-15	0.00%	1.440	0.20%	0.012	0.00%	0.002	0.00%	0.015	0.00%	0.003
-14	0.00%	1.414	0.50%	0.012	0.00%	0.002	0.00%	0.014	0.00%	0.003
-13	0.00%	1.419	2.70%	0.012	0.00%	0.002	0.20%	0.015	0.00%	0.003
-12	0.00%	1.396	6.50%	0.012	0.00%	0.002	1.20%	0.015	0.00%	0.003
-11	0.10%	1.385	14.20%	0.012	0.20%	0.002	6.20%	0.015	0.20%	0.003
-10	0.50%	1.406	33.80%	0.012	1.60%	0.002	26.50%	0.015	1.60%	0.003
-9	16.20%	1.389	81.00%	0.012	22.40%	0.002	64.50%	0.015	22.40%	0.003
-7	11.20%	1.353	73.30%	0.012	12.20%	0.002	61.30%	0.015	12.80%	0.003
-6	0.00%	1.292	21.60%	0.012	0.50%	0.002	11.40%	0.015	0.50%	0.003
-5	0.00%	1.242	3.80%	0.012	0.00%	0.002	0.60%	0.015	0.00%	0.003
-4	0.00%	1.214	0.10%	0.012	0.00%	0.002	0.00%	0.015	0.00%	0.003
-3	0.00%	1.196	0.00%	0.012	0.00%	0.002	0.00%	0.014	0.00%	0.003
-2	0.00%	1.175	0.00%	0.012	0.00%	0.002	0.10%	0.015	0.00%	0.003

Table 3.2: Error rate and average time for, $\alpha_\ell = -8$ vs. $\alpha_r \in \{-2, -3, -5, \dots, -19, -20\}$ with $n = 1$

The performance of M. Gambini, T. Kruskal and T. Mann-Whitney are similar regarding their error rates, e.g., they are equal to 0% when $\alpha_r \leq -12$ and when $\alpha_r > -6$. Their error rates increase when α_r approaches α_ℓ , up to 16.2% for M. Gambini and 22.4% for T. Kruskal and T. Mann-Whitney, when $\alpha_r = -9$. These three methods present the best behavior for $n = 1$ and $\alpha_\ell = -8$ with respect to error.

Figure 3.5 shows the behavior of the error generated by different methods under consideration. Note that the smallest percentages are generated by M. Gambini, T. Kruskal and T. Mann-Whitney.

Figure 3.6, left, shows that the average time of the execution of M. Gambini has the same behavior observed in the $\alpha_\ell = -3$ situation (Section 3.1). The plot to the right of Figure 3.6 presents the behavior of the average times of the non-parametrics methods, which continue being shorter than the former second. T. Kruskal is the

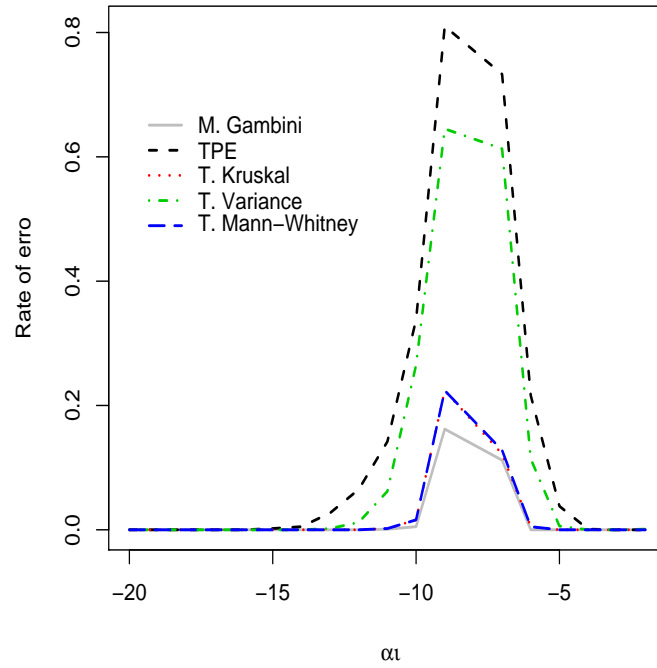


Figure 3.5: Error rate in edge detection for Gambini, Kruskal, Mann-Whitney, Variance and TPE, $\alpha_\ell = -8$ vs. $\alpha_r \in \{-2, -4, -5, \dots, -19, -20\}$ with $n = 1$

method that obtains the shortest execution times, followed by **Mann-Whitney**.

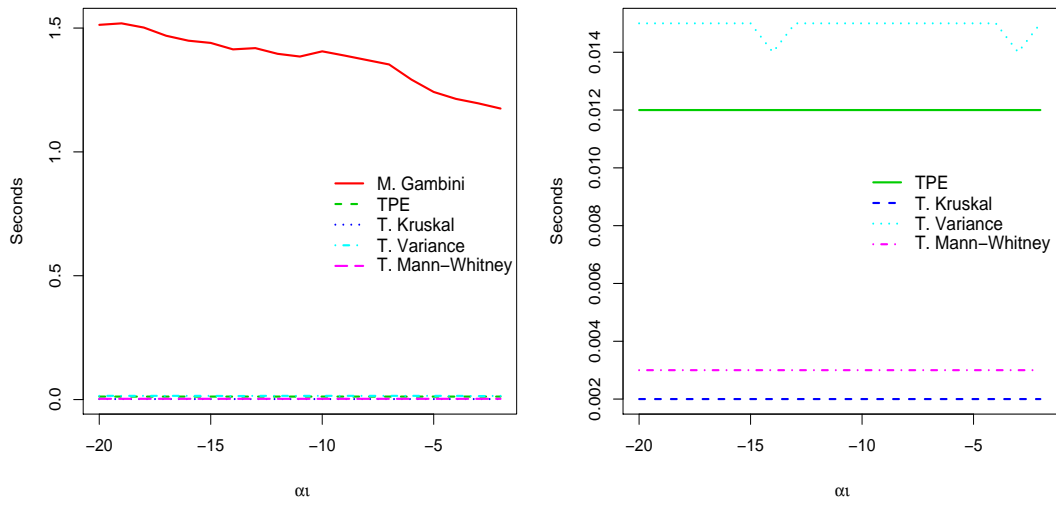


Figure 3.6: Average execution time in seconds for Gambini, Kruskal, Mann-Whitney, Variance and TPE, $\alpha_\ell = -8$ vs. $\alpha_r \in \{-2, -4, -5, \dots, -19, -20\}$ with $n = 1$

3.3 Homogeneous areas with $n = 1$ and $\alpha_\ell = -12$

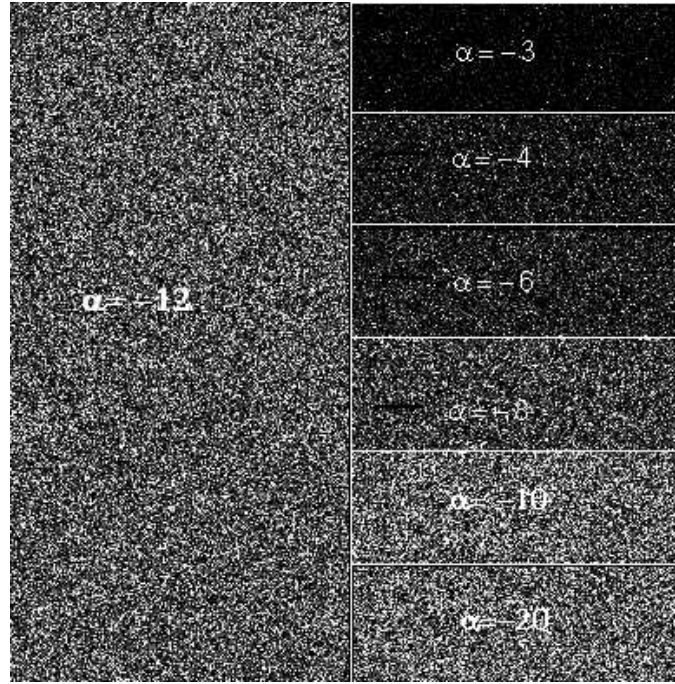


Figure 3.7: Synthetic images from $\mathcal{G}_1^0(\alpha, 1, 1)$, $\gamma = 1$ and $\alpha_\ell = -12$ to the left against $\alpha_r = \{-3, -4, -6, -8, -10, -20\}$ to the right

Figure 3.7, left, is an image formed by samples from the $\mathcal{G}_1^0(-12, 1, 1)$, representing homogeneous areas. Figure 3.7, right, presents samples from the $\mathcal{G}_1^0(\alpha_r, 1, 1)$ distribution with $\alpha_r = -3$ up to $\alpha_r = -20$ representing areas with different degrees of roughness. Table 3.3 contain the percentages of error and average time for $n = 1$, $\alpha_\ell = -12$. We note that the **TPE** method presents high rates of error for almost all values of α_r and that it only gets an error rate equal to zero when $\alpha_r \geq -5$. **M. Gambini**, **T. Kruskal** and **T. Mann-Whitney** display similar behaviors, but **M. Gambini** presents smaller percentages of error. When $\alpha_r = -11$ the method with greater percentage of error is **TPE** with 90.6%, the method with the smallest percentage of error is **M. Gambini** with (40.3%). In the average execution time we noted the difference in the times of execution between the non-parametrics methods and **M. Gambini**, the latter being approximately 626 times slower than by

T. Kruskal for $\alpha_r = -2$, and 823 times slower for $\alpha_r = -20$.

α_r	M. Gambini		TPE		T. Kruskal		T. Variance		T. M-Whitney	
	Error rate	Time	Error rate	Time	Error rate	Time	Error rate	Time	Error rate	Time
-20	0.00%	1.646	1.10%	0.012	0.00%	0.002	0.00%	0.015	0.00%	0.003
-19	0.00%	1.640	3.00%	0.012	0.00%	0.002	0.20%	0.015	0.00%	0.003
-18	0.00%	1.609	7.10%	0.012	0.00%	0.002	0.60%	0.015	0.00%	0.003
-17	0.00%	1.612	13.50%	0.012	0.20%	0.002	4.40%	0.015	0.20%	0.003
-16	0.00%	1.634	23.50%	0.012	0.40%	0.002	12.50%	0.015	0.40%	0.003
-15	0.80%	1.608	39.00%	0.012	1.60%	0.002	27.70%	0.015	1.60%	0.003
-14	6.90%	1.598	67.70%	0.012	11.30%	0.002	48.30%	0.015	11.30%	0.003
-13	40.30%	1.622	92.50%	0.012	45.90%	0.002	75.90%	0.015	45.40%	0.003
-11	38.30%	1.544	90.60%	0.012	40.70%	0.002	76.00%	0.015	41.20%	0.003
-10	3.20%	1.512	53.90%	0.012	5.80%	0.002	45.10%	0.015	5.80%	0.003
-9	0.00%	1.469	23.90%	0.012	0.20%	0.002	11.80%	0.015	0.20%	0.003
-8	0.00%	1.399	9.00%	0.012	0.00%	0.002	1.30%	0.014	0.00%	0.003
-7	0.00%	1.387	2.10%	0.012	0.00%	0.002	0.00%	0.015	0.00%	0.003
-6	0.00%	1.343	0.20%	0.012	0.00%	0.002	0.00%	0.015	0.00%	0.003
-5	0.00%	1.315	0.00%	0.012	0.00%	0.002	0.00%	0.015	0.00%	0.003
-4	0.00%	1.281	0.00%	0.012	0.00%	0.002	0.00%	0.015	0.00%	0.003
-3	0.00%	1.277	0.00%	0.012	0.00%	0.002	0.00%	0.015	0.00%	0.003
-2	0.00%	1.252	0.00%	0.012	0.00%	0.002	0.00%	0.015	0.00%	0.003

Table 3.3: Error rate and average time for $\alpha_\ell = -12$ vs. $\alpha_r \in \{-2, -3, -5, \dots, -19, -20\}$ with $n = 1$

Figure 3.8 shows the behavior of the percentages of error generated by different methods under consideration for $\alpha_\ell = -12$ and $n = 1$; it is observed that the greater percentages of error are generated by **TPE** and **T. Variance**.

M. Gambini, **T. Kruskal** and **Mann-Whitney** have similar behaviors, and differ when α_r is near α_ℓ .

Figure 3.9, left, shows that the average execution time of the **M. Gambini** diminishes as the value of α_r increases. Figure 3.9, right, shows the behavior of the average execution times of the non-parametrics methods. The **T. Kruskal** has the smallest execution time followed by **T. Mann-Whitney**, the execution time of the non-parametrics methods are not sensitive to the value of α_r .

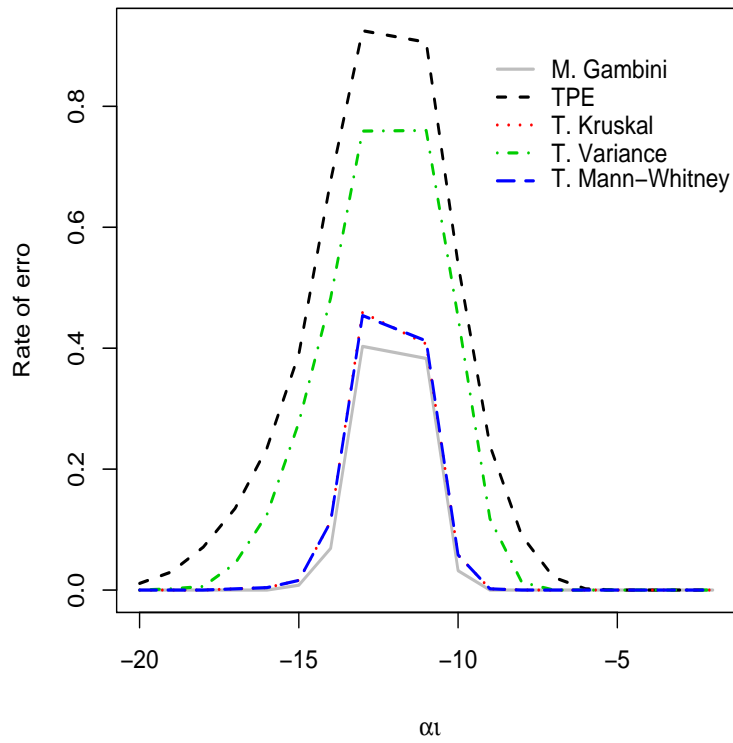


Figure 3.8: Error rate in edge detection for Gambini, Kruskal, Mann-Whitney, Variance and TPE, $\alpha_\ell = -12$ vs. $\alpha_r \in \{-2, -4, -5, \dots, -19, -20\}$ with $n = 1$

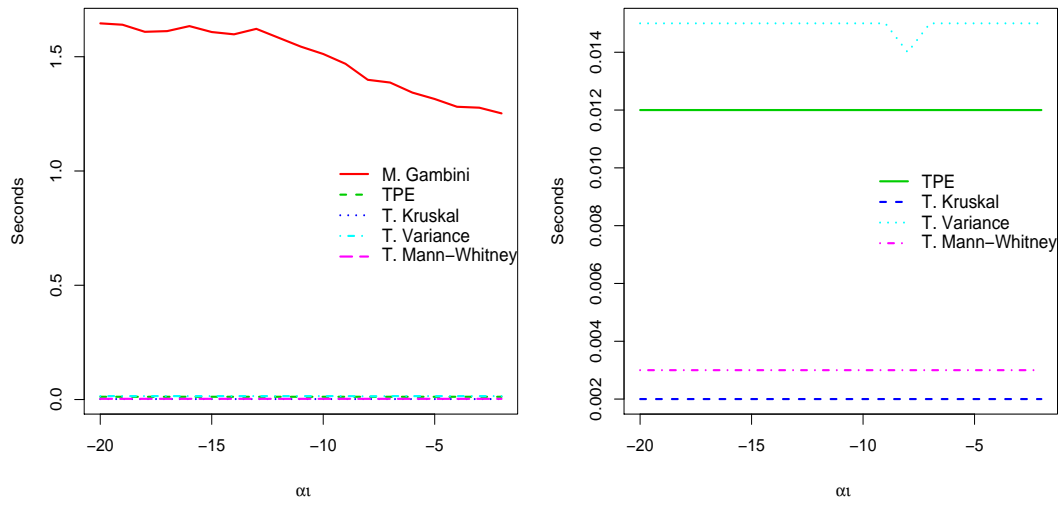


Figure 3.9: Average execution time in seconds for Gambini, Kruskal, Mann-Whitney, Variance and TPE, $\alpha_\ell = -12$ vs. $\alpha_r \in \{-2, -4, -5, \dots, -19, -20\}$ with $n = 1$

3.4 Homogeneous areas with $n = 1$ and $\alpha_\ell = -18$

In the left side of Figure 3.10 we find an image generated from $\mathcal{G}_1^0(-18, 1, 1)$, which represents homogeneous areas, and on the right side there are images generated with $\alpha_r = -4$ up to $\alpha_r = -20$, that represent areas with different degrees of roughness.

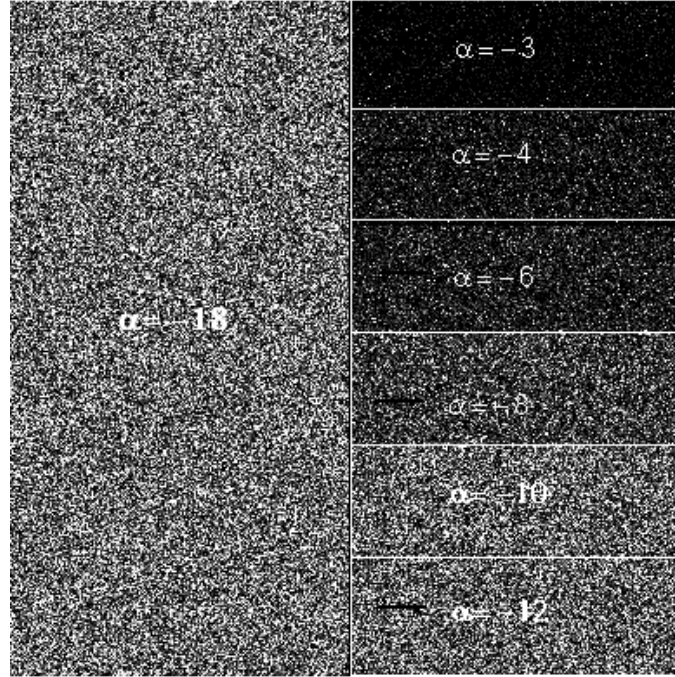


Figure 3.10: Synthetic images $\mathcal{G}_1^0(\alpha, 1, 1)$, $\gamma = 1$ and $\alpha_\ell = -18$ to the left against $\alpha_r = \{-3, -4, -6, -8, -10, -12\}$ to the right

Table 3.4 contains the error rate and average time of the methods under evaluation for $\alpha_\ell = -18$. We note that **M. Gambini**, **T. Kruskal** and **T. Mann-Whitney** present percentage of error zero in the cases for which the image to the right of the edge is generated from $\alpha_r \geq -13$; the error rate increases as α_r approaches α_ℓ . Note also that the highest percentage of error of these methods occurs for $\alpha_r = -17$ and $\alpha_r = -19$, however, this error rate is lower in comparison with **T. Variance** and **TPE**.

TPE presents zero error rate when α_r is a distant from α_ℓ , but this percentage begins to increase when α_r approaches $\alpha_\ell = -18$, reaching 98% when $\alpha_r = -17$.

T. Variance behaves similarly to **TPE**. The **T. Mann-Whitney** presented error rate similarly to **T. Kruskal**.

Note that the average execution time of **T. Kruskal** is approximately 1000 times smaller than that of **M. Gambini** when $\alpha_r = -19$. Figure 3.12 shows that the runtime of **M. Gambini** decreases when α_r is close to zero, but it does not get close to the times of the non-parametrics methods. The faster method is **T. Kruskal** followed by **T. Mann-Whitney**; the slower method is **T. Variance**, which, however, never exceeds 0,015 second.

α_r	M. Gambini		TPE		T. Kruskal		T. Variance		T. M-Whitney	
	Error rate	Time	Error rate	Time	Error rate	Time	Error rate	Time	Error rate	Time
-20	23.80%	1.995	84.40%	0.012	24.20%	0.002	67.50%	0.015	24.20%	0.003
-19	64.40%	2.013	97.50%	0.012	65.00%	0.002	79.40%	0.015	64.90%	0.003
-17	62.70%	1.893	98.00%	0.012	63.60%	0.002	79.60%	0.015	63.80%	0.003
-16	19.70%	1.853	83.50%	0.012	21.40%	0.002	62.10%	0.015	21.40%	0.003
-15	2.60%	1.777	56.30%	0.012	4.00%	0.002	39.40%	0.015	4.10%	0.003
-14	0.30%	1.746	33.30%	0.012	0.90%	0.002	18.80%	0.015	0.90%	0.003
-13	0.00%	1.669	17.50%	0.012	0.00%	0.002	4.10%	0.015	0.00%	0.003
-12	0.00%	1.638	7.00%	0.012	0.00%	0.002	1.00%	0.015	0.00%	0.003
-11	0.00%	1.600	2.70%	0.012	0.00%	0.002	0.20%	0.015	0.00%	0.003
-10	0.00%	1.564	0.40%	0.012	0.00%	0.002	0.00%	0.015	0.00%	0.003
-9	0.00%	1.538	0.50%	0.012	0.00%	0.002	0.00%	0.015	0.00%	0.003
-8	0.00%	1.508	0.00%	0.012	0.00%	0.002	0.00%	0.015	0.00%	0.003
-7	0.00%	1.495	0.00%	0.012	0.00%	0.002	0.00%	0.015	0.00%	0.003
-6	0.00%	1.461	0.00%	0.012	0.00%	0.002	0.00%	0.015	0.00%	0.003
-5	0.00%	1.436	0.00%	0.012	0.00%	0.002	0.00%	0.015	0.00%	0.003
-4	0.00%	1.406	0.00%	0.012	0.00%	0.002	0.00%	0.015	0.00%	0.003
-3	0.00%	1.404	0.00%	0.012	0.00%	0.002	0.00%	0.015	0.00%	0.003
-2	0.00%	1.387	0.00%	0.012	0.00%	0.002	0.00%	0.015	0.00%	0.003

Table 3.4: Error rate and average time for, $\alpha_\ell = -18$ vs. $\alpha_r \in \{-2, -3, -5, \dots, -19, -20\}$ with $n = 1$

Figure 3.11 shows **T. Kruskal** and **T. Mann-Whitney** behaves similarly to **M. Gambini**, these three methods are the best performing over. All methods present error in the detection of the edge when the generated images come from distributions with very nearby parameters of roughness.

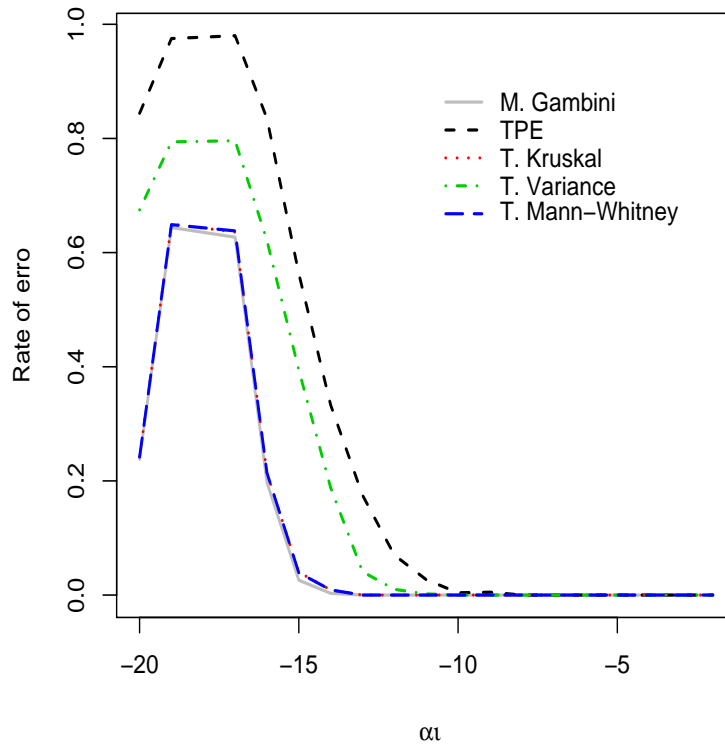


Figure 3.11: Error rate for Gambini, Kruskal, Mann-Whitney, Variance and TPE, $\alpha_\ell = -18$ vs. $\alpha_r \in \{-2, -4, -5, \dots, -19, -20\}$ with $n = 1$

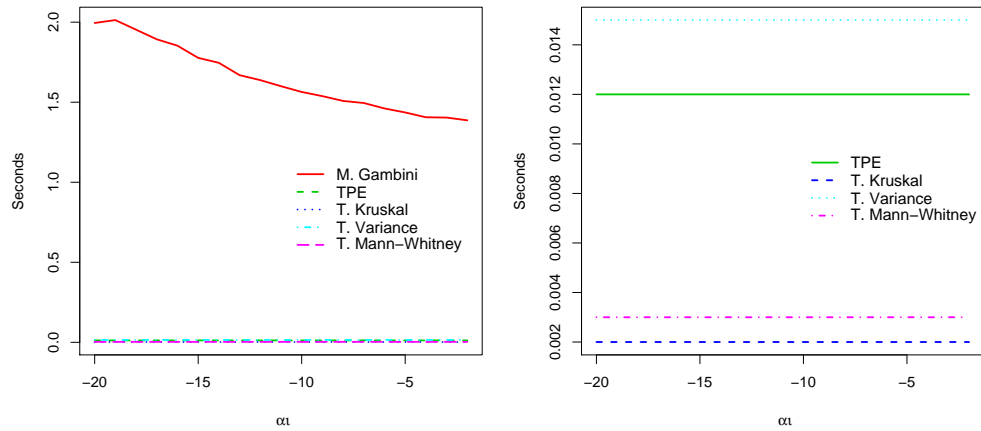


Figure 3.12: Average execution time in seconds for Gambini, Kruskal, Mann-Whitney, Variance and TPE, $\alpha_\ell = -18$ vs. $\alpha_r \in \{-2, -4, -5, \dots, -19, -20\}$ with $n = 1$

3.5 Extremely heterogeneous areas with $n = 3$ and $\alpha_\ell = -3$

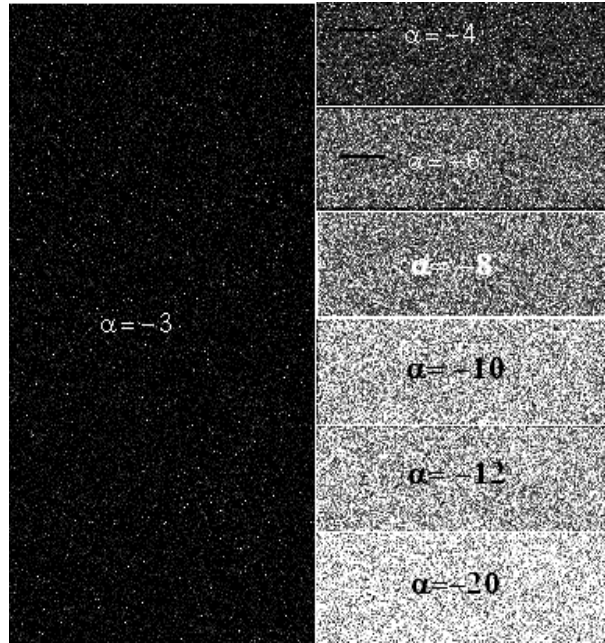


Figure 3.13: Synthetic images $\mathcal{G}_I^0(\alpha, 1, 3)$, $\gamma = 1$ and $\alpha_\ell = -3$ to the left against $\alpha_r = \{-4, -6, -8, -10, -12, -20\}$ to the right

Figure 3.13 shows images of samples generated from $\mathcal{G}_I^0(\alpha, 1, 3)$ with different values of α . On the left side of the figure we find an image generated from $\mathcal{G}_I^0(-3, 1, 3)$.

Table 3.5 presents the error rate and average time obtained by the methods used in the simulation. Note that the percentages of errors of all methods are zero except for method **T. Variance** which presents error rates of 5.9%, 3.4% and 0.3% for $\alpha_r = -5, -4$ and -2 , respectively. In Table 3.5 it is noteworthy the difference in execution times between non-parametrics methods and **M. Gambini**. The **T. Kruskal** is 545 times faster than **M. Gambini**, for $\alpha_r = -2$. Figure 3.14, left, shows that the average execution time of the **M. Gambini** decreases as the value of α_r increases.

Figure 3.14, right, shows that **T. Kruskal** has the smaller execution times, followed by the method of **T. Mann-Whitney**.

	M. Gambini		TPE		T. Kruskal		T. Variance		T. M-Whitney	
α_r	Error rate	Time	Error rate	Time	Error rate	Time	Error rate	Time	Error rate	Time
-20	0.00%	1.252	0.00%	0.012	0.00%	0.002	0.00%	0.015	0.00%	0.003
-19	0.00%	1.216	0.00%	0.012	0.00%	0.002	0.00%	0.015	0.00%	0.003
-18	0.00%	1.205	0.00%	0.012	0.00%	0.002	0.00%	0.014	0.00%	0.003
-17	0.00%	1.355	0.00%	0.012	0.00%	0.002	0.00%	0.015	0.00%	0.003
-16	0.00%	1.144	0.00%	0.012	0.00%	0.002	0.00%	0.015	0.00%	0.003
-15	0.00%	1.136	0.00%	0.012	0.00%	0.002	0.00%	0.015	0.00%	0.003
-14	0.00%	1.132	0.00%	0.012	0.00%	0.002	0.00%	0.015	0.00%	0.003
-13	0.00%	1.141	0.00%	0.012	0.00%	0.002	0.00%	0.015	0.00%	0.003
-12	0.00%	1.151	0.00%	0.012	0.00%	0.002	0.00%	0.015	0.00%	0.003
-11	0.00%	1.137	0.00%	0.012	0.00%	0.002	0.00%	0.015	0.00%	0.003
-10	0.00%	1.127	0.00%	0.012	0.00%	0.002	0.00%	0.014	0.00%	0.003
-9	0.00%	1.127	0.00%	0.012	0.00%	0.002	0.00%	0.015	0.00%	0.003
-8	0.00%	1.149	0.00%	0.012	0.00%	0.002	0.00%	0.015	0.00%	0.003
-7	0.00%	1.142	0.00%	0.012	0.00%	0.002	0.00%	0.015	0.00%	0.003
-6	0.00%	1.127	0.00%	0.012	0.00%	0.002	0.00%	0.015	0.00%	0.003
-5	0.00%	1.137	0.00%	0.012	0.00%	0.002	0.30%	0.015	0.00%	0.003
-4	0.00%	1.117	0.00%	0.012	0.00%	0.002	3.40%	0.015	0.00%	0.003
-2	0.00%	1.090	0.00%	0.012	0.00%	0.002	5.90%	0.015	0.00%	0.003

Table 3.5: Error rate and average time for, $\alpha_\ell = -3$ vs. $\alpha_r \in \{-2, -4, -5, \dots, -19, -20\}$ with $n = 3$

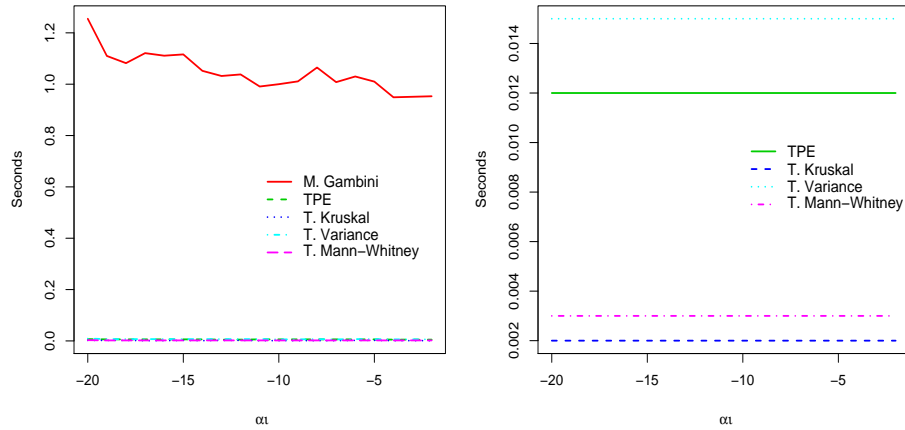


Figure 3.14: Average execution time for Gambini, Kruskal, Mann-Whitney, Variance and TPE, $\alpha_\ell = -3$ vs. $\alpha_r \in \{-2, -4, -5, \dots, -19, -20\}$ with $n = 3$

3.6 Heterogeneous areas with $n = 3$ and $\alpha_\ell = -8$

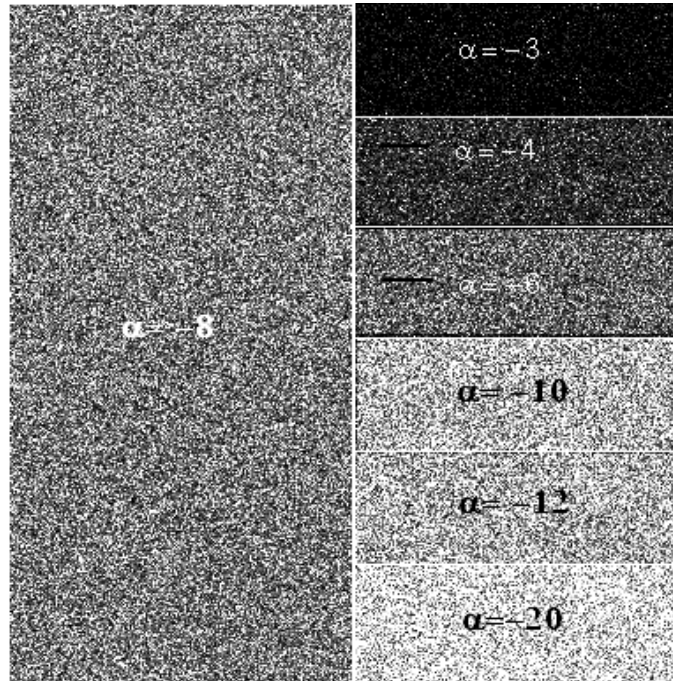


Figure 3.15: Synthetic images $\mathcal{G}_I^0(\alpha, 1, 3)$, $\gamma = 1$ and $\alpha_\ell = -8$ to the left against $\alpha_r = \{-3, -4, -6, -10, -12, -20\}$ to the right

Table 3.6 contains the percentages of error and average time for $\alpha_\ell = -8$, $n = 3$. We note that **T. Kruskal**, **T. Mann-Whitney** and **M. Gambini** do not present errors for any α_r , which makes the best behavior. **TPE** has 58% of error for $\alpha_r = 9$ and 12% for $\alpha_r = -7$; for the other values of α_r the percentage of error is zero; the method **TPE** has difficulties in finding the edge when α_r is very close to α_ℓ . The method **T. Variance** presents large percentages of error around α_ℓ .

Figure 3.16 compares the behavior of the percentages of error generated by the different methods in study. Note that the greater percentages of error are generated by **TPE** and **T. Variance**. The methods with better behavior are **M. Gambini**, **T. Kruskal** and **T. Mann-Whitney** because they have zero error rate.

Table 3.6 shows that **M. Gambini** continues to display the largest execution times. **T. Kruskal** is approximately 578 times faster than the **M. Gambini** for

	M. Gambini		TPE		T. Kruskal		T. Variance		T. M-Whitney	
α_r	Error rate	Time	Error rate	Time	Error rate	Time	Error rate	Time	Error rate	Time
-20	0.00%	1.351	0.00%	0.012	0.00%	0.002	0.00%	0.015	0.00%	0.003
-19	0.00%	1.186	0.00%	0.012	0.00%	0.002	0.00%	0.015	0.00%	0.003
-18	0.00%	1.229	0.00%	0.012	0.00%	0.002	0.00%	0.015	0.00%	0.003
-17	0.00%	1.277	0.00%	0.012	0.00%	0.002	0.00%	0.015	0.00%	0.003
-16	0.00%	1.268	0.00%	0.012	0.00%	0.002	0.00%	0.015	0.00%	0.003
-15	0.00%	1.506	0.00%	0.012	0.00%	0.002	0.00%	0.015	0.00%	0.003
-14	0.00%	1.231	0.00%	0.012	0.00%	0.002	0.00%	0.015	0.00%	0.003
-13	0.00%	1.196	0.00%	0.012	0.00%	0.002	0.00%	0.015	0.00%	0.003
-12	0.00%	1.232	0.00%	0.012	0.00%	0.002	0.00%	0.015	0.00%	0.003
-11	0.00%	1.262	0.00%	0.012	0.00%	0.002	0.40%	0.015	0.00%	0.003
-10	0.00%	1.252	0.00%	0.012	0.00%	0.002	20.90%	0.015	0.00%	0.003
-9	0.00%	1.279	57.90%	0.012	0.00%	0.002	32.20%	0.015	0.00%	0.003
-7	0.00%	1.269	11.90%	0.012	0.00%	0.002	48.80%	0.015	0.00%	0.003
-6	0.00%	1.237	0.00%	0.012	0.00%	0.002	3.00%	0.015	0.00%	0.003
-5	0.00%	1.172	0.00%	0.012	0.00%	0.002	0.00%	0.015	0.00%	0.003
-4	0.00%	1.141	0.00%	0.012	0.00%	0.002	0.00%	0.015	0.00%	0.003
-3	0.00%	1.136	0.00%	0.012	0.00%	0.002	0.00%	0.015	0.00%	0.003
-2	0.00%	1.157	0.00%	0.012	0.00%	0.002	0.20%	0.015	0.00%	0.003

Table 3.6: Error rate and average time for, $\alpha_\ell = -8$ vs. $\alpha_r \in \{-2, -4, -5, \dots, -19, -20\}$ with $n = 3$

$\alpha_r = -2$ and 675 times faster when $\alpha_r = -20$.

Figure 3.17 corroborates the behavior of the execution times of M. Gambini. The execution times of the non-parametric methods are almost constant when α_r varies, the fastest method being T. Kruskal, followed by the method of T. Mann-Whitney.

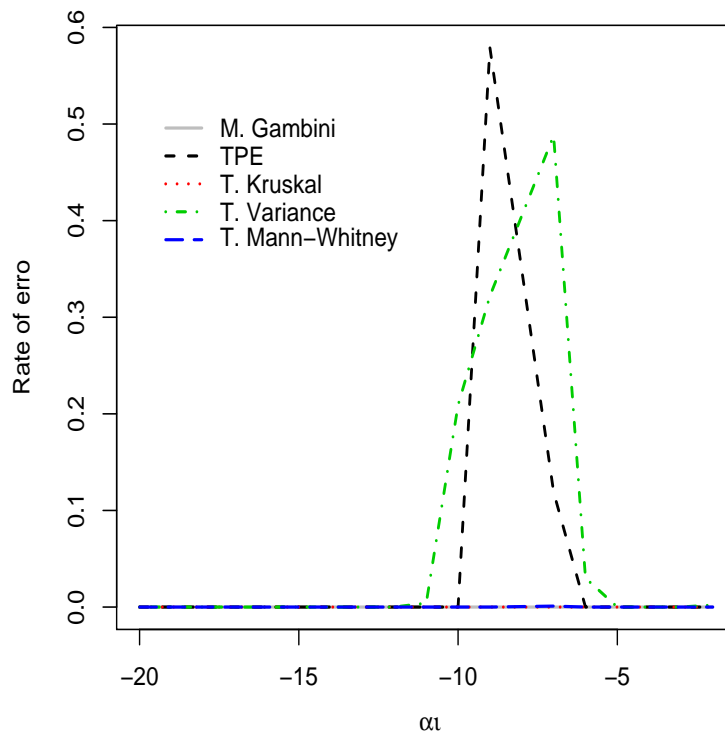


Figure 3.16: Error rate in edge detection for Gambini, Kruskal, Mann-Whitney, Variance and TPE, $\alpha_\ell = -8$ vs. $\alpha_r \in \{-2, -4, -5, \dots, -19, -20\}$ with $n = 3$

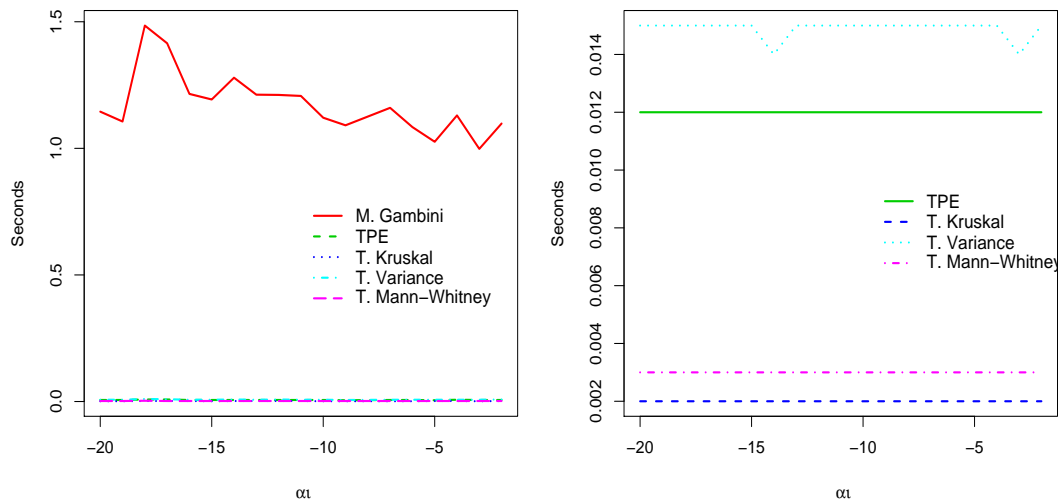


Figure 3.17: Average execution time in seconds for Gambini, Kruskal, Mann-Whitney, Variance and TPE, $\alpha_\ell = -8$ vs. $\alpha_r \in \{-2, -4, -5, \dots, -19, -20\}$ with $n = 3$

3.7 Homogeneous areas with $n = 3$ and $\alpha_\ell = -12$

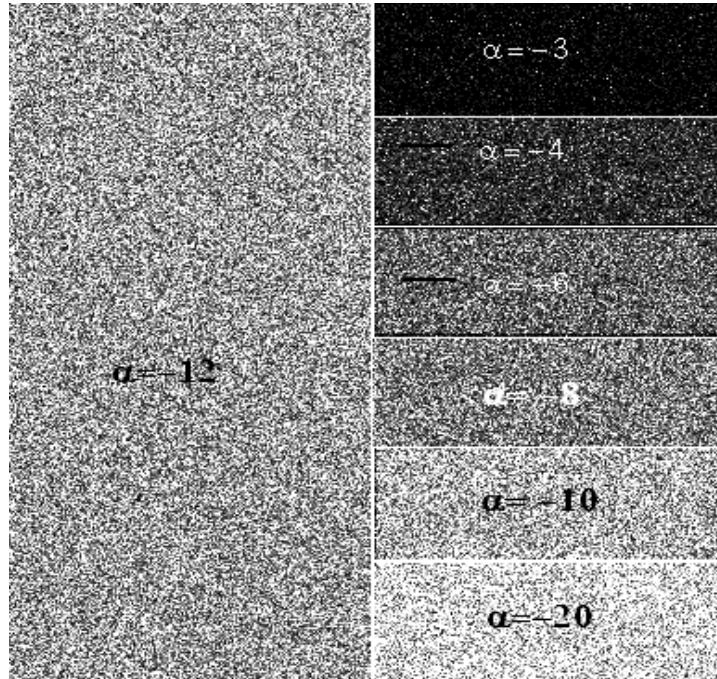


Figure 3.18: Synthetic images from $\mathcal{G}_I^0(\alpha, 1, 3)$, $\gamma = 1$ and $\alpha_\ell = -12$ to the left against $\alpha_r = \{-3, -4, -6, -8, -10, -20\}$ to the right

Figure 3.18 shows images of samples generated from $\mathcal{G}_I^0(\alpha, 1, 3)$ and different values of the parameter α and $\gamma = 1$. The image at the left side of the figure generated from $\mathcal{G}_I^0(-12, 1, 3)$ which represents homogeneous areas.

The table 3.7 contains the error rate and average time for $\alpha_\ell = -12$, $n = 3$ and different values of α_r . Note that **M. Gambini**, **T. Kruskal** and **T. Mann-Whitney** are the best performing over. The **M. Gambini** has the smallest percentage of error when $\alpha_r = -13$, and the largest percentage of error when $\alpha_r = -11$ with 26%. For $\alpha_r = -14$, the methods with the best behavior are **T. Kruskal** and **M. Gambini** followed by **T. Mann-Whitney**. The **T. Variance** presents 89% of error when $\alpha_r = -11$ and 50% when $\alpha_r = -13$, with which this method presents under performance.

	M. Gambini		TPE		T. Kruskal		T. Variance		T. M-Whitney	
α_r	Error rate	Time	Error rate	Time	Error rate	Time	Error rate	Time	Error rate	Time
-20	0.00%	1.555	0.00%	0.006	0.00%	0.001	0.00%	0.007	0.00%	0.002
-19	0.00%	1.963	0.00%	0.006	0.00%	0.001	0.00%	0.007	0.00%	0.002
-18	0.00%	1.509	0.00%	0.006	0.00%	0.002	0.00%	0.008	0.00%	0.002
-17	0.00%	1.598	0.00%	0.007	0.00%	0.002	0.00%	0.009	0.00%	0.003
-16	0.00%	1.639	0.00%	0.008	0.00%	0.002	0.00%	0.009	0.00%	0.003
-15	0.00%	1.636	2.00%	0.007	0.00%	0.002	21.50%	0.008	0.00%	0.002
-14	0.40%	1.452	1.50%	0.007	0.10%	0.002	22.50%	0.009	0.10%	0.002
-13	14.90%	1.430	49.50%	0.007	31.50%	0.002	50.30%	0.008	31.60%	0.002
-11	26.40%	1.491	41.70%	0.007	24.50%	0.002	88.80%	0.008	25.20%	0.002
-10	0.00%	1.417	71.20%	0.006	0.00%	0.002	16.40%	0.008	0.00%	0.002
-9	0.00%	1.448	0.00%	0.006	0.00%	0.001	0.00%	0.008	0.00%	0.002
-8	0.00%	1.405	0.00%	0.007	0.00%	0.002	0.10%	0.009	0.00%	0.002
-7	0.00%	1.315	0.00%	0.007	0.00%	0.002	0.00%	0.008	0.00%	0.002
-6	0.00%	1.098	0.00%	0.005	0.00%	0.002	0.00%	0.007	0.00%	0.002
-5	0.00%	1.038	0.00%	0.005	0.00%	0.001	0.00%	0.006	0.00%	0.002
-4	0.00%	1.074	0.00%	0.005	0.00%	0.001	0.00%	0.006	0.00%	0.002
-3	0.00%	0.982	0.00%	0.005	0.00%	0.002	0.00%	0.006	0.00%	0.002
-2	0.00%	0.938	0.00%	0.006	0.00%	0.001	0.10%	0.006	0.00%	0.002

Table 3.7: Error rate and average time for, $\alpha_\ell = -12$ vs. $\alpha_r \in \{-2, -4, -5, \dots, -19, -20\}$ with $n = 3$

Figure 3.19 shows the behavior of the different methods according to the percentage of error generated in the detection of edges. Note that the method with the best behavior is the **M. Gambini** followed by **T. Kruskal** and **T. Mann-Whitney**.

The average execution time of the methods display the same behavior as before, that for ($n = 1$); the non-parametrics methods are faster than **M. Gambini**; **T. Kruskal** is 938 times faster than **M. Gambini** for $\alpha_r = -2$ and 1963 times faster for $\alpha_r = -19$, as presented in Table 3.7 and Figure 3.20

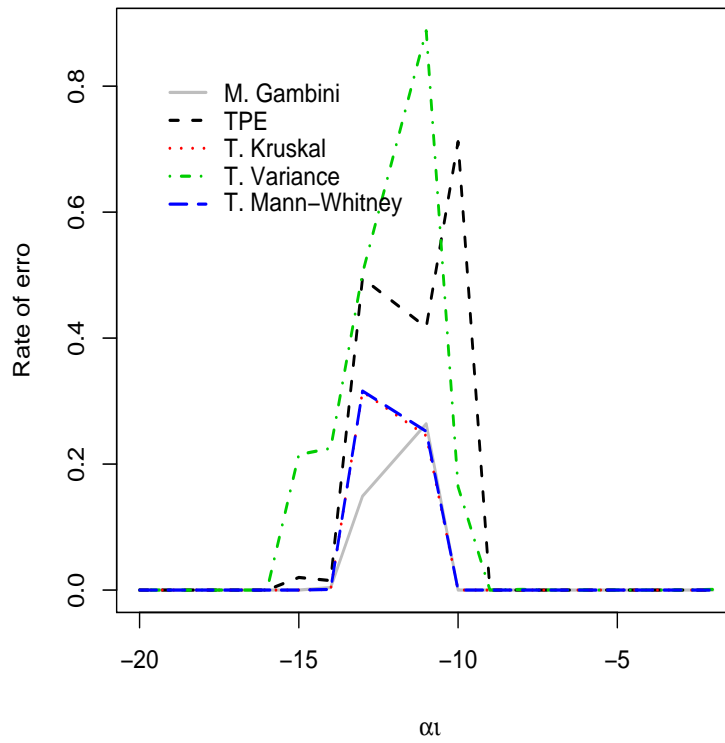


Figure 3.19: Error rate in edge detection for Gambini, Kruskal, Mann-Whitney, Variance and TPE, $\alpha_\ell = -12$ vs. $\alpha_r \in \{-2, -4, -5, \dots, -19, -20\}$ with $n = 3$

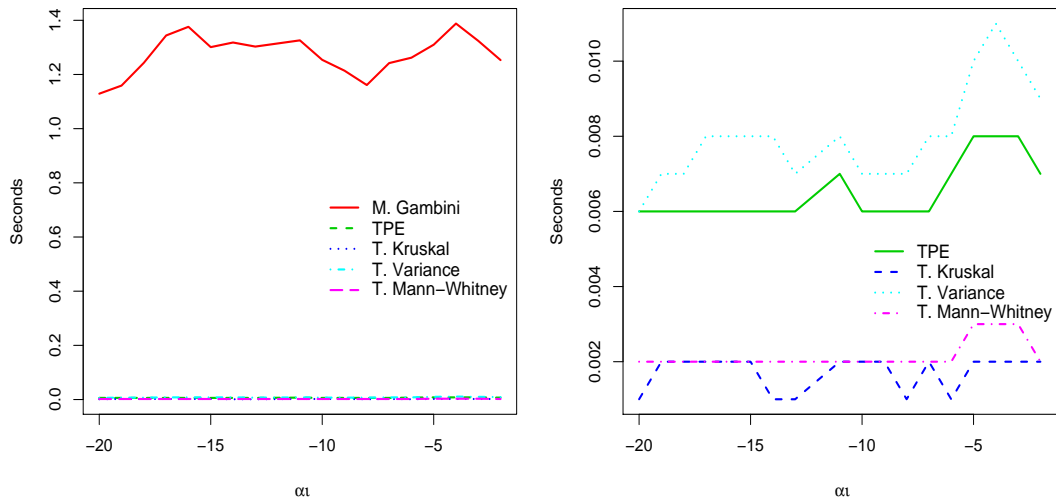


Figure 3.20: Average execution time in seconds for Gambini, Kruskal, Mann-Whitney, Variance and TPE, $\alpha_\ell = -12$ vs. $\alpha_r \in \{-2, -4, -5, \dots, -19, -20\}$ with $n = 3$

3.8 Homogeneous areas with $n = 3$ and $\alpha_\ell = -18$

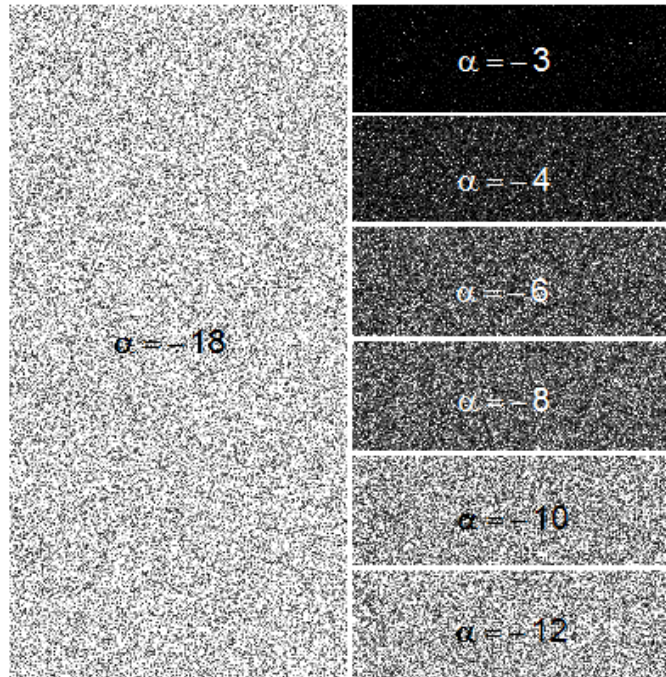


Figure 3.21: Synthetic images $\mathcal{G}_1^0(\alpha, 1, 3)$, $\gamma = 1$ and $\alpha_\ell = -18$ to the left against $\alpha_r = \{-3, -4, -6, -8, -10, -20\}$ to the right

Table 3.8 contains the error rate and average execution times of the methods under study when detecting the edge in a 20×100 image generated with $\alpha_\ell = -18$ and $n = 3$. We note that the **M. Gambini**, **T. Kruskal** and **T. Mann-Whitney** present percentages of error equal to zero in the cases where $\alpha_r \geq -16$. The **T. Kruskal** and **T. Mann-Whitney** presents smaller percentages of error in comparison with **M. Gambini** for $\alpha_r = -17, -19, -20$; **T. Kruskal** and **T. Mann-Whitney** appears to be the methods with the smaller percentages of error in the detection of edges when $\alpha_\ell = -18$ and $n = 3$. The **TPE** presents percentage of error zero when α_r is distant enough from α_ℓ , but this percentage begins to increase as α_r approaches $\alpha_\ell = -18$, obtaining 99.5% of error when $\alpha_r = -17$. The **T. Variance** presents behavior similar to the **TPE**.

α_r	M. Gambini		TPE		T. Kruskal		T. Variance		T. M-Whitney	
	Error rate	Time	Error rate	Time	Error rate	Time	Error rate	Time	Error rate	Time
-20	0.30%	1.866	7.50%	0.005	0.50%	0.001	76.80%	0.006	0.50%	0.002
-19	15.70%	1.417	33.30%	0.005	13.10%	0.001	83.20%	0.006	13.10%	0.002
-17	31.30%	1.324	99.50%	0.006	11.20%	0.001	87.00%	0.006	11.20%	0.002
-16	0.00%	1.278	2.90%	0.005	0.00%	0.002	20.00%	0.006	0.00%	0.002
-15	0.00%	1.206	0.00%	0.005	0.00%	0.001	13.30%	0.006	0.00%	0.002
-14	0.00%	1.351	6.10%	0.005	0.00%	0.002	17.20%	0.007	0.00%	0.002
-13	0.00%	1.182	0.00%	0.006	0.00%	0.001	0.00%	0.006	0.00%	0.002
-12	0.00%	1.097	0.00%	0.006	0.00%	0.001	0.00%	0.006	0.00%	0.002
-11	0.00%	1.303	0.00%	0.005	0.00%	0.001	0.00%	0.007	0.00%	0.002
-10	0.00%	1.264	0.00%	0.005	0.00%	0.001	0.00%	0.007	0.00%	0.002
-9	0.00%	1.133	0.00%	0.005	0.00%	0.001	0.00%	0.007	0.00%	0.002
-8	0.00%	1.046	0.00%	0.005	0.00%	0.001	0.00%	0.006	0.00%	0.002
-7	0.00%	1.378	0.00%	0.005	0.00%	0.001	0.00%	0.006	0.00%	0.002
-6	0.00%	1.097	0.00%	0.005	0.00%	0.001	0.00%	0.006	0.00%	0.002
-5	0.00%	1.062	0.00%	0.005	0.00%	0.001	0.00%	0.006	0.00%	0.002
-4	0.00%	1.056	0.00%	0.005	0.00%	0.001	0.00%	0.006	0.00%	0.002
-3	0.00%	1.055	0.00%	0.005	0.00%	0.001	0.00%	0.006	0.00%	0.002
-2	0.00%	1.021	0.00%	0.005	0.00%	0.001	0.00%	0.006	0.00%	0.002

Table 3.8: Error rate and average time for $\alpha_\ell = -18$ vs. $\alpha_r \in \{-2, -4, -5, \dots, -19, -20\}$ with $n = 3$

Figure 3.22 shows that **T. Kruskal** and **T. Mann-Whitney** presents the lowest error rate in detecting edges, followed by **M. Gambini**. All methods present error greater than zero when the generated images were obtained from distributions with roughness parameters very close in value.

The average time of the **T. Kruskal** is approximately 1000 times smaller than that of **M. Gambini** when $\alpha_r = -2$ and 1866 times faster when $\alpha_r = -20$, as it is observed in the Table 3.8.

Figure 3.23 shows that the **M. Gambini** runtime decreases when α_r is close to zero, but this time is never less than 1 second. Among the non-parametric methods, the fastest is **T. Kruskal** followed by **T. Mann-Whitney**; lower is the **T. Variance** although that it never surpasses 0.010seconds.

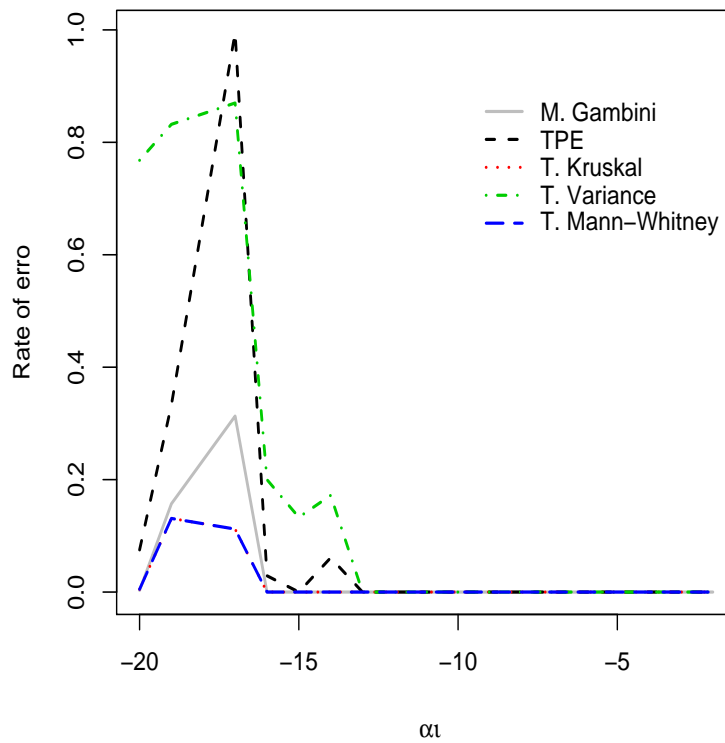


Figure 3.22: Error rate in edge detection for Gambini, Kruskal, Mann-Whitney, Variance and TPE, $\alpha_\ell = -18$ vs. $\alpha_r \in \{-2, -4, -5, \dots, -19, -20\}$ with $n = 3$

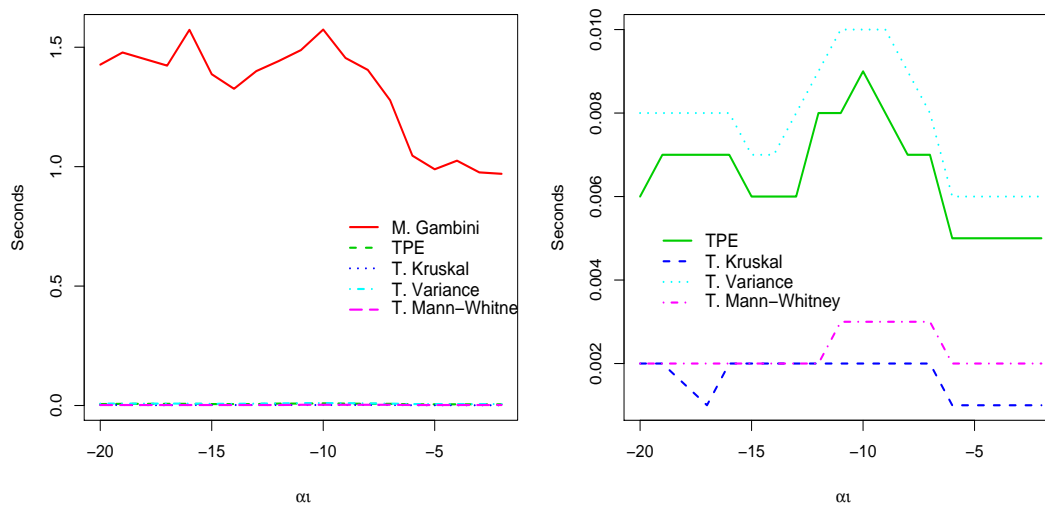


Figure 3.23: Average execution time in seconds for Gambini, Kruskal, Mann-Whitney, Variance and TPE, $\alpha_\ell = -18$ vs. $\alpha_r \in \{-2, -4, -5, \dots, -19, -20\}$ with $n = 3$

3.9 Extremely heterogeneous areas with $n = 8$ and $\alpha_\ell = -3$

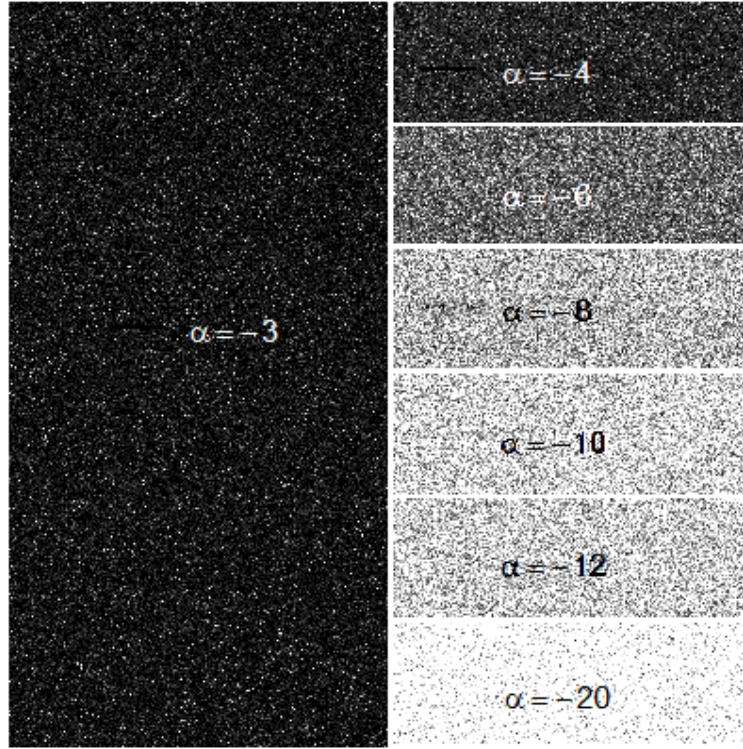


Figure 3.24: Synthetic images $\mathcal{G}_I^0(\alpha, 1, 8)$, $\gamma = 1$ and $\alpha_\ell = -3$ to the left against $\alpha_r = \{-4, -6, -8, -10, -12, -20\}$ to the right

Figure 3.24, left, show an image generated from $\mathcal{G}_I^0(-3, 1, 8)$ which represents extremely heterogeneous areas. Figure 3.24, right, we have images generated with $\alpha_r = -4$ until $\alpha_r = -20$ that represent areas with different degrees of roughness.

The table 3.9 presents the percentages of errors and average time obtained by the methods considered in the simulation. Note that the error rate of all methods are zero, except for **T. Variance** that presents percentages of error of 6.2% and 3.6% for $\alpha_r = -2$ and $\alpha_r = -4$, respectively. All methods present excellent behavior in the detection of edges when $\alpha_\ell = -3$ and $n = 8$.

The Table 3.9 contains the average execution time for $\alpha_\ell = -3$ and $n = 8$. The

	M. Gambini		TPE		T. Kruskal		T. Variance		T. M-Whitney	
α_r	Error rate	Time	Error rate	Time	Error rate	Time	Error rate	Time	Error rate	Time
-20	0.00%	1.255	0.00%	0.007	0.00%	0.002	0.00%	0.009	0.00%	0.003
-19	0.00%	1.110	0.00%	0.006	0.00%	0.002	0.00%	0.007	0.00%	0.002
-18	0.00%	1.082	0.00%	0.006	0.00%	0.002	0.00%	0.007	0.00%	0.002
-17	0.00%	1.121	0.00%	0.006	0.00%	0.001	0.00%	0.007	0.00%	0.002
-16	0.00%	1.111	0.00%	0.006	0.00%	0.001	0.00%	0.007	0.00%	0.002
-15	0.00%	1.116	0.00%	0.006	0.00%	0.002	0.00%	0.007	0.00%	0.002
-14	0.00%	1.052	0.00%	0.006	0.00%	0.001	0.00%	0.007	0.00%	0.002
-13	0.00%	1.032	0.00%	0.005	0.00%	0.002	0.00%	0.007	0.00%	0.002
-12	0.00%	1.038	0.00%	0.005	0.00%	0.002	0.00%	0.007	0.00%	0.002
-11	0.00%	0.991	0.00%	0.006	0.00%	0.001	0.10%	0.007	0.00%	0.002
-10	0.00%	1.000	0.00%	0.006	0.00%	0.001	0.00%	0.006	0.00%	0.002
-9	0.00%	1.011	0.00%	0.006	0.00%	0.001	0.00%	0.006	0.00%	0.002
-8	0.00%	1.065	0.00%	0.006	0.00%	0.001	0.00%	0.007	0.00%	0.002
-7	0.00%	1.008	0.00%	0.006	0.00%	0.001	0.00%	0.006	0.00%	0.002
-6	0.00%	1.030	0.00%	0.006	0.00%	0.002	0.00%	0.007	0.00%	0.002
-5	0.00%	1.010	0.00%	0.006	0.00%	0.002	0.10%	0.007	0.00%	0.002
-4	0.00%	0.949	0.10%	0.005	0.00%	0.001	3.60%	0.006	0.00%	0.002
-2	0.00%	0.953	0.00%	0.005	0.00%	0.001	6.20%	0.006	0.00%	0.002

Table 3.9: Error rate and average time for $\alpha_\ell = -3$ vs. $\alpha_r \in \{-2, -4, -5, \dots, -19, -20\}$ with $n = 8$

difference between the runtimes of the non-parametrics methods and that of M. Gambini method remain. The Kruskal Wallis is 953 times faster than M. Gambini for $\alpha_r = -2$.

In figure 3.25, left, it is noted that the average execution time of M. Gambini diminishes as the value of α_r increases. In figure 3.25, right, it is noted that T. Kruskal yield the smallest runtimes followed by the T. Mann-Whitney method.

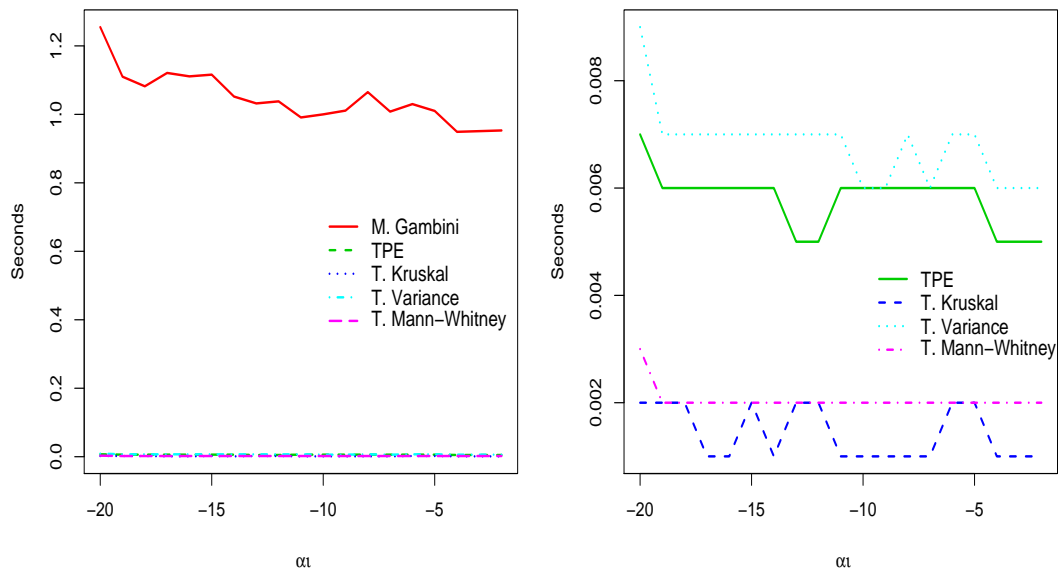


Figure 3.25: Average execution time in seconds for Gambini, Kruskal, Mann-Whitney, Variance and TPE, $\alpha_\ell = -3$ vs. $\alpha_r \in \{-2, -4, -5, \dots, -19, -20\}$ with $n = 8$

3.10 Heterogeneous areas with $n = 8$ and $\alpha_\ell = -8$

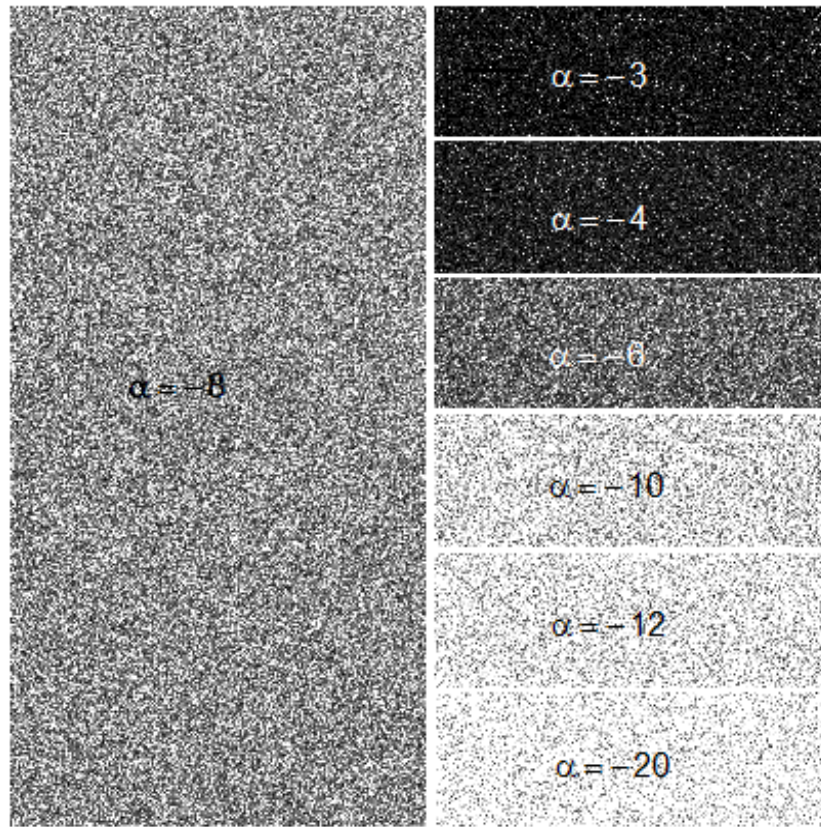


Figure 3.26: Synthetic images $\mathcal{G}_I^0(\alpha, 1, 8)$, $\gamma = 1$ and $\alpha_\ell = -8$ to the left against $\alpha_r = \{-3, -4, -6, -10, -12, -20\}$ to the right

Table 3.10 contains the error rate and average time for $\alpha_\ell = -8$, $n = 8$ and different values of the α_r . Note that **T. Kruskal** does not present errors in the detection of edges for any value of α_r . **M. Gambini** and **T. Mann-Whitney** methods have the same behavior as **T. Kruskal** method except for $\alpha_r = -7$ where its percentage of error is 0.2% and 0.1% respectively. These three methods achieve the best results when $\alpha_\ell = -8$ and $n = 8$.

TPE method reaches 66% of error when $\alpha_r = -7$ and 10,3% when $\alpha_r = -9$, for the other values of α_r the percentage of error is zero. **T. Variance** method display high percentage of errors when α_ℓ is close to α_r .

	M. Gambini		TPE		T. Kruskal		T. Variance		T. M-Whitney	
α_r	Error rate	Time	Error rate	Time	Error rate	Time	Error rate	Time	Error rate	Time
-20	0.00%	1.145	0.00%	0.006	0.00%	0.001	0.00%	0.007	0.00%	0.002
-19	0.00%	1.106	0.00%	0.006	0.00%	0.001	0.00%	0.007	0.00%	0.002
-18	0.00%	1.485	0.00%	0.008	0.00%	0.002	0.00%	0.010	0.00%	0.003
-17	0.00%	1.415	0.00%	0.008	0.00%	0.002	0.00%	0.009	0.00%	0.002
-16	0.00%	1.215	0.00%	0.006	0.00%	0.002	0.00%	0.007	0.00%	0.002
-15	0.00%	1.193	0.00%	0.006	0.00%	0.001	0.00%	0.007	0.00%	0.002
-14	0.00%	1.279	0.00%	0.006	0.00%	0.002	0.00%	0.008	0.00%	0.002
-13	0.00%	1.212	0.00%	0.006	0.00%	0.002	0.00%	0.007	0.00%	0.002
-12	0.00%	1.211	0.00%	0.006	0.00%	0.002	0.10%	0.008	0.00%	0.002
-11	0.00%	1.207	0.00%	0.006	0.00%	0.002	0.70%	0.007	0.00%	0.002
-10	0.00%	1.121	0.00%	0.006	0.00%	0.001	4.40%	0.007	0.00%	0.002
-9	0.00%	1.091	10.30%	0.005	0.00%	0.001	41.50%	0.006	0.00%	0.002
-7	0.20%	1.160	66.50%	0.006	0.00%	0.001	58.00%	0.007	0.10%	0.002
-6	0.00%	1.084	0.00%	0.006	0.00%	0.001	1.20%	0.007	0.00%	0.002
-5	0.00%	1.026	0.00%	0.005	0.00%	0.002	0.00%	0.007	0.00%	0.002
-4	0.00%	1.130	0.00%	0.007	0.00%	0.002	0.00%	0.007	0.00%	0.002
-3	0.00%	0.998	0.00%	0.006	0.00%	0.001	0.00%	0.007	0.00%	0.002
-2	0.00%	1.098	0.00%	0.006	0.00%	0.002	0.10%	0.008	0.00%	0.002

Table 3.10: Error rate and average time for $\alpha_\ell = -8$ vs. $\alpha_r \in \{-2, -4, -5, \dots, -19, -20\}$ with $n = 8$

Figure 3.27 compares the behavior of the percentages of error generated by the different methods under study. We observe that the largest percentages of error are generated by **TPE** and **T. Variance**.

Regarding runtime, the Table 3.10 shows that **M. Gambini** is the slowest method. **T. Kruskal** is approximately 550 times faster than **M. Gambini** for $\alpha_r = -2$ and 1145 times faster when $\alpha_r = -20$. Figure 3.28 corroborates the behavior of the times of **M. Gambini**. The execution times of non-parametric methods are smaller than 0.010 seconds, being **T. Kruskal** the fastest method, whose execution time does not exceed 0.02 second in any situation.

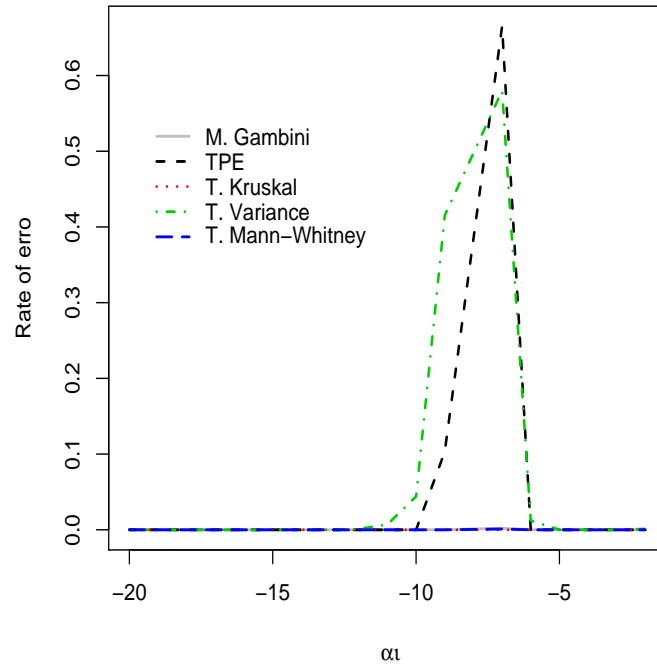


Figure 3.27: Error rate in edge detection for Gambini, Kruskal, Mann-Whitney, Variance and TPE, $\alpha_\ell = -8$ vs. $\alpha_r \in \{-2, -4, -5, \dots, -19, -20\}$ with $n = 8$

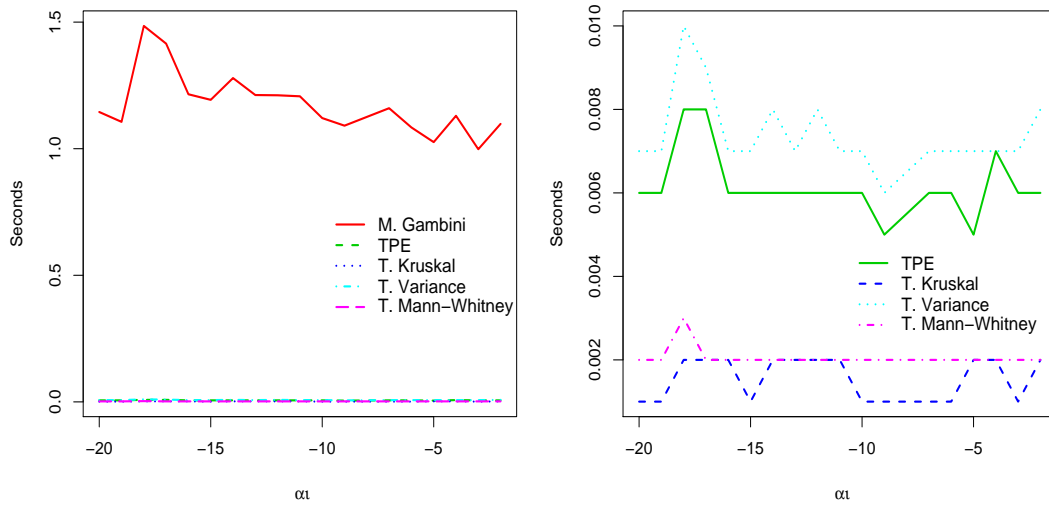


Figure 3.28: Average execution time in seconds for Gambini, Kruskal, Mann-Whitney, Variance and TPE, $\alpha_\ell = -8$ vs. $\alpha_r \in \{-2, -4, -5, \dots, -19, -20\}$ with $n = 8$

3.11 Homogeneous areas with $n = 8$ and $\alpha_\ell = -12$

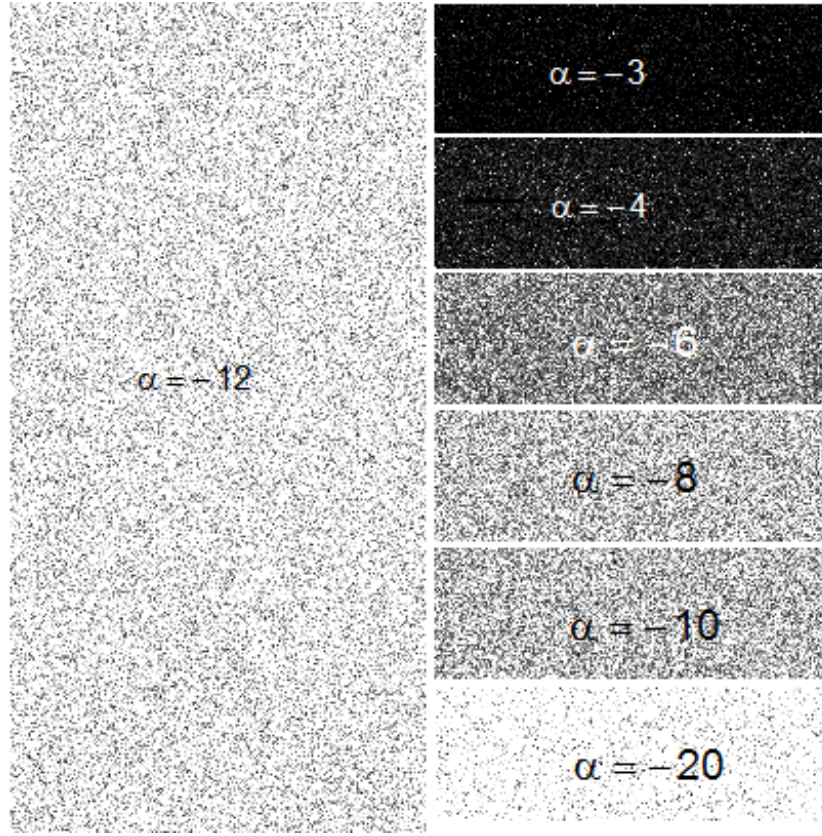


Figure 3.29: Synthetic images $\mathcal{G}_1^0(\alpha, 1, 8)$, $\gamma = 1$ and $\alpha_\ell = -12$ to the left against $\alpha_r = \{-3, -4, -6, -8, -10, -20\}$ to the right

Table 3.11 presents the error rates and average execution times achieved by the different methods in the simulation, with $n = 8$ and $\alpha_\ell = -12$. We note that **T. Variance** obtains errors between 35.5% and 67.9% when α_r is between -14 and -9 . **TPE** obtains errors between 17.7% and 37.3% when α_r is between -13 and -10 . **T. Mann-Whitney** detects satisfactorily the edge when $\alpha_r \leq -14$; it obtains 0.4% of error when $\alpha_r = -13$ and for $\alpha_r \geq -11$ it obtains 0% of error in edge detection. **T. Kruskal** and **M. Gambini** behave similarly, obtaining 0.4% and 0.3% errors, respectively, when $\alpha_r = -13$; the maximum error that these methods generate are 1.2% and 1.3% when α_r is equal to -11 .

	M. Gambini		TPE		T. Kruskal		T. Variance		T. M-Whitney	
α_r	Error rate	Time	Error rate	Time	Error rate	Time	Error rate	Time	Error rate	Time
-20	0.00%	1.129	0.00%	0.006	0.00%	0.001	0.00%	0.006	0.00%	0.002
-19	0.00%	1.159	0.00%	0.006	0.00%	0.002	0.00%	0.007	0.00%	0.002
-18	0.00%	1.243	0.00%	0.006	0.00%	0.002	0.10%	0.007	0.00%	0.002
-17	0.00%	1.344	0.00%	0.006	0.00%	0.002	0.00%	0.008	0.00%	0.002
-16	0.00%	1.376	0.00%	0.006	0.00%	0.002	0.20%	0.008	0.00%	0.002
-15	0.00%	1.301	0.00%	0.006	0.00%	0.002	0.50%	0.008	0.00%	0.002
-14	0.00%	1.318	0.00%	0.006	0.00%	0.001	35.50%	0.008	0.00%	0.002
-13	0.30%	1.303	37.30%	0.006	0.40%	0.001	47.10%	0.007	0.40%	0.002
-11	1.20%	1.326	11.70%	0.007	1.30%	0.002	67.90%	0.008	1.30%	0.002
-10	0.00%	1.254	17.70%	0.006	0.00%	0.002	5.90%	0.007	0.00%	0.002
-9	0.00%	1.214	0.00%	0.006	0.00%	0.002	0.60%	0.007	0.00%	0.002
-8	0.00%	1.161	0.00%	0.006	0.00%	0.001	0.00%	0.007	0.00%	0.002
-7	0.00%	1.242	0.00%	0.006	0.00%	0.002	0.00%	0.008	0.00%	0.002
-6	0.00%	1.262	0.00%	0.007	0.00%	0.001	0.00%	0.008	0.00%	0.002
-5	0.00%	1.310	0.00%	0.008	0.00%	0.002	0.00%	0.010	0.00%	0.003
-4	0.00%	1.388	0.00%	0.008	0.00%	0.002	0.00%	0.011	0.00%	0.003
-3	0.00%	1.324	0.00%	0.008	0.00%	0.002	0.00%	0.010	0.00%	0.003
-2	0.00%	1.253	0.00%	0.007	0.00%	0.002	0.00%	0.009	0.00%	0.002

Table 3.11: Error rate and average time for $\alpha_\ell = -12$ vs. $\alpha_r \in \{-2, -4, -5, \dots, -19, -20\}$ with $n = 8$

Figure 3.30 shows that M. Gambini, T. Kruskal and T. Mann-Whitney have the same behavior and widely surpass the performance of the other methods.

Table 3.11 shows that the execution time in seconds required by M. Gambini is approximately 1000 times slower than the one required by any of the rank-based methods; this feature is also shown in the graph on the left of figure 3.31. In the graphic to the right, we compare the runtimes of the non-parametrics methods. We note that T. Kruskal and T. Mann-Whitney are the fastest methods. Therefore, T. Kruskal achieves the smallest errors in the detection of edges with the smallest computing time.

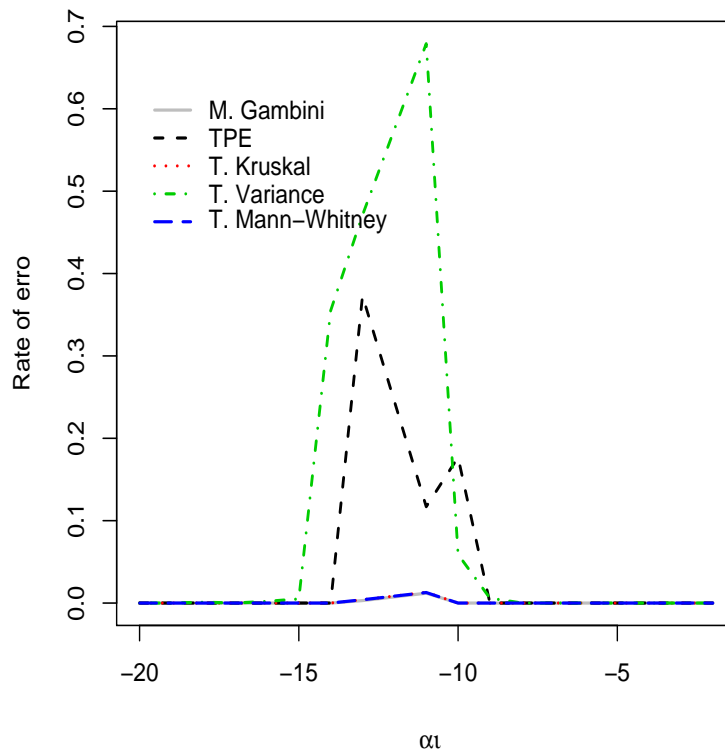


Figure 3.30: Error rate in detection of edge for Gambini, Kruskal, Mann-Whitney, Variance and TPE, $\alpha_\ell = -12$ vs. $\alpha_r \in \{-2, -4, -5, \dots, -19, -20\}$ with $n = 8$

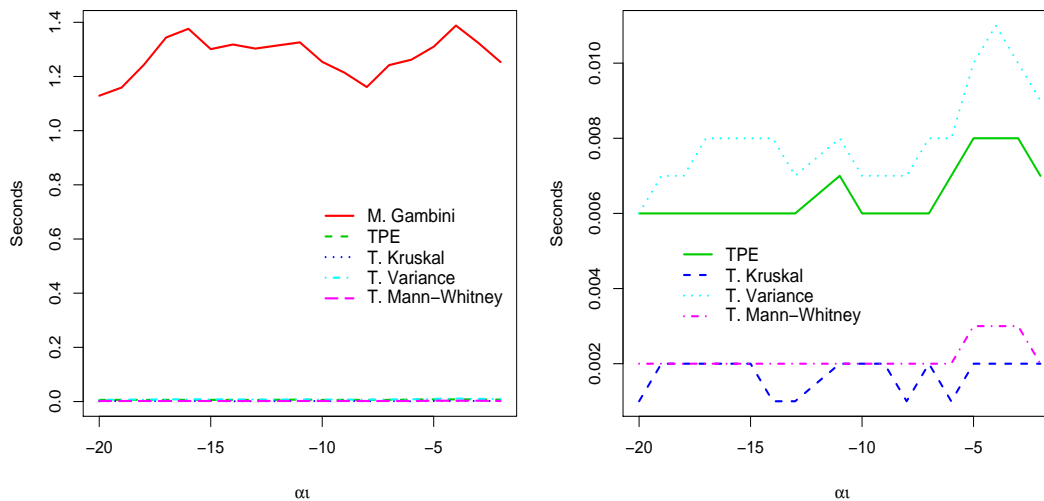


Figure 3.31: Average execution time in seconds for Gambini, Kruskal, Mann-Whitney, Variance and TPE, $\alpha_\ell = -12$ vs. $\alpha_r \in \{-2, -4, -5, \dots, -19, -20\}$ with $n = 8$

3.12 Homogeneous areas with $n = 8$ $\alpha_\ell = -18$

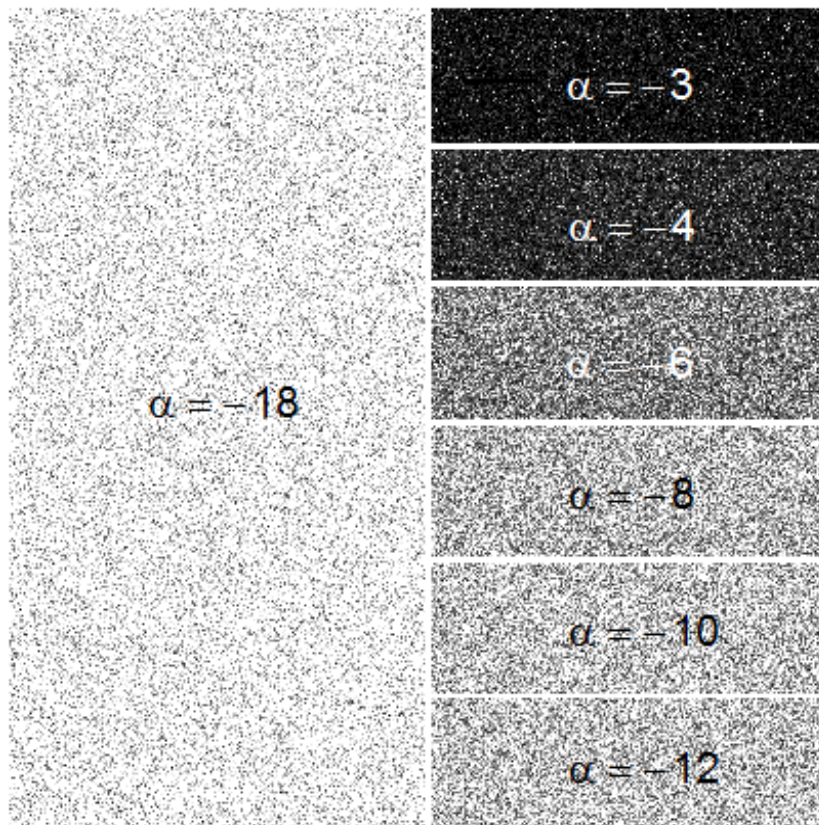


Figure 3.32: Synthetic images $\mathcal{G}_1^0(\alpha, 1, 8)$, $\gamma = 1$ and $\alpha_\ell = -18$ to the left against $\alpha_r = \{-3, -4, -6, -8, -10, -20\}$ to the right

Figure 3.32 depicts a typical sample of the situation considered in this section.

Table 3.12 presents the errors of the different methods, with $n = 8$ and $\alpha_\ell = -18$, it can be seen that the percentages error of **T. Variance** exceeds 11% when $\alpha_r < -15$, while **TPE** obtains errors of 38.3%, 34% and 64% when α_r takes values $-17, -19$ and -20 , respectively. **T. Mann-Whitney** obtains 0% of error for $\alpha_r = -20$, 3.4% when $\alpha_r = -19$ and 0.30% for $\alpha_r = -16$; for $\alpha_r \geq -15$, it obtains 0% of error. **T. Kruskal** and **M. Gambini** behave similarly, obtaining errors of 3.1% and 3.4%, respectively, when $\alpha_r = -19$; for $\alpha_r > -15$, these two methods always find the edge and, thus, obtain 0% of error.

	M. Gambini		TPE		T. Kruskal		T. Variance		T. M-Whitney	
α_r	Error rate	Time	Error rate	Time	Error rate	Time	Error rate	Time	Error rate	Time
-20	0.00%	1.427	63.70%	0.006	0.00%	0.002	60.40%	0.008	0.00%	0.002
-19	3.10%	1.478	34.90%	0.007	3.40%	0.002	43.70%	0.008	3.40%	0.002
-17	1.70%	1.423	38.30%	0.007	1.50%	0.001	66.40%	0.008	1.60%	0.002
-16	0.20%	1.573	1.90%	0.007	0.30%	0.002	69.60%	0.008	0.30%	0.002
-15	0.00%	1.387	0.10%	0.006	0.00%	0.002	11.50%	0.007	0.00%	0.002
-14	0.00%	1.326	0.00%	0.006	0.00%	0.002	0.50%	0.007	0.00%	0.002
-13	0.00%	1.400	0.00%	0.006	0.00%	0.002	0.00%	0.008	0.00%	0.002
-12	0.00%	1.442	0.00%	0.008	0.00%	0.002	0.00%	0.009	0.00%	0.002
-11	0.00%	1.488	0.00%	0.008	0.00%	0.002	0.00%	0.010	0.00%	0.003
-10	0.00%	1.574	0.00%	0.009	0.00%	0.002	0.00%	0.010	0.00%	0.003
-9	0.00%	1.455	0.00%	0.008	0.00%	0.002	0.00%	0.010	0.00%	0.003
-8	0.00%	1.405	0.00%	0.007	0.00%	0.002	0.00%	0.009	0.00%	0.003
-7	0.00%	1.278	0.00%	0.007	0.00%	0.002	0.00%	0.008	0.00%	0.003
-6	0.00%	1.046	0.00%	0.005	0.00%	0.001	0.00%	0.006	0.00%	0.002
-5	0.00%	0.989	0.00%	0.005	0.00%	0.001	0.00%	0.006	0.00%	0.002
-4	0.00%	1.025	0.00%	0.005	0.00%	0.001	0.00%	0.006	0.00%	0.002
-3	0.00%	0.976	0.00%	0.005	0.00%	0.001	0.00%	0.006	0.00%	0.002
-2	0.00%	0.970	0.00%	0.005	0.00%	0.001	0.00%	0.006	0.00%	0.002

Table 3.12: Error rate and average time for, $\alpha_\ell = -18$ vs. $\alpha_r \in \{-2, -4, -5, \dots, -19, -20\}$ with $n = 8$

Figure 3.33 suggests that the smaller errors and more stable performances are obtained by T. Kruskal, T. Mann-Whitney and M. Gambini.

Table 3.12 shows that M. Gambini continues to display the largest execution times; T. Kruskal is approximately 970 times faster than M. Gambini when $\alpha_r = -2$ and 713 times faster when $\alpha_r = -20$. The execution times of M. Gambini reduce as α_r increases, which can be seen in Figure 3.34. To the right of Figure 3.34, we compare the time in seconds required by the non-parametric methods, noting that T. Kruskal and T. Mann-Whitney require the smallest execution times.

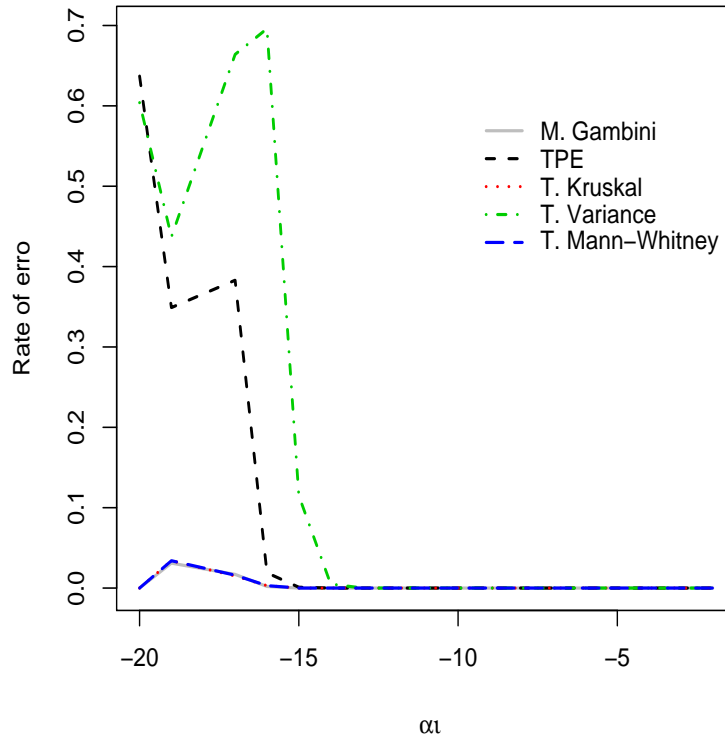


Figure 3.33: Error rate in detection of edge for Gambini, Kruskal, Mann-Whitney, Variance and TPE, $\alpha_\ell = -18$ vs. $\alpha_r \in \{-2, -4, -5, \dots, -19, -20\}$ with $n = 8$

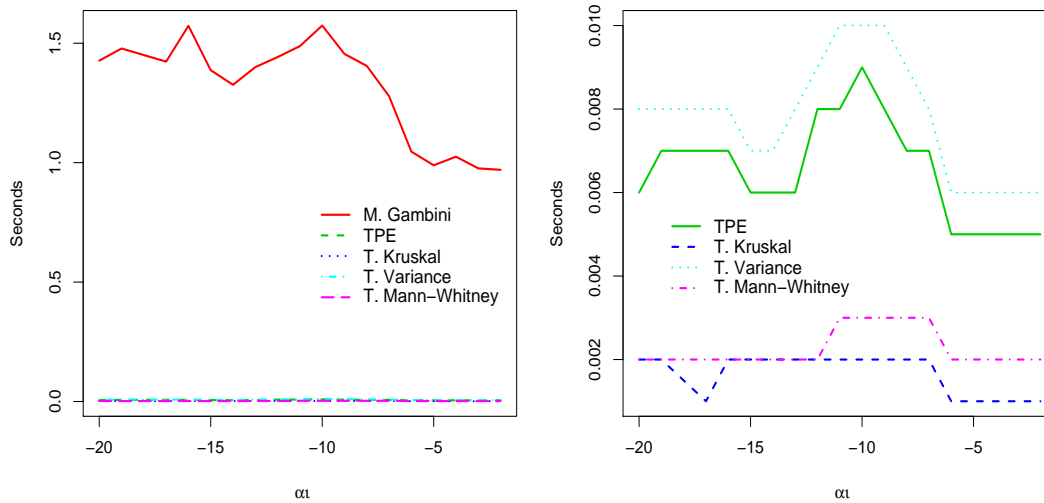


Figure 3.34: Average execution time in seconds for Gambini, Kruskal, Mann-Whitney, Variance and TPE, $\alpha_\ell = -18$ vs. $\alpha_r \in \{-2, -4, -5, \dots, -19, -20\}$ with $n = 8$

This Chapter presented the Monte Carlo experience designed to assess the performance of five edge detection methods with respect to the error in finding an edge and to the execution time. Next Chapter will describe the conclusions.

Chapter 4

Conclusions

Resumo

O objetivo deste trabalho foi estudar técnicas alternativas de detecção de bordas em imagens speckled, tendo como ponto de partida Gambini et al. (2006, 2008). O modelo utilizado para descrever os dados com ruído speckled é a distribuição \mathcal{G}_I^0 , a qual Mejail et al. (2001, 2003) mostra que pode ser usada como um modelo universal neste caso.

Os métodos sob avaliação buscam identificar a borda entre regiões com diferentes graus de rugosidade determinada por α , o parâmetro de rugosidade da distribuição $\mathcal{G}_I^0(\alpha, \gamma, n)$.

Considerando os resultados obtidos através das simulações de Monte Carlo, pode-se concluir que o detector de **T. Kruskal** e o detector de **T. Mann-Whitney** são ligeiramente melhores do que **M. Gambini**. Comparados com os detectores **TPE** e **T. Variance**, **T. Kruskal** e **T. Mann-Whitney** fornecem os melhores resultados.

Todos os métodos sob estudo apresentam bom desempenho quando a borda separa áreas com rugosidade muito diferente. Quando a imagem gerada representa zonas homogêneas, as taxas de erro de todos os métodos são relativamente elevadas. No entanto, esse problema é atenuado com o aumento do número de looks n , que torna a detecção de bordas mais confiável.

O detector **T. Kruskal** fornece os melhores resultados, tanto no que respeita ao erro como no que tange ao tempo de execução. Este último é, em muitos casos, 1000 vezes menor do que do **M. Gambini**.

Como conclusão final, em relação ao erro e ao tempo de execução, este trabalho fornece evidência de que a técnica de **M. Gambini** pode ser substituída com sucesso por **T. Kruskal**. O ganho reside em ter um algoritmo de até 1000 vezes mais rápido, sem comprometer a qualidade dos resultados.

Conclusions

The aim of this thesis was to considerer alternative techniques for edge detection in speckled imagery, having as starting point the results in Gambini et al. (2006, 2008). The techniques here assessed do not try to eliminate speckle, but to extract information from its statistical properties. The model used to describe these data is the \mathcal{G}_I^0 distribution, which, as shown by Mejail et al. (2001, 2003), can be used as an universal model.

The methods under assessment aim at identifying edges between regions with different degrees of roughness, which, in turn, is determined by α , the roughness parameter of the $\mathcal{G}_I^0(\alpha, \gamma, n)$ distribution. Homogenous, e.g., pastures, heterogeneous regions, e.g., forests, and very heterogeneous regions, e.g., urban, targets are considered.

We describe a new edge detector based on the **T. Kruskal** test which proved to be an useful alternative to the approach of **M. Gambini**, which is based on the likelihood function of the data.

In order to make a comparison of the five methods, a Monte Carlo experiment was carried out, and two measures of quality were assessed: error in detecting an edge in a known position and execution time. Several situations were considered, namely, when the areas on each side of the edge have the same mean and the same number of looks differing only on the roughness.

From the experimental results it was observed that the **T. Kruskal** and **T. Mann-Whitney** detectors performed slightly better than **M. Gambini**. Compared with the **TPE**, **T. Variance** detectors, **T. Kruskal** and **T. Mann-Whitney** performed much better.

All methods under study perform well when the edge separates areas with very different roughnesses. When the generated image represents homogenous zones, the percentages of error of all methods are relatively high. Nevertheless, this problem is alleviated by the increase of the number of looks n , which causes the detection of edges to be more accurate.

The **T. Mann-Whitney** and **T. Kruskal** detectors display the best results, both with respect to error and execution time. The latter is, in many cases, 1000 times smaller than **M. Gambini**.

The **TPE** method yields good results in the detection of edges when α_ℓ differs from α_r by at least three units.

As a final conclusion, regarding the error and the execution time, we provide evidence that the **M. Gambini** technique can be successfully replaced by **T. Kruskal**. The latter can be up to 1000 times faster than the former.

Appendix A

Simulation results for $n = 1$

TABLE 1. Error rate and average execution time for $\alpha_\ell = -3$										
	M. Gambini		TPE		T. Kruskal		T. Variance		T. M-Whitney	
α_r	Error	Time	Error	Time	Error	Time	Error	Time	Error	Time
-20	0.00%	1.415	0.00%	0.012	0.00%	0.002	0.00%	0.015	0.00%	0.003
-19	0.00%	1.401	0.00%	0.012	0.00%	0.002	0.00%	0.015	0.00%	0.003
-18	0.00%	1.376	0.00%	0.012	0.00%	0.002	0.00%	0.015	0.00%	0.003
-17	0.00%	1.362	0.00%	0.012	0.00%	0.002	0.00%	0.015	0.00%	0.003
-16	0.00%	1.352	0.00%	0.012	0.00%	0.002	0.00%	0.015	0.00%	0.003
-15	0.00%	1.338	0.00%	0.012	0.00%	0.002	0.00%	0.015	0.00%	0.003
-14	0.00%	1.307	0.00%	0.012	0.00%	0.002	0.00%	0.015	0.00%	0.003
-13	0.00%	1.287	0.00%	0.012	0.00%	0.002	0.00%	0.015	0.00%	0.003
-12	0.00%	1.275	0.00%	0.012	0.00%	0.002	0.00%	0.015	0.00%	0.003
-11	0.00%	1.257	0.00%	0.012	0.00%	0.002	0.00%	0.015	0.00%	0.003
-10	0.00%	1.238	0.00%	0.012	0.00%	0.002	0.00%	0.015	0.00%	0.003
-9	0.00%	1.221	0.00%	0.012	0.00%	0.002	0.00%	0.015	0.00%	0.003
-8	0.00%	1.198	0.00%	0.012	0.00%	0.002	0.00%	0.015	0.00%	0.003
-7	0.00%	1.189	0.10%	0.012	0.00%	0.002	0.00%	0.015	0.00%	0.003
-6	0.00%	1.168	0.00%	0.012	0.00%	0.002	0.00%	0.015	0.00%	0.003
-5	0.00%	1.158	0.40%	0.012	0.00%	0.002	0.60%	0.015	0.00%	0.003
-4	0.10%	1.140	15.40%	0.012	0.00%	0.002	16.90%	0.015	0.00%	0.003
-2	0.00%	1.101	2.80%	0.012	0.00%	0.002	9.30%	0.015	0.00%	0.003

TABLE 2. Error rates and average execution time for $\alpha_\ell = -4$

α_r	M. Gambini		TPE		T. Kruskal		T. Variance		T. M-Whitney	
	Error	Time	Error	Time	Error	Time	Error	Time	Error	Time
-20	0.00%	1.455	0.00%	0.012	0.00%	0.002	0.00%	0.015	0.00%	0.003
-19	0.00%	1.423	0.00%	0.012	0.00%	0.002	0.00%	0.015	0.00%	0.003
-18	0.00%	1.412	0.00%	0.012	0.00%	0.002	0.00%	0.015	0.00%	0.003
-17	0.00%	1.379	0.00%	0.012	0.00%	0.002	0.00%	0.015	0.00%	0.003
-16	0.00%	1.349	0.00%	0.012	0.00%	0.002	0.00%	0.015	0.00%	0.003
-15	0.00%	1.357	0.00%	0.012	0.00%	0.002	0.00%	0.015	0.00%	0.003
-14	0.00%	1.322	0.00%	0.012	0.00%	0.002	0.00%	0.015	0.00%	0.003
-13	0.00%	1.313	0.00%	0.012	0.00%	0.002	0.00%	0.015	0.00%	0.003
-12	0.00%	1.288	0.00%	0.012	0.00%	0.002	0.00%	0.015	0.00%	0.003
-11	0.00%	1.277	0.00%	0.012	0.00%	0.002	0.00%	0.015	0.00%	0.003
-10	0.00%	1.258	0.00%	0.012	0.00%	0.002	0.00%	0.015	0.00%	0.003
-9	0.00%	1.246	0.00%	0.012	0.00%	0.002	0.00%	0.015	0.00%	0.003
-8	0.00%	1.233	0.10%	0.012	0.00%	0.002	0.00%	0.015	0.00%	0.003
-7	0.00%	1.222	0.80%	0.012	0.00%	0.002	0.00%	0.015	0.00%	0.003
-6	0.00%	1.197	4.90%	0.012	0.10%	0.002	2.10%	0.015	0.10%	0.003
-5	0.70%	1.176	36.20%	0.012	1.90%	0.002	29.10%	0.015	1.90%	0.003
-3	0.00%	1.144	18.60%	0.012	0.10%	0.002	14.90%	0.015	0.10%	0.003
-2	0.00%	1.112	0.00%	0.012	0.00%	0.002	1.40%	0.015	0.00%	0.003

TABLE 3. Error rates and average execution time for $\alpha_\ell = -6$

α_r	M. Gambini		TPE		T. Kruskal		T. Variance		T. M-Whitney	
	Error	Time	Error	Time	Error	Time	Error	Time	Error	Time
-20	0.00%	1.483	0.00%	0.012	0.00%	0.002	0.00%	0.015	0.00%	0.003
-19	0.00%	1.467	0.00%	0.012	0.00%	0.002	0.00%	0.015	0.00%	0.003
-18	0.00%	1.464	0.00%	0.012	0.00%	0.002	0.00%	0.015	0.00%	0.003
-17	0.00%	1.448	0.00%	0.012	0.00%	0.002	0.00%	0.015	0.00%	0.003
-16	0.00%	1.429	0.00%	0.012	0.00%	0.002	0.00%	0.014	0.00%	0.003
-15	0.00%	1.404	0.00%	0.012	0.00%	0.002	0.00%	0.015	0.00%	0.003
-14	0.00%	1.402	0.00%	0.012	0.00%	0.002	0.00%	0.015	0.00%	0.003
-13	0.00%	1.369	0.00%	0.012	0.00%	0.002	0.00%	0.015	0.00%	0.003
-12	0.00%	1.360	0.00%	0.012	0.00%	0.002	0.00%	0.015	0.00%	0.003
-11	0.00%	1.342	0.70%	0.012	0.00%	0.002	0.00%	0.015	0.00%	0.003
-10	0.00%	1.318	1.40%	0.012	0.00%	0.002	0.10%	0.015	0.00%	0.003
-9	0.00%	1.316	4.60%	0.012	0.00%	0.002	1.50%	0.015	0.00%	0.003
-8	0.10%	1.293	18.90%	0.012	0.20%	0.002	12.50%	0.015	0.20%	0.003
-7	5.50%	1.309	64.00%	0.012	6.40%	0.002	51.10%	0.015	6.40%	0.003
-5	2.70%	1.238	51.10%	0.012	3.20%	0.002	39.80%	0.015	3.20%	0.003
-4	0.00%	1.194	6.60%	0.012	0.00%	0.002	1.30%	0.015	0.00%	0.003
-3	0.00%	1.172	0.20%	0.012	0.00%	0.002	0.00%	0.015	0.00%	0.003
-2	0.00%	1.155	0.00%	0.012	0.00%	0.002	0.10%	0.015	0.00%	0.003

TABLE 4. Error rates and average execution time for $\alpha_\ell = -8$

	M. Gambini		TPE		T. Kruskal		T. Variance		T. M-Whitney	
α_r	Error	Time	Error	Time	Error	Time	Error	Time	Error	Time
-20	0.00%	1.513	0.00%	0.012	0.00%	0.002	0.00%	0.015	0.00%	0.003
-19	0.00%	1.519	0.00%	0.012	0.00%	0.002	0.00%	0.015	0.00%	0.003
-18	0.00%	1.502	0.00%	0.012	0.00%	0.002	0.00%	0.015	0.00%	0.003
-17	0.00%	1.469	0.00%	0.012	0.00%	0.002	0.00%	0.015	0.00%	0.003
-16	0.00%	1.449	0.00%	0.012	0.00%	0.002	0.00%	0.015	0.00%	0.003
-15	0.00%	1.440	0.20%	0.012	0.00%	0.002	0.00%	0.015	0.00%	0.003
-14	0.00%	1.414	0.50%	0.012	0.00%	0.002	0.00%	0.014	0.00%	0.003
-13	0.00%	1.419	2.70%	0.012	0.00%	0.002	0.20%	0.015	0.00%	0.003
-12	0.00%	1.396	6.50%	0.012	0.00%	0.002	1.20%	0.015	0.00%	0.003
-11	0.10%	1.385	14.20%	0.012	0.20%	0.002	6.20%	0.015	0.20%	0.003
-10	0.50%	1.406	33.80%	0.012	1.60%	0.002	26.50%	0.015	1.60%	0.003
-9	16.20%	1.389	81.00%	0.012	22.40%	0.002	64.50%	0.015	22.40%	0.003
-7	11.20%	1.353	73.30%	0.012	12.20%	0.002	61.30%	0.015	12.80%	0.003
-6	0.00%	1.292	21.60%	0.012	0.50%	0.002	11.40%	0.015	0.50%	0.003
-5	0.00%	1.242	3.80%	0.012	0.00%	0.002	0.60%	0.015	0.00%	0.003
-4	0.00%	1.214	0.10%	0.012	0.00%	0.002	0.00%	0.015	0.00%	0.003
-3	0.00%	1.196	0.00%	0.012	0.00%	0.002	0.00%	0.014	0.00%	0.003
-2	0.00%	1.175	0.00%	0.012	0.00%	0.002	0.10%	0.015	0.00%	0.003

TABLE 5. Error rates and average execution time for $\alpha_\ell = -10$

	M. Gambini		TPE		T. Kruskal		T. Variance		T. M-Whitney	
α_r	Error	Time	Error	Time	Error	Time	Error	Time	Error	Time
-20	0.00%	1.600	0.10%	0.012	0.00%	0.002	0.00%	0.015	0.00%	0.003
-19	0.00%	1.561	0.50%	0.012	0.00%	0.002	0.00%	0.015	0.00%	0.003
-18	0.00%	1.542	0.40%	0.012	0.00%	0.002	0.00%	0.015	0.00%	0.003
-17	0.00%	1.526	0.80%	0.012	0.00%	0.002	0.10%	0.015	0.00%	0.003
-16	0.00%	1.520	2.70%	0.012	0.00%	0.002	0.20%	0.015	0.00%	0.003
-15	0.00%	1.512	6.90%	0.012	0.00%	0.002	2.00%	0.015	0.00%	0.003
-14	0.00%	1.501	14.10%	0.012	0.00%	0.002	5.20%	0.015	0.00%	0.003
-13	0.30%	1.524	28.30%	0.012	0.40%	0.002	15.00%	0.015	0.40%	0.003
-12	5.50%	1.641	53.80%	0.013	5.50%	0.002	41.90%	0.016	5.50%	0.003
-11	32.30%	1.491	87.90%	0.012	30.20%	0.002	71.30%	0.014	30.20%	0.003
-9	22.70%	1.431	85.50%	0.011	25.20%	0.002	69.60%	0.014	25.20%	0.003
-8	0.60%	1.390	38.70%	0.012	1.80%	0.002	27.00%	0.014	1.90%	0.003
-7	0.00%	1.332	13.10%	0.012	0.00%	0.002	3.40%	0.014	0.00%	0.003
-6	0.00%	1.304	2.80%	0.012	0.00%	0.002	0.10%	0.014	0.00%	0.003
-5	0.00%	1.264	0.20%	0.012	0.00%	0.002	0.00%	0.014	0.00%	0.003
-4	0.00%	1.242	0.00%	0.012	0.00%	0.002	0.00%	0.014	0.00%	0.002
-3	0.00%	1.217	0.00%	0.012	0.00%	0.002	0.00%	0.015	0.00%	0.003
-2	0.00%	1.199	0.00%	0.012	0.00%	0.002	0.10%	0.014	0.00%	0.003

TABLE 6. Error rates and average execution time for $\alpha_\ell = -12$

	M. Gambini		TPE		T. Kruskal		T. Variance		T. M-Whitney	
α_r	Error	Time	Error	Time	Error	Time	Error	Time	Error	Time
-20	0.00%	1.646	1.10%	0.012	0.00%	0.002	0.00%	0.015	0.00%	0.003
-19	0.00%	1.640	3.00%	0.012	0.00%	0.002	0.20%	0.015	0.00%	0.003
-18	0.00%	1.609	7.10%	0.012	0.00%	0.002	0.60%	0.015	0.00%	0.003
-17	0.00%	1.612	13.50%	0.012	0.20%	0.002	4.40%	0.015	0.20%	0.003
-16	0.00%	1.634	23.50%	0.012	0.40%	0.002	12.50%	0.015	0.40%	0.003
-15	0.80%	1.608	39.00%	0.012	1.60%	0.002	27.70%	0.015	1.60%	0.003
-14	6.90%	1.598	67.70%	0.012	11.30%	0.002	48.30%	0.015	11.30%	0.003
-13	40.30%	1.622	92.50%	0.012	45.90%	0.002	75.90%	0.015	45.40%	0.003
-11	38.30%	1.544	90.60%	0.012	40.70%	0.002	76.00%	0.015	41.20%	0.003
-10	3.20%	1.512	53.90%	0.012	5.80%	0.002	45.10%	0.015	5.80%	0.003
-9	0.00%	1.469	23.90%	0.012	0.20%	0.002	11.80%	0.015	0.20%	0.003
-8	0.00%	1.399	9.00%	0.012	0.00%	0.002	1.30%	0.014	0.00%	0.003
-7	0.00%	1.387	2.10%	0.012	0.00%	0.002	0.00%	0.015	0.00%	0.003
-6	0.00%	1.343	0.20%	0.012	0.00%	0.002	0.00%	0.015	0.00%	0.003
-5	0.00%	1.315	0.00%	0.012	0.00%	0.002	0.00%	0.015	0.00%	0.003
-4	0.00%	1.281	0.00%	0.012	0.00%	0.002	0.00%	0.015	0.00%	0.003
-3	0.00%	1.277	0.00%	0.012	0.00%	0.002	0.00%	0.015	0.00%	0.003
-2	0.00%	1.252	0.00%	0.012	0.00%	0.002	0.00%	0.015	0.00%	0.003

TABLE 7. Error rates and average execution time for $\alpha_\ell = -14$

	M. Gambini		TPE		T. Kruskal		T. Variance		T. M-Whitney	
α_r	Error	Time	Error	Time	Error	Time	Error	Time	Error	Time
-20	0.00%	1.726	11.00%	0.012	0.00%	0.002	3.40%	0.015	0.00%	0.003
-19	0.00%	1.747	17.30%	0.012	0.40%	0.002	7.20%	0.015	0.40%	0.003
-18	0.30%	1.699	32.70%	0.012	0.70%	0.002	17.50%	0.015	0.70%	0.003
-17	2.50%	1.721	52.50%	0.012	4.80%	0.002	35.60%	0.015	4.80%	0.003
-16	12.10%	1.734	72.60%	0.012	17.90%	0.002	57.70%	0.015	17.90%	0.003
-15	50.20%	1.774	94.90%	0.012	52.90%	0.002	78.60%	0.015	54.10%	0.003
-13	46.10%	1.719	95.60%	0.013	51.20%	0.002	76.60%	0.015	51.30%	0.003
-12	5.80%	1.613	67.40%	0.012	6.40%	0.002	52.40%	0.015	6.40%	0.003
-11	0.70%	1.574	34.00%	0.012	1.10%	0.002	21.80%	0.015	1.10%	0.003
-10	0.00%	1.512	15.30%	0.012	0.10%	0.002	3.50%	0.015	0.10%	0.003
-9	0.00%	1.479	5.70%	0.012	0.00%	0.002	0.70%	0.015	0.00%	0.003
-8	0.00%	1.443	1.00%	0.012	0.00%	0.002	0.00%	0.015	0.00%	0.003
-7	0.00%	1.417	0.30%	0.012	0.00%	0.002	0.00%	0.015	0.00%	0.003
-6	0.00%	1.387	0.10%	0.012	0.00%	0.002	0.00%	0.015	0.00%	0.003
-5	0.00%	1.345	0.00%	0.012	0.00%	0.002	0.00%	0.015	0.00%	0.003
-4	0.00%	1.340	0.00%	0.012	0.00%	0.002	0.00%	0.015	0.00%	0.003
-3	0.00%	1.315	0.00%	0.012	0.00%	0.002	0.00%	0.015	0.00%	0.003
-2	0.00%	1.302	0.00%	0.012	0.00%	0.002	0.00%	0.015	0.00%	0.003

TABLE 8. Error rates and average execution time for $\alpha_\ell = -16$

	M. Gambini		TPE		T. Kruskal		T. Variance		T. M-Whitney	
α_r	Error	Time	Error	Time	Error	Time	Error	Time	Error	Time
-20	0.80%	1.811	37.50%	0.012	1.30%	0.002	27.90%	0.015	1.30%	0.003
-19	4.60%	1.867	59.60%	0.012	8.10%	0.002	44.60%	0.015	8.10%	0.003
-18	18.00%	1.844	81.80%	0.012	20.80%	0.003	66.40%	0.015	20.80%	0.003
-17	57.30%	1.861	97.00%	0.012	59.60%	0.002	80.60%	0.015	59.70%	0.003
-15	55.30%	1.819	96.50%	0.012	57.40%	0.002	78.40%	0.015	57.60%	0.003
-14	11.90%	1.742	74.30%	0.012	12.60%	0.002	59.00%	0.015	12.50%	0.003
-13	1.40%	1.656	43.30%	0.012	2.20%	0.002	33.60%	0.015	2.20%	0.003
-12	0.10%	1.635	24.30%	0.012	0.20%	0.002	10.20%	0.015	0.20%	0.003
-11	0.00%	1.589	12.10%	0.012	0.00%	0.002	1.70%	0.015	0.00%	0.003
-10	0.00%	1.544	3.60%	0.012	0.00%	0.002	0.30%	0.015	0.00%	0.003
-9	0.00%	1.513	1.60%	0.012	0.00%	0.002	0.00%	0.015	0.00%	0.003
-8	0.00%	1.493	0.30%	0.012	0.00%	0.002	0.00%	0.015	0.00%	0.003
-7	0.00%	1.457	0.10%	0.012	0.00%	0.002	0.00%	0.015	0.00%	0.003
-6	0.00%	1.429	0.00%	0.012	0.00%	0.002	0.00%	0.015	0.00%	0.003
-5	0.00%	1.406	0.00%	0.012	0.00%	0.002	0.00%	0.015	0.00%	0.003
-4	0.00%	1.359	0.00%	0.012	0.00%	0.002	0.00%	0.015	0.00%	0.003
-3	0.00%	1.352	0.00%	0.012	0.00%	0.002	0.00%	0.015	0.00%	0.003
-2	0.00%	1.350	0.00%	0.012	0.00%	0.002	0.10%	0.015	0.00%	0.003

TABLE 9. Error rates and average execution time for $\alpha_\ell = -18$

	M. Gambini		TPE		T. Kruskal		T. Variance		T. M-Whitney	
α_r	Error	Time	Error	Time	Error	Time	Error	Time	Error	Time
-20	23.80%	1.995	84.40%	0.012	24.20%	0.002	67.50%	0.015	24.20%	0.003
-19	64.40%	2.013	97.50%	0.012	65.00%	0.002	79.40%	0.015	64.90%	0.003
-17	62.70%	1.893	98.00%	0.012	63.60%	0.002	79.60%	0.015	63.80%	0.003
-16	19.70%	1.853	83.50%	0.012	21.40%	0.002	62.10%	0.015	21.40%	0.003
-15	2.60%	1.777	56.30%	0.012	4.00%	0.002	39.40%	0.015	4.10%	0.003
-14	0.30%	1.746	33.30%	0.012	0.90%	0.002	18.80%	0.015	0.90%	0.003
-13	0.00%	1.669	17.50%	0.012	0.00%	0.002	4.10%	0.015	0.00%	0.003
-12	0.00%	1.638	7.00%	0.012	0.00%	0.002	1.00%	0.015	0.00%	0.003
-11	0.00%	1.600	2.70%	0.012	0.00%	0.002	0.20%	0.015	0.00%	0.003
-10	0.00%	1.564	0.40%	0.012	0.00%	0.002	0.00%	0.015	0.00%	0.003
-9	0.00%	1.538	0.50%	0.012	0.00%	0.002	0.00%	0.015	0.00%	0.003
-8	0.00%	1.508	0.00%	0.012	0.00%	0.002	0.00%	0.015	0.00%	0.003
-7	0.00%	1.495	0.00%	0.012	0.00%	0.002	0.00%	0.015	0.00%	0.003
-6	0.00%	1.461	0.00%	0.012	0.00%	0.002	0.00%	0.015	0.00%	0.003
-5	0.00%	1.436	0.00%	0.012	0.00%	0.002	0.00%	0.015	0.00%	0.003
-4	0.00%	1.406	0.00%	0.012	0.00%	0.002	0.00%	0.015	0.00%	0.003
-3	0.00%	1.404	0.00%	0.012	0.00%	0.002	0.00%	0.015	0.00%	0.003
-2	0.00%	1.387	0.00%	0.012	0.00%	0.002	0.00%	0.015	0.00%	0.003

TABLE 10. Error rates and average execution time for $\alpha_\ell = -20$

	M. Gambini		TPE		T. Kruskal		T. Variance		T. M-Whitney	
α_r	Error	Time	Error	Time	Error	Time	Error	Time	Error	Time
-19	65.40%	2.067	98.20%	0.012	68.60%	0.002	81.50%	0.015	69.50%	0.003
-18	25.70%	1.964	86.70%	0.012	28.80%	0.002	68.30%	0.015	29.10%	0.003
-17	6.10%	1.883	63.20%	0.012	8.30%	0.002	48.00%	0.015	8.10%	0.003
-16	1.50%	1.837	42.80%	0.012	2.70%	0.002	27.80%	0.015	2.70%	0.003
-15	0.20%	1.769	21.70%	0.012	0.80%	0.002	12.30%	0.015	0.80%	0.003
-14	0.00%	1.773	12.50%	0.013	0.00%	0.002	2.90%	0.015	0.00%	0.003
-13	0.00%	1.731	5.60%	0.013	0.00%	0.002	1.20%	0.015	0.00%	0.003
-12	0.00%	1.725	3.80%	0.013	0.00%	0.002	0.00%	0.015	0.00%	0.003
-11	0.00%	1.649	1.40%	0.013	0.00%	0.002	0.00%	0.015	0.00%	0.003
-10	0.00%	1.595	0.10%	0.012	0.00%	0.002	0.00%	0.015	0.00%	0.003
-9	0.00%	1.563	0.00%	0.013	0.00%	0.002	0.00%	0.015	0.00%	0.003
-8	0.00%	1.528	0.00%	0.012	0.00%	0.002	0.00%	0.015	0.00%	0.003
-7	0.00%	1.503	0.00%	0.012	0.00%	0.002	0.00%	0.015	0.00%	0.003
-6	0.00%	1.492	0.00%	0.012	0.00%	0.002	0.00%	0.015	0.00%	0.003
-5	0.00%	1.473	0.00%	0.012	0.00%	0.002	0.00%	0.015	0.00%	0.003
-4	0.00%	1.452	0.00%	0.012	0.00%	0.002	0.00%	0.015	0.00%	0.003
-3	0.00%	1.444	0.00%	0.012	0.00%	0.002	0.00%	0.015	0.00%	0.003
-2	0.00%	1.406	0.00%	0.012	0.00%	0.002	0.00%	0.015	0.00%	0.003

Appendix B

Simulation results for $n = 3$

TABLE 11. Error rates and average execution time for $\alpha_\ell = -3$										
	M. Gambini		TPE		T. Kruskal		T. Variance		T. M-Whitney	
α_r	Error	Time	Error	Time	Error	Time	Error	Time	Error	Time
-20	0.00%	1.252	0.00%	0.012	0.00%	0.002	0.00%	0.015	0.00%	0.003
-19	0.00%	1.216	0.00%	0.012	0.00%	0.002	0.00%	0.015	0.00%	0.003
-18	0.00%	1.205	0.00%	0.012	0.00%	0.002	0.00%	0.014	0.00%	0.003
-17	0.00%	1.355	0.00%	0.012	0.00%	0.002	0.00%	0.015	0.00%	0.003
-16	0.00%	1.144	0.00%	0.012	0.00%	0.002	0.00%	0.015	0.00%	0.003
-15	0.00%	1.136	0.00%	0.012	0.00%	0.002	0.00%	0.015	0.00%	0.003
-14	0.00%	1.132	0.00%	0.012	0.00%	0.002	0.00%	0.015	0.00%	0.003
-13	0.00%	1.141	0.00%	0.012	0.00%	0.002	0.00%	0.015	0.00%	0.003
-12	0.00%	1.151	0.00%	0.012	0.00%	0.002	0.00%	0.015	0.00%	0.003
-11	0.00%	1.137	0.00%	0.012	0.00%	0.002	0.00%	0.015	0.00%	0.003
-10	0.00%	1.127	0.00%	0.012	0.00%	0.002	0.00%	0.014	0.00%	0.003
-9	0.00%	1.127	0.00%	0.012	0.00%	0.002	0.00%	0.015	0.00%	0.003
-8	0.00%	1.149	0.00%	0.012	0.00%	0.002	0.00%	0.015	0.00%	0.003
-7	0.00%	1.142	0.00%	0.012	0.00%	0.002	0.00%	0.015	0.00%	0.003
-6	0.00%	1.127	0.00%	0.012	0.00%	0.002	0.00%	0.015	0.00%	0.003
-5	0.00%	1.137	0.00%	0.012	0.00%	0.002	0.30%	0.015	0.00%	0.003
-4	0.00%	1.117	0.00%	0.012	0.00%	0.002	3.40%	0.015	0.00%	0.003
-2	0.00%	1.090	0.00%	0.012	0.00%	0.002	5.90%	0.015	0.00%	0.003

TABLE 12. Error rates and average execution time for $\alpha_\ell = -4$

	M. Gambini		TPE		T. Kruskal		T. Variance		T. M-Whitney	
α_r	Error	Time	Error	Time	Error	Time	Error	Time	Error	Time
-20	0.00%	1.272	0.00%	0.012	0.00%	0.002	0.00%	0.015	0.00%	0.003
-19	0.00%	1.171	0.00%	0.012	0.00%	0.002	0.00%	0.015	0.00%	0.003
-18	0.00%	1.188	0.00%	0.012	0.00%	0.002	0.00%	0.015	0.00%	0.003
-17	0.00%	1.178	0.00%	0.012	0.00%	0.002	0.00%	0.014	0.00%	0.003
-16	0.00%	1.250	0.00%	0.012	0.00%	0.002	0.00%	0.015	0.00%	0.003
-15	0.00%	1.256	0.00%	0.012	0.00%	0.002	0.00%	0.014	0.00%	0.003
-14	0.00%	1.445	0.00%	0.012	0.00%	0.002	0.00%	0.014	0.00%	0.003
-13	0.00%	1.164	0.00%	0.012	0.00%	0.002	0.00%	0.014	0.00%	0.003
-12	0.00%	1.149	0.00%	0.012	0.00%	0.002	0.00%	0.015	0.00%	0.003
-11	0.00%	1.132	0.00%	0.012	0.00%	0.002	0.00%	0.014	0.00%	0.003
-10	0.00%	1.127	0.00%	0.012	0.00%	0.002	0.00%	0.014	0.00%	0.003
-9	0.00%	1.136	0.00%	0.012	0.00%	0.002	0.00%	0.015	0.00%	0.003
-8	0.00%	1.152	0.00%	0.012	0.00%	0.002	0.00%	0.015	0.00%	0.003
-7	0.00%	1.164	0.00%	0.012	0.00%	0.002	0.00%	0.015	0.00%	0.003
-6	0.00%	1.145	0.00%	0.012	0.00%	0.002	0.00%	0.015	0.00%	0.003
-5	0.00%	1.133	0.50%	0.012	0.00%	0.002	13.40%	0.015	0.00%	0.003
-3	0.00%	1.112	4.00%	0.012	0.00%	0.002	7.50%	0.015	0.00%	0.003
-2	0.00%	1.082	0.00%	0.012	0.00%	0.002	1.00%	0.015	0.00%	0.003

TABLE 13. Error rates and average execution time for $\alpha_\ell = -6$

	M. Gambini		TPE		T. Kruskal		T. Variance		T. M-Whitney	
α_r	Error	Time	Error	Time	Error	Time	Error	Time	Error	Time
-20	0.00%	1.306	0.00%	0.012	0.00%	0.002	0.00%	0.015	0.00%	0.003
-19	0.00%	1.211	0.00%	0.012	0.00%	0.002	0.00%	0.015	0.00%	0.003
-18	0.00%	1.180	0.00%	0.012	0.00%	0.002	0.00%	0.015	0.00%	0.003
-17	0.00%	1.375	0.00%	0.012	0.00%	0.002	0.00%	0.015	0.00%	0.003
-16	0.00%	1.231	0.00%	0.013	0.00%	0.002	0.00%	0.015	0.00%	0.003
-15	0.00%	1.175	0.00%	0.012	0.00%	0.002	0.00%	0.015	0.00%	0.003
-14	0.00%	1.207	0.00%	0.012	0.00%	0.002	0.00%	0.014	0.00%	0.003
-13	0.00%	1.263	0.00%	0.012	0.00%	0.002	0.00%	0.015	0.00%	0.003
-12	0.00%	1.235	0.00%	0.012	0.00%	0.002	0.00%	0.015	0.00%	0.003
-11	0.00%	1.185	0.00%	0.012	0.00%	0.002	0.00%	0.015	0.00%	0.003
-10	0.00%	1.179	0.00%	0.012	0.00%	0.002	0.00%	0.015	0.00%	0.003
-9	0.00%	1.228	0.00%	0.012	0.00%	0.002	0.00%	0.015	0.00%	0.003
-8	0.00%	1.218	0.00%	0.012	0.00%	0.002	0.10%	0.015	0.00%	0.003
-7	0.10%	1.276	9.30%	0.012	0.00%	0.002	44.80%	0.015	0.00%	0.003
-5	0.00%	1.170	0.10%	0.012	0.00%	0.002	49.20%	0.015	0.10%	0.003
-4	0.00%	1.166	0.10%	0.012	0.00%	0.002	0.00%	0.015	0.00%	0.003
-3	0.00%	1.141	0.00%	0.012	0.00%	0.002	0.10%	0.015	0.00%	0.003
-2	0.00%	1.124	0.00%	0.012	0.00%	0.002	0.10%	0.015	0.00%	0.003

TABLE 14. Error rates and average execution time for $\alpha_\ell = -8$

α_r	M. Gambini		TPE		T. Kruskal		T. Variance		T. M-Whitney	
	Error	Time	Error	Time	Error	Time	Error	Time	Error	Time
-20	0.00%	1.351	0.00%	0.012	0.00%	0.002	0.00%	0.015	0.00%	0.003
-19	0.00%	1.186	0.00%	0.012	0.00%	0.002	0.00%	0.015	0.00%	0.003
-18	0.00%	1.229	0.00%	0.012	0.00%	0.002	0.00%	0.015	0.00%	0.003
-17	0.00%	1.277	0.00%	0.012	0.00%	0.002	0.00%	0.015	0.00%	0.003
-16	0.00%	1.268	0.00%	0.012	0.00%	0.002	0.00%	0.015	0.00%	0.003
-15	0.00%	1.506	0.00%	0.012	0.00%	0.002	0.00%	0.015	0.00%	0.003
-14	0.00%	1.231	0.00%	0.012	0.00%	0.002	0.00%	0.015	0.00%	0.003
-13	0.00%	1.196	0.00%	0.012	0.00%	0.002	0.00%	0.015	0.00%	0.003
-12	0.00%	1.232	0.00%	0.012	0.00%	0.002	0.00%	0.015	0.00%	0.003
-11	0.00%	1.262	0.00%	0.012	0.00%	0.002	0.40%	0.015	0.00%	0.003
-10	0.00%	1.252	0.00%	0.012	0.00%	0.002	20.90%	0.015	0.00%	0.003
-9	0.00%	1.279	57.90%	0.012	0.00%	0.002	32.20%	0.015	0.00%	0.003
-7	0.00%	1.269	11.90%	0.012	0.00%	0.002	48.80%	0.015	0.00%	0.003
-6	0.00%	1.237	0.00%	0.012	0.00%	0.002	3.00%	0.015	0.00%	0.003
-5	0.00%	1.172	0.00%	0.012	0.00%	0.002	0.00%	0.015	0.00%	0.003
-4	0.00%	1.141	0.00%	0.012	0.00%	0.002	0.00%	0.015	0.00%	0.003
-3	0.00%	1.136	0.00%	0.012	0.00%	0.002	0.00%	0.015	0.00%	0.003
-2	0.00%	1.157	0.00%	0.012	0.00%	0.002	0.20%	0.015	0.00%	0.003

TABLE 15. Error rates and average execution time for $\alpha_\ell = -10$

α_r	M. Gambini		TPE		T. Kruskal		T. Variance		T. M-Whitney	
	Error	Time	Error	Time	Error	Time	Error	Time	Error	Time
-20	0.00%	1.369	0.00%	0.013	0.00%	0.002	0.00%	0.015	0.00%	0.003
-19	0.00%	1.337	0.00%	0.012	0.00%	0.002	0.00%	0.015	0.00%	0.003
-18	0.00%	1.277	0.00%	0.012	0.00%	0.002	0.00%	0.015	0.00%	0.003
-17	0.00%	1.348	0.00%	0.012	0.00%	0.002	0.00%	0.015	0.00%	0.003
-16	0.00%	1.280	0.00%	0.012	0.00%	0.002	0.00%	0.015	0.00%	0.003
-15	0.00%	1.298	0.00%	0.012	0.00%	0.002	0.00%	0.015	0.00%	0.003
-14	0.00%	1.273	0.00%	0.012	0.00%	0.002	0.00%	0.015	0.00%	0.003
-13	0.00%	1.349	19.90%	0.012	0.00%	0.002	5.00%	0.015	0.00%	0.003
-12	0.00%	1.297	0.50%	0.012	0.00%	0.002	56.20%	0.015	0.00%	0.003
-11	0.10%	1.278	87.80%	0.012	0.00%	0.002	33.10%	0.015	0.00%	0.003
-9	1.20%	1.312	3.80%	0.012	0.40%	0.002	74.50%	0.015	0.40%	0.003
-8	0.00%	1.296	47.30%	0.012	0.00%	0.002	6.10%	0.015	0.00%	0.003
-7	0.00%	1.235	0.00%	0.012	0.00%	0.002	0.00%	0.015	0.00%	0.003
-6	0.00%	1.169	0.00%	0.012	0.00%	0.002	0.00%	0.015	0.00%	0.003
-5	0.00%	1.164	0.00%	0.012	0.00%	0.002	0.00%	0.015	0.00%	0.003
-4	0.00%	1.183	0.00%	0.012	0.00%	0.002	0.00%	0.015	0.00%	0.003
-3	0.00%	1.146	0.00%	0.012	0.00%	0.002	0.00%	0.015	0.00%	0.003
-2	0.00%	1.123	0.00%	0.012	0.00%	0.002	0.20%	0.015	0.00%	0.003

TABLE 16. Error rates and average execution time for $\alpha_\ell = -12$

α_r	M. Gambini		TPE		T. Kruskal		T. Variance		T. M-Whitney	
	Error	Time	Error	Time	Error	Time	Error	Time	Error	Time
-20	0.00%	1.555	0.00%	0.006	0.00%	0.001	0.00%	0.007	0.00%	0.002
-19	0.00%	1.963	0.00%	0.006	0.00%	0.001	0.00%	0.007	0.00%	0.002
-18	0.00%	1.509	0.00%	0.006	0.00%	0.002	0.00%	0.008	0.00%	0.002
-17	0.00%	1.598	0.00%	0.007	0.00%	0.002	0.00%	0.009	0.00%	0.003
-16	0.00%	1.639	0.00%	0.008	0.00%	0.002	0.00%	0.009	0.00%	0.003
-15	0.00%	1.636	2.00%	0.007	0.00%	0.002	21.50%	0.008	0.00%	0.002
-14	0.40%	1.452	1.50%	0.007	0.10%	0.002	22.50%	0.009	0.10%	0.002
-13	14.90%	1.430	49.50%	0.007	31.50%	0.002	50.30%	0.008	31.60%	0.002
-11	26.40%	1.491	41.70%	0.007	24.50%	0.002	88.80%	0.008	25.20%	0.002
-10	0.00%	1.417	71.20%	0.006	0.00%	0.002	16.40%	0.008	0.00%	0.002
-9	0.00%	1.448	0.00%	0.006	0.00%	0.001	0.00%	0.008	0.00%	0.002
-8	0.00%	1.405	0.00%	0.007	0.00%	0.002	0.10%	0.009	0.00%	0.002
-7	0.00%	1.315	0.00%	0.007	0.00%	0.002	0.00%	0.008	0.00%	0.002
-6	0.00%	1.098	0.00%	0.005	0.00%	0.002	0.00%	0.007	0.00%	0.002
-5	0.00%	1.038	0.00%	0.005	0.00%	0.001	0.00%	0.006	0.00%	0.002
-4	0.00%	1.074	0.00%	0.005	0.00%	0.001	0.00%	0.006	0.00%	0.002
-3	0.00%	0.982	0.00%	0.005	0.00%	0.002	0.00%	0.006	0.00%	0.002
-2	0.00%	0.938	0.00%	0.006	0.00%	0.001	0.10%	0.006	0.00%	0.002

TABLE 17. Error rates and average execution time for $\alpha_\ell = -14$

α_r	M. Gambini		TPE		T. Kruskal		T. Variance		T. M-Whitney	
	Error	Time	Error	Time	Error	Time	Error	Time	Error	Time
-20	0.00%	1.738	0.00%	0.006	0.00%	0.002	0.50%	0.007	0.00%	0.002
-19	0.00%	1.644	0.00%	0.007	0.00%	0.002	0.00%	0.008	0.00%	0.003
-18	0.00%	1.784	1.20%	0.007	0.00%	0.002	2.30%	0.008	0.00%	0.002
-17	0.00%	1.494	0.00%	0.007	0.00%	0.002	0.60%	0.008	0.00%	0.002
-16	0.50%	1.604	37.20%	0.006	1.30%	0.002	11.20%	0.008	1.30%	0.002
-15	0.00%	1.607	56.90%	0.006	0.00%	0.002	85.40%	0.008	0.00%	0.002
-13	0.70%	1.607	35.80%	0.007	0.00%	0.002	88.60%	0.008	0.00%	0.002
-12	0.00%	1.547	4.20%	0.007	0.00%	0.002	43.10%	0.008	0.00%	0.002
-11	0.00%	1.506	0.40%	0.007	0.00%	0.002	1.30%	0.008	0.00%	0.002
-10	0.00%	1.354	0.00%	0.007	0.00%	0.002	0.10%	0.008	0.00%	0.002
-9	0.00%	1.324	0.00%	0.007	0.00%	0.002	0.00%	0.008	0.00%	0.002
-8	0.00%	1.141	0.00%	0.006	0.00%	0.002	0.00%	0.007	0.00%	0.002
-7	0.00%	1.190	0.00%	0.006	0.00%	0.002	0.00%	0.008	0.00%	0.002
-6	0.00%	1.302	0.00%	0.006	0.00%	0.002	0.00%	0.007	0.00%	0.002
-5	0.00%	1.124	0.00%	0.006	0.00%	0.001	0.00%	0.007	0.00%	0.002
-4	0.00%	1.540	0.00%	0.006	0.00%	0.002	0.00%	0.007	0.00%	0.002
-3	0.00%	1.119	0.00%	0.006	0.00%	0.002	0.00%	0.007	0.00%	0.002
-2	0.00%	1.140	0.00%	0.006	0.00%	0.001	0.00%	0.007	0.00%	0.002

TABLE 18. Error rates and average execution time for $\alpha_\ell = -16$

	M. Gambini		TPE		T. Kruskal		T. Variance		T. M-Whitney	
α_r	Error	Time	Error	Time	Error	Time	Error	Time	Error	Time
-20	0.00%	1.586	0.00%	0.012	0.00%	0.002	28.10%	0.015	0.00%	0.003
-19	0.00%	1.264	0.60%	0.012	0.00%	0.002	7.80%	0.015	0.00%	0.003
-18	0.00%	1.419	50.30%	0.012	0.00%	0.002	51.60%	0.015	0.00%	0.003
-17	0.00%	1.366	26.80%	0.012	0.00%	0.002	17.30%	0.015	0.00%	0.003
-15	41.30%	1.413	100.00%	0.012	43.70%	0.002	84.70%	0.015	43.60%	0.003
-14	0.00%	1.456	6.20%	0.012	1.50%	0.002	30.40%	0.015	1.60%	0.003
-13	0.00%	1.418	0.00%	0.012	0.00%	0.002	12.20%	0.015	0.00%	0.003
-12	0.00%	1.369	0.00%	0.013	0.00%	0.002	0.60%	0.015	0.00%	0.003
-11	0.00%	1.395	0.00%	0.012	0.00%	0.002	0.00%	0.015	0.00%	0.003
-10	0.00%	1.266	0.00%	0.012	0.00%	0.002	0.00%	0.015	0.00%	0.003
-9	0.00%	1.252	0.00%	0.012	0.00%	0.002	0.00%	0.015	0.00%	0.003
-8	0.00%	1.238	0.00%	0.012	0.00%	0.002	0.00%	0.015	0.00%	0.003
-7	0.00%	1.334	0.00%	0.012	0.00%	0.002	0.00%	0.015	0.00%	0.003
-6	0.00%	1.255	0.00%	0.012	0.00%	0.002	0.00%	0.015	0.00%	0.003
-5	0.00%	1.229	0.00%	0.012	0.00%	0.002	0.00%	0.015	0.00%	0.003
-4	0.00%	1.248	0.00%	0.012	0.00%	0.002	0.00%	0.015	0.00%	0.003
-3	0.00%	1.144	0.00%	0.012	0.00%	0.002	0.00%	0.015	0.00%	0.003
-2	0.00%	1.230	0.00%	0.012	0.00%	0.002	0.00%	0.015	0.00%	0.003

TABLE 19. Error rates and average execution time for $\alpha_\ell = -18$

	M. Gambini		TPE		T. Kruskal		T. Variance		T. M-Whitney	
α_r	Error	Time	Error	Time	Error	Time	Error	Time	Error	Time
-20	0.30%	1.866	7.50%	0.005	0.50%	0.001	76.80%	0.006	0.50%	0.002
-19	15.70%	1.417	33.30%	0.005	13.10%	0.001	83.20%	0.006	13.10%	0.002
-17	31.30%	1.324	99.50%	0.006	11.20%	0.001	87.00%	0.006	11.20%	0.002
-16	0.00%	1.278	2.90%	0.005	0.00%	0.002	20.00%	0.006	0.00%	0.002
-15	0.00%	1.206	0.00%	0.005	0.00%	0.001	13.30%	0.006	0.00%	0.002
-14	0.00%	1.351	6.10%	0.005	0.00%	0.002	17.20%	0.007	0.00%	0.002
-13	0.00%	1.182	0.00%	0.006	0.00%	0.001	0.00%	0.006	0.00%	0.002
-12	0.00%	1.097	0.00%	0.006	0.00%	0.001	0.00%	0.006	0.00%	0.002
-11	0.00%	1.303	0.00%	0.005	0.00%	0.001	0.00%	0.007	0.00%	0.002
-10	0.00%	1.264	0.00%	0.005	0.00%	0.001	0.00%	0.007	0.00%	0.002
-9	0.00%	1.133	0.00%	0.005	0.00%	0.001	0.00%	0.007	0.00%	0.002
-8	0.00%	1.046	0.00%	0.005	0.00%	0.001	0.00%	0.006	0.00%	0.002
-7	0.00%	1.378	0.00%	0.005	0.00%	0.001	0.00%	0.006	0.00%	0.002
-6	0.00%	1.097	0.00%	0.005	0.00%	0.001	0.00%	0.006	0.00%	0.002
-5	0.00%	1.062	0.00%	0.005	0.00%	0.001	0.00%	0.006	0.00%	0.002
-4	0.00%	1.056	0.00%	0.005	0.00%	0.001	0.00%	0.006	0.00%	0.002
-3	0.00%	1.055	0.00%	0.005	0.00%	0.001	0.00%	0.006	0.00%	0.002
-2	0.00%	1.021	0.00%	0.005	0.00%	0.001	0.00%	0.006	0.00%	0.002

TABLE 20. Error rates and average execution time for $\alpha_\ell = -20$

	M. Gambini		TPE		T. Kruskal		T. Variance		T. M-Whitney	
α_r	Error	Time	Error	Time	Error	Time	Error	Time	Error	Time
-19	87.40%	2.411	100.00%	0.007	89.30%	0.002	77.70%	0.008	89.90%	0.002
-18	1.00%	2.052	45.80%	0.006	0.00%	0.002	19.70%	0.007	0.50%	0.002
-17	3.60%	1.636	10.50%	0.006	3.30%	0.001	48.60%	0.007	3.30%	0.002
-16	0.00%	1.387	0.00%	0.006	0.00%	0.001	2.20%	0.007	0.00%	0.002
-15	0.00%	1.474	0.00%	0.006	0.00%	0.001	1.60%	0.007	0.00%	0.002
-14	0.00%	1.253	0.00%	0.006	0.00%	0.002	0.00%	0.007	0.00%	0.002
-13	0.00%	1.693	0.00%	0.006	0.00%	0.001	0.00%	0.007	0.00%	0.002
-12	0.00%	1.645	0.00%	0.006	0.00%	0.002	0.00%	0.007	0.00%	0.002
-11	0.00%	1.248	0.00%	0.006	0.00%	0.001	0.00%	0.006	0.00%	0.002
-10	0.00%	1.264	0.00%	0.005	0.00%	0.001	0.00%	0.006	0.00%	0.002
-9	0.00%	1.092	0.00%	0.005	0.00%	0.001	0.00%	0.006	0.00%	0.002
-8	0.00%	1.153	0.00%	0.005	0.00%	0.001	0.00%	0.006	0.00%	0.002
-7	0.00%	1.281	0.00%	0.005	0.00%	0.001	0.00%	0.007	0.00%	0.002
-6	0.00%	1.056	0.00%	0.006	0.00%	0.001	0.00%	0.006	0.00%	0.002
-5	0.00%	1.081	0.00%	0.005	0.00%	0.001	0.00%	0.006	0.00%	0.002
-4	0.00%	1.140	0.00%	0.006	0.00%	0.001	0.00%	0.006	0.00%	0.002
-3	0.00%	1.177	0.00%	0.006	0.00%	0.002	0.00%	0.007	0.00%	0.002
-2	0.00%	1.587	0.00%	0.007	0.00%	0.002	0.00%	0.008	0.00%	0.002

Appendix C

Simulation results for $n = 8$

TABLE 21. Error rates and average execution time for $\alpha_\ell = -3$										
	M. Gambini		TPE		T. Kruskal		T. Variance		T. M-Whitney	
α_r	Error	Time	Error	Time	Error	Time	Error	Time	Error	Time
-20	0.00%	1.255	0.00%	0.007	0.00%	0.002	0.00%	0.009	0.00%	0.003
-19	0.00%	1.110	0.00%	0.006	0.00%	0.002	0.00%	0.007	0.00%	0.002
-18	0.00%	1.082	0.00%	0.006	0.00%	0.002	0.00%	0.007	0.00%	0.002
-17	0.00%	1.121	0.00%	0.006	0.00%	0.001	0.00%	0.007	0.00%	0.002
-16	0.00%	1.111	0.00%	0.006	0.00%	0.001	0.00%	0.007	0.00%	0.002
-15	0.00%	1.116	0.00%	0.006	0.00%	0.002	0.00%	0.007	0.00%	0.002
-14	0.00%	1.052	0.00%	0.006	0.00%	0.001	0.00%	0.007	0.00%	0.002
-13	0.00%	1.032	0.00%	0.005	0.00%	0.002	0.00%	0.007	0.00%	0.002
-12	0.00%	1.038	0.00%	0.005	0.00%	0.002	0.00%	0.007	0.00%	0.002
-11	0.00%	0.991	0.00%	0.006	0.00%	0.001	0.10%	0.007	0.00%	0.002
-10	0.00%	1.000	0.00%	0.006	0.00%	0.001	0.00%	0.006	0.00%	0.002
-9	0.00%	1.011	0.00%	0.006	0.00%	0.001	0.00%	0.006	0.00%	0.002
-8	0.00%	1.065	0.00%	0.006	0.00%	0.001	0.00%	0.007	0.00%	0.002
-7	0.00%	1.008	0.00%	0.006	0.00%	0.001	0.00%	0.006	0.00%	0.002
-6	0.00%	1.030	0.00%	0.006	0.00%	0.002	0.00%	0.007	0.00%	0.002
-5	0.00%	1.010	0.00%	0.006	0.00%	0.002	0.10%	0.007	0.00%	0.002
-4	0.00%	0.949	0.10%	0.005	0.00%	0.001	3.60%	0.006	0.00%	0.002
-2	0.00%	0.953	0.00%	0.005	0.00%	0.001	6.20%	0.006	0.00%	0.002

TABLE 22. Error rates and average execution time for $\alpha_\ell = -4$

α_r	M. Gambini		TPE		T. Kruskal		T. Variance		T. M-Whitney	
	Error	Time	Error	Time	Error	Time	Error	Time	Error	Time
-20	0.00%	0.983	0.00%	0.005	0.00%	0.001	0.00%	0.006	0.00%	0.002
-19	0.00%	1.125	0.00%	0.006	0.00%	0.001	0.00%	0.007	0.00%	0.002
-18	0.00%	0.988	0.00%	0.005	0.00%	0.001	0.00%	0.006	0.00%	0.002
-17	0.00%	1.035	0.00%	0.005	0.00%	0.001	0.00%	0.006	0.00%	0.002
-16	0.00%	0.978	0.00%	0.005	0.00%	0.001	0.00%	0.006	0.00%	0.002
-15	0.00%	1.002	0.00%	0.005	0.00%	0.001	0.00%	0.006	0.00%	0.002
-14	0.00%	0.974	0.00%	0.005	0.00%	0.001	0.00%	0.006	0.00%	0.002
-13	0.00%	0.984	0.00%	0.005	0.00%	0.001	0.00%	0.006	0.00%	0.002
-12	0.00%	0.975	0.00%	0.005	0.00%	0.001	0.00%	0.006	0.00%	0.002
-11	0.00%	0.989	0.00%	0.005	0.00%	0.001	0.00%	0.006	0.00%	0.002
-10	0.00%	0.958	0.00%	0.005	0.00%	0.001	0.00%	0.006	0.00%	0.002
-9	0.00%	0.975	0.00%	0.005	0.00%	0.001	0.00%	0.006	0.00%	0.002
-8	0.00%	0.965	0.00%	0.005	0.00%	0.001	0.00%	0.006	0.00%	0.002
-7	0.00%	0.974	0.00%	0.005	0.00%	0.001	0.00%	0.006	0.00%	0.002
-6	0.00%	0.970	0.00%	0.005	0.00%	0.001	0.10%	0.006	0.00%	0.002
-5	0.00%	0.959	3.10%	0.005	0.00%	0.001	6.50%	0.006	0.00%	0.002
-3	0.00%	0.937	1.20%	0.005	0.00%	0.001	4.20%	0.006	0.00%	0.002
-2	0.00%	0.914	0.00%	0.005	0.00%	0.001	0.50%	0.006	0.00%	0.002

TABLE 23. Error rates and average execution time for $\alpha_\ell = -6$

α_r	M. Gambini		TPE		T. Kruskal		T. Variance		T. M-Whitney	
	Error	Time	Error	Time	Error	Time	Error	Time	Error	Time
-20	0.00%	1.105	0.00%	0.006	0.00%	0.001	0.00%	0.007	0.00%	0.002
-19	0.00%	1.303	0.00%	0.007	0.00%	0.002	0.00%	0.008	0.00%	0.002
-18	0.00%	1.364	0.00%	0.007	0.00%	0.002	0.00%	0.009	0.00%	0.002
-17	0.00%	1.282	0.00%	0.006	0.00%	0.002	0.00%	0.008	0.00%	0.002
-16	0.00%	1.160	0.00%	0.006	0.00%	0.002	0.00%	0.007	0.00%	0.002
-15	0.00%	1.257	0.00%	0.006	0.00%	0.002	0.00%	0.008	0.00%	0.002
-14	0.00%	1.224	0.00%	0.006	0.00%	0.002	0.00%	0.008	0.00%	0.002
-13	0.00%	1.186	0.00%	0.006	0.00%	0.001	0.00%	0.007	0.00%	0.002
-12	0.00%	1.246	0.00%	0.006	0.00%	0.002	0.00%	0.008	0.00%	0.002
-11	0.00%	1.180	0.00%	0.006	0.00%	0.002	0.00%	0.007	0.00%	0.002
-10	0.00%	1.132	0.00%	0.006	0.00%	0.001	0.00%	0.007	0.00%	0.002
-9	0.00%	1.220	0.00%	0.006	0.00%	0.002	0.00%	0.008	0.00%	0.002
-8	0.00%	1.176	0.00%	0.006	0.00%	0.002	0.40%	0.008	0.00%	0.002
-7	0.00%	1.244	12.30%	0.006	0.00%	0.001	46.50%	0.007	0.00%	0.002
-5	0.00%	1.131	4.90%	0.006	0.00%	0.002	14.40%	0.007	0.00%	0.002
-4	0.00%	1.153	0.00%	0.006	0.00%	0.002	0.00%	0.008	0.00%	0.002
-3	0.00%	1.179	0.00%	0.006	0.00%	0.002	0.10%	0.008	0.00%	0.002
-2	0.00%	1.113	0.00%	0.006	0.00%	0.001	0.30%	0.008	0.00%	0.002

TABLE 24. Error rates and average execution time for $\alpha_\ell = -8$

α_r	M. Gambini		TPE		T. Kruskal		T. Variance		T. M-Whitney	
	Error	Time	Error	Time	Error	Time	Error	Time	Error	Time
-20	0.00%	1.145	0.00%	0.006	0.00%	0.001	0.00%	0.007	0.00%	0.002
-19	0.00%	1.106	0.00%	0.006	0.00%	0.001	0.00%	0.007	0.00%	0.002
-18	0.00%	1.485	0.00%	0.008	0.00%	0.002	0.00%	0.010	0.00%	0.003
-17	0.00%	1.415	0.00%	0.008	0.00%	0.002	0.00%	0.009	0.00%	0.002
-16	0.00%	1.215	0.00%	0.006	0.00%	0.002	0.00%	0.007	0.00%	0.002
-15	0.00%	1.193	0.00%	0.006	0.00%	0.001	0.00%	0.007	0.00%	0.002
-14	0.00%	1.279	0.00%	0.006	0.00%	0.002	0.00%	0.008	0.00%	0.002
-13	0.00%	1.212	0.00%	0.006	0.00%	0.002	0.00%	0.007	0.00%	0.002
-12	0.00%	1.211	0.00%	0.006	0.00%	0.002	0.10%	0.008	0.00%	0.002
-11	0.00%	1.207	0.00%	0.006	0.00%	0.002	0.70%	0.007	0.00%	0.002
-10	0.00%	1.121	0.00%	0.006	0.00%	0.001	4.40%	0.007	0.00%	0.002
-9	0.00%	1.091	10.30%	0.005	0.00%	0.001	41.50%	0.006	0.00%	0.002
-7	0.20%	1.160	66.50%	0.006	0.00%	0.001	58.00%	0.007	0.10%	0.002
-6	0.00%	1.084	0.00%	0.006	0.00%	0.001	1.20%	0.007	0.00%	0.002
-5	0.00%	1.026	0.00%	0.005	0.00%	0.002	0.00%	0.007	0.00%	0.002
-4	0.00%	1.130	0.00%	0.007	0.00%	0.002	0.00%	0.007	0.00%	0.002
-3	0.00%	0.998	0.00%	0.006	0.00%	0.001	0.00%	0.007	0.00%	0.002
-2	0.00%	1.098	0.00%	0.006	0.00%	0.002	0.10%	0.008	0.00%	0.002

TABLE 25. Error rates and average execution time for $\alpha_\ell = -10$

α_r	M. Gambini		TPE		T. Kruskal		T. Variance		T. M-Whitney	
	Error	Time	Error	Time	Error	Time	Error	Time	Error	Time
-20	0.00%	1.159	0.00%	0.006	0.00%	0.002	0.00%	0.007	0.00%	0.002
-19	0.00%	1.251	0.00%	0.007	0.00%	0.002	0.00%	0.007	0.00%	0.002
-18	0.00%	1.279	0.00%	0.006	0.00%	0.002	0.00%	0.007	0.00%	0.002
-17	0.00%	1.124	0.00%	0.006	0.00%	0.001	0.00%	0.006	0.00%	0.002
-16	0.00%	1.074	0.00%	0.005	0.00%	0.001	0.00%	0.006	0.00%	0.002
-15	0.00%	1.067	0.00%	0.005	0.00%	0.001	0.00%	0.006	0.00%	0.002
-14	0.00%	1.079	0.00%	0.005	0.00%	0.001	0.00%	0.006	0.00%	0.002
-13	0.00%	1.113	0.00%	0.005	0.00%	0.001	0.80%	0.006	0.00%	0.002
-12	0.00%	1.093	0.00%	0.005	0.00%	0.001	11.50%	0.006	0.00%	0.002
-11	0.00%	1.079	31.80%	0.005	0.00%	0.001	63.90%	0.006	0.00%	0.002
-9	0.00%	1.103	8.20%	0.005	0.00%	0.001	46.50%	0.006	0.00%	0.002
-8	0.00%	1.067	0.10%	0.005	0.00%	0.001	2.30%	0.006	0.00%	0.002
-7	0.00%	1.035	0.00%	0.005	0.00%	0.002	0.00%	0.006	0.00%	0.002
-6	0.00%	1.008	0.00%	0.005	0.00%	0.001	0.00%	0.006	0.00%	0.002
-5	0.00%	0.987	0.00%	0.005	0.00%	0.001	0.00%	0.006	0.00%	0.002
-4	0.00%	0.967	0.00%	0.005	0.00%	0.001	0.00%	0.006	0.00%	0.002
-3	0.00%	0.955	0.00%	0.005	0.00%	0.002	0.00%	0.006	0.00%	0.002
-2	0.00%	0.938	0.00%	0.005	0.00%	0.001	0.10%	0.006	0.00%	0.002

TABLE 26. Error rates and average execution time for $\alpha_\ell = -12$

	M. Gambini		TPE		T. Kruskal		T. Variance		T. M-Whitney	
α_r	Error	Time	Error	Time	Error	Time	Error	Time	Error	Time
-20	0.00%	1.129	0.00%	0.006	0.00%	0.001	0.00%	0.006	0.00%	0.002
-19	0.00%	1.159	0.00%	0.006	0.00%	0.002	0.00%	0.007	0.00%	0.002
-18	0.00%	1.243	0.00%	0.006	0.00%	0.002	0.10%	0.007	0.00%	0.002
-17	0.00%	1.344	0.00%	0.006	0.00%	0.002	0.00%	0.008	0.00%	0.002
-16	0.00%	1.376	0.00%	0.006	0.00%	0.002	0.20%	0.008	0.00%	0.002
-15	0.00%	1.301	0.00%	0.006	0.00%	0.002	0.50%	0.008	0.00%	0.002
-14	0.00%	1.318	0.00%	0.006	0.00%	0.001	35.50%	0.008	0.00%	0.002
-13	0.30%	1.303	37.30%	0.006	0.40%	0.001	47.10%	0.007	0.40%	0.002
-11	1.20%	1.326	11.70%	0.007	1.30%	0.002	67.90%	0.008	1.30%	0.002
-10	0.00%	1.254	17.70%	0.006	0.00%	0.002	5.90%	0.007	0.00%	0.002
-9	0.00%	1.214	0.00%	0.006	0.00%	0.002	0.60%	0.007	0.00%	0.002
-8	0.00%	1.161	0.00%	0.006	0.00%	0.001	0.00%	0.007	0.00%	0.002
-7	0.00%	1.242	0.00%	0.006	0.00%	0.002	0.00%	0.008	0.00%	0.002
-6	0.00%	1.262	0.00%	0.007	0.00%	0.001	0.00%	0.008	0.00%	0.002
-5	0.00%	1.310	0.00%	0.008	0.00%	0.002	0.00%	0.010	0.00%	0.003
-4	0.00%	1.388	0.00%	0.008	0.00%	0.002	0.00%	0.011	0.00%	0.003
-3	0.00%	1.324	0.00%	0.008	0.00%	0.002	0.00%	0.010	0.00%	0.003
-2	0.00%	1.253	0.00%	0.007	0.00%	0.002	0.00%	0.009	0.00%	0.002

TABLE 27. Error rates and average execution time for $\alpha_\ell = -14$

	M. Gambini		TPE		T. Kruskal		T. Variance		T. M-Whitney	
α_r	Error	Time	Error	Time	Error	Time	Error	Time	Error	Time
-20	0.00%	1.250	0.00%	0.006	0.00%	0.001	0.00%	0.007	0.00%	0.002
-19	0.00%	1.631	0.00%	0.008	0.00%	0.002	0.40%	0.010	0.00%	0.003
-18	0.00%	1.390	0.00%	0.007	0.00%	0.002	0.90%	0.008	0.00%	0.002
-17	0.00%	1.385	0.50%	0.007	0.00%	0.002	5.40%	0.008	0.00%	0.002
-16	0.00%	1.392	7.90%	0.007	0.10%	0.002	63.50%	0.008	0.10%	0.002
-15	0.10%	1.274	91.70%	0.006	0.10%	0.001	60.20%	0.007	0.10%	0.002
-13	39.70%	1.149	60.90%	0.005	31.70%	0.001	78.00%	0.006	31.80%	0.002
-12	0.00%	1.110	0.10%	0.005	0.00%	0.001	20.50%	0.006	0.00%	0.002
-11	0.00%	1.104	0.00%	0.005	0.00%	0.001	7.70%	0.006	0.00%	0.002
-10	0.00%	1.078	0.00%	0.005	0.00%	0.001	0.10%	0.006	0.00%	0.002
-9	0.00%	1.086	0.00%	0.005	0.00%	0.001	0.00%	0.006	0.00%	0.002
-8	0.00%	1.028	0.00%	0.005	0.00%	0.001	0.00%	0.006	0.00%	0.002
-7	0.00%	1.080	0.00%	0.005	0.00%	0.001	0.00%	0.006	0.00%	0.002
-6	0.00%	1.026	0.00%	0.005	0.00%	0.001	0.00%	0.006	0.00%	0.002
-5	0.00%	0.984	0.00%	0.005	0.00%	0.001	0.00%	0.006	0.00%	0.002
-4	0.00%	0.983	0.00%	0.005	0.00%	0.002	0.00%	0.006	0.00%	0.002
-3	0.00%	0.950	0.00%	0.005	0.00%	0.001	0.00%	0.006	0.00%	0.002
-2	0.00%	0.948	0.00%	0.005	0.00%	0.001	0.10%	0.006	0.00%	0.002

TABLE 28. Error rates and average execution time for $\alpha_\ell = -16$

	M. Gambini		TPE		T. Kruskal		T. Variance		T. M-Whitney	
α_r	Error	Time	Error	Time	Error	Time	Error	Time	Error	Time
-20	0.00%	1.199	0.40%	0.006	0.00%	0.001	4.90%	0.006	0.00%	0.002
-19	0.00%	1.273	0.80%	0.006	0.00%	0.001	47.60%	0.007	0.00%	0.002
-18	0.00%	1.473	4.80%	0.007	0.00%	0.002	13.00%	0.008	0.00%	0.002
-17	10.20%	1.406	61.90%	0.006	9.90%	0.001	87.00%	0.007	9.90%	0.002
-15	5.40%	1.627	37.10%	0.007	6.20%	0.002	78.00%	0.009	6.20%	0.003
-14	0.00%	1.586	8.10%	0.007	0.00%	0.002	8.90%	0.010	0.00%	0.003
-13	0.00%	1.457	0.10%	0.007	0.00%	0.002	4.70%	0.009	0.00%	0.002
-12	0.00%	1.454	0.00%	0.007	0.00%	0.002	3.50%	0.008	0.00%	0.002
-11	0.00%	1.383	0.00%	0.007	0.00%	0.002	0.00%	0.008	0.00%	0.002
-10	0.00%	1.319	0.00%	0.007	0.00%	0.002	0.00%	0.008	0.00%	0.002
-9	0.00%	1.208	0.00%	0.006	0.00%	0.002	0.00%	0.007	0.00%	0.002
-8	0.00%	1.204	0.00%	0.006	0.00%	0.001	0.00%	0.007	0.00%	0.002
-7	0.00%	1.223	0.00%	0.006	0.00%	0.002	0.00%	0.008	0.00%	0.002
-6	0.00%	1.192	0.00%	0.006	0.00%	0.002	0.00%	0.007	0.00%	0.002
-5	0.00%	1.038	0.00%	0.005	0.00%	0.001	0.00%	0.006	0.00%	0.002
-4	0.00%	1.069	0.00%	0.005	0.00%	0.002	0.00%	0.007	0.00%	0.002
-3	0.00%	0.990	0.00%	0.005	0.00%	0.001	0.00%	0.006	0.00%	0.002
-2	0.00%	0.973	0.00%	0.005	0.00%	0.001	0.10%	0.006	0.00%	0.002

TABLE 29. Error rates and average execution time for $\alpha_\ell = -18$

	M. Gambini		TPE		T. Kruskal		T. Variance		T. M-Whitney	
α_r	Error	Time	Error	Time	Error	Time	Error	Time	Error	Time
-20	0.00%	1.427	63.70%	0.006	0.00%	0.002	60.40%	0.008	0.00%	0.002
-19	3.10%	1.478	34.90%	0.007	3.40%	0.002	43.70%	0.008	3.40%	0.002
-17	1.70%	1.423	38.30%	0.007	1.50%	0.001	66.40%	0.008	1.80%	0.002
-16	0.20%	1.573	1.90%	0.007	0.30%	0.002	69.60%	0.008	0.30%	0.002
-15	0.00%	1.387	0.10%	0.006	0.00%	0.002	11.50%	0.007	0.00%	0.002
-14	0.00%	1.326	0.00%	0.006	0.00%	0.002	0.50%	0.007	0.00%	0.002
-13	0.00%	1.400	0.00%	0.006	0.00%	0.002	0.00%	0.008	0.00%	0.002
-12	0.00%	1.442	0.00%	0.008	0.00%	0.002	0.00%	0.009	0.00%	0.002
-11	0.00%	1.488	0.00%	0.008	0.00%	0.002	0.00%	0.010	0.00%	0.003
-10	0.00%	1.574	0.00%	0.009	0.00%	0.002	0.00%	0.010	0.00%	0.003
-9	0.00%	1.455	0.00%	0.008	0.00%	0.002	0.00%	0.010	0.00%	0.003
-8	0.00%	1.405	0.00%	0.007	0.00%	0.002	0.00%	0.009	0.00%	0.003
-7	0.00%	1.278	0.00%	0.007	0.00%	0.002	0.00%	0.008	0.00%	0.003
-6	0.00%	1.046	0.00%	0.005	0.00%	0.001	0.00%	0.006	0.00%	0.002
-5	0.00%	0.989	0.00%	0.005	0.00%	0.001	0.00%	0.006	0.00%	0.002
-4	0.00%	1.025	0.00%	0.005	0.00%	0.001	0.00%	0.006	0.00%	0.002
-3	0.00%	0.976	0.00%	0.005	0.00%	0.001	0.00%	0.006	0.00%	0.002
-2	0.00%	0.970	0.00%	0.005	0.00%	0.001	0.00%	0.006	0.00%	0.002

TABLE 30. Error rates and average execution time for $\alpha_\ell = -20$

	M. Gambini		TPE		T. Kruskal		T. Variance		T. M-Whitney	
α_r	Error	Time	Error	Time	Error	Time	Error	Time	Error	Time
-19	5.80%	1.368	58.70%	0.006	5.50%	0.001	93.80%	0.007	5.50%	0.002
-18	0.00%	1.384	2.00%	0.006	0.10%	0.002	40.80%	0.007	0.20%	0.002
-17	0.00%	1.546	15.90%	0.006	0.00%	0.001	10.50%	0.008	0.00%	0.002
-16	0.00%	1.241	0.00%	0.006	0.00%	0.001	3.30%	0.007	0.00%	0.002
-15	0.00%	1.227	0.00%	0.005	0.00%	0.001	0.10%	0.007	0.00%	0.002
-14	0.00%	1.231	0.00%	0.005	0.00%	0.001	0.00%	0.007	0.00%	0.002
-13	0.00%	1.209	0.00%	0.006	0.00%	0.002	0.00%	0.007	0.00%	0.002
-12	0.00%	1.141	0.00%	0.006	0.00%	0.001	0.00%	0.006	0.00%	0.002
-11	0.00%	1.135	0.00%	0.005	0.00%	0.001	0.00%	0.007	0.00%	0.002
-10	0.00%	1.188	0.00%	0.006	0.00%	0.001	0.00%	0.007	0.00%	0.002
-9	0.00%	1.111	0.00%	0.006	0.00%	0.001	0.00%	0.007	0.00%	0.002
-8	0.00%	1.111	0.00%	0.006	0.00%	0.001	0.00%	0.007	0.00%	0.002
-7	0.00%	1.128	0.00%	0.006	0.00%	0.001	0.00%	0.007	0.00%	0.002
-6	0.00%	1.144	0.00%	0.006	0.00%	0.001	0.00%	0.007	0.00%	0.002
-5	0.00%	1.085	0.00%	0.005	0.00%	0.001	0.00%	0.007	0.00%	0.002
-4	0.00%	1.029	0.00%	0.006	0.00%	0.001	0.00%	0.007	0.00%	0.002
-3	0.00%	1.111	0.00%	0.006	0.00%	0.002	0.00%	0.008	0.00%	0.002
-2	0.00%	1.044	0.00%	0.005	0.00%	0.001	0.00%	0.007	0.00%	0.002

Appendix D

Ox Codes

This appendix presents the program written in the matrix programming language Ox that was used in the simulation corresponding to the detection of edges. This program provides the following results:

- Estimation of parameters of the \mathcal{G}_j^0 distribution for the method of moments.
- Detection of edges and times in seconds for the used methods.

```
#include <oxstd.h>
#include <oxprob.h>
#import <solvenle> decl
g_mm, g_m1, n=8, rep=1, erro=5;

sist_ec_gama12(const avF, const vX) {
    decl alfa, beta, c;
    alfa=vX[0];
    beta=vX[1];
    c=((g_mm^2)*(gammafact(n))*(gammafact(n+1)))/(g_m1*((gammafact(n+0.5))^2));
    avF[0] = ( ((gammafact( ((-1.0)*alfa)-0.5))^2)/(( gammafact((-1.0)*alfa))*
    (gammafact((( -1.0)*alfa)-1))))- c | g_mm-(beta/n)^(0.5)
    *(gammafact((-1)*alfa-0.5)*(gammafact(n+0.5))/ (gammafact((-1)*alfa)
```

```

    * (gammafact(n)))));
    return 1;
}

```

```

estimacion(const vg0) { decl v_solucao=<-1.0,0> ; decl mc=0, m1=0,
mmc=0, mm=0; g_mm=0; g_m1=0; mc = meanc(vg0); m1=meanr(mc) ;
mmc=meanc(vg0.^0.5); mm=meanr(mmc); g_mm = mm; g_m1 = m1;
SolveNLE(sist_ec_gama12, &v_solucao);

```

```

return (v_solucao); } prob(const z, const vX) {
    decl alfa, beta, ln;
    alfa=vX[0];
    beta=vX[1];
    ln= (n*log(n))+ log(gammafact(n-alfa)) + (n-1)*log(z)
        - alfa*log(beta)-log(gammafact(-alfa))
        -log(gammafact(n)) -(n-alfa)*log(beta+(n*z));
    return (ln);
}

```

```

postos(const z) {
    decl x, y,p,s, sum, i, contador, j, r, prom=0;
    y=vec(z)~vecrindex(z);
    p=sortbyc(y,0~1);
    s=sortcindex(sortcindex(p[] [0] '))+1;
    p=p~s;
    i=0;
    sum=0;
    contador=1;
    r=p;
    for(i=0;i<rows(p)-1;i++){ //1

```

```

    contador=1;
    while(p[i][0]==p[i+1][0]){ //2
        contador++;
        i++;
    } //2
    if(contador!=1)
    { //3
        sum=0;
        for(j=(i-contador)+1; j<i+1;j++){ //4
            sum+=p[j][2];
        } //4
        prom=sum/contador;
        for(j=i-contador+1;j<i+1;j++){ //5
            r[j][2]=prom;
        } //5
    } //3
    else{
        r[i][2]=p[i][2];
    }
} //1
r=sortbyc(r,1);
p=r[][2];
p=shape(p,rows(z),columns(z));
return p;
}

varia(const g0, paso) {
    decl COL, N1, N2, contador, est, j, p, q, v, w;
    contador=0;
    COL=columns(g0);
    N1=sizerc(g0);

```

```

est=zeros(COL-paso, 2);
decl N3, pu, pv, pos, pos2, sumu, sumu2, sumv ,
sumv2, medu2, suma4, T, NT;
for(j=paso; j<=(COL-paso); j=j+paso)
{
    p=g0[] [j-paso:j-1];
    q=g0[] [j:j+(paso-1)];
    N2=sizerc(p);
    N3=sizerc(q);
    NT=N2+N3;
    v=sumc(p);
    w=sumc(q);
    v=sumr(v);
    w=sumr(w);
    pu=fabs(p-(v/N2));
    pv=fabs(q-(w/N3));
    pos=postos(pu~pv);
    p=pos[] [:paso-1];
    q=pos[] [paso:];
    p=p.^2;
    q=q.^2;
    sumu=sumr(sumc(p));
    sumv=sumr(sumc(q));
    medu2=((sumu + sumv)/(N2+N3));
    p=p.^2;
    q=q.^2;
    sumu2=sumr(sumc(p));
    sumv2=sumr(sumc(q));
    T=(sumu -N2*medu2)/((( (N2*N3)/(NT*(NT-1)))*(sumu2+sumv2)
    - ((N2*N3)/(NT-1))*(medu2^2))^0.5);

```

```

        est[contador][0]=j;
        est[contador][1]=(fabs(T));
        contador=contador+1;
        v=w=pu=pv=0;
    }
    savemat("Q_1.txt", est);
    return est[(maxcindex(est[][]) [0][1])] [0];
}

/*****

MAIN PROGRAM

*****/
main() { decl g1, g2a, g2, g2b, g0,gp, alfs; decl v,w, j,i,t, p, q,
desv1=0, desv2=0; decl si=0, sf=0, stot=0; decl contador=0, COL, N1,
N2, Cuenta=0, Ran=0, valor=0, Rp=0, k=0, d=0, RANG=0; decl
mediafila, mediaTrangos; decl extimer1, extimer2, extimer3,
extimer4, extimer5, T ; decl ttimer1=0, ttimer2=0, ttimer3=0,
ttimer4=0, ttimer5=0; decl Ez, alpha1, alpha2, B1, B2, alfai; decl
tdados, limite, fil; decl e, porc1=0, porc2=0, porc3=0, porc4=0,
porc5=0; ranseed("LE"); ranseed({2,11,111,1111});

/*****
declaração de alphas e betas
para a geração dos dados
*****/
tdados=100; fil=20; limite=50;
Ez=1;    // E[Z]
    alpha1=3;  // ALPHA Backscatter 1
for(alpha2=20; alpha2>1; alpha2--)
{
    porc1=0, porc2=0, porc3=0, porc4=0, porc5=0;

```

```

println(" Antes ", " alfa1 =", alpha1, "   alfa =", alpha2);
if(alpha2==alpha1 && alpha2!=2)
{
    alpha2=alpha2-1;
}
println(" Depois ", " alfa1 =", alpha1, "   alfa2 =", alpha2);
B1= Ez* n*(gammafact(alpha1)*gammafact(n))
/(gammafact(alpha1-1)*gammafact(n+1));
B2= Ez* n*(gammafact(alpha2)*gammafact(n))
/(gammafact(alpha2-1)*gammafact(n+1));
g1=rangamma(fil, tdados, n, n);
contador=0;
for(e=1; e<=rep; e++)
{
    g2a=rangamma(fil, limite, alpha1, 1/B1);
    g2b=rangamma(fil, tdados-limite, alpha2, 1/B2);
    g2=g2a~g2b;
    gp=g1./g2;
    g0=(gp);
    savemat("go_2.txt",  g0);
    N1=rows(g0);
    COL=columns(g0);
    contador=0;
    decl est=zeros(COL-1,2), alfai=zeros(COL-1,2);
    /*****
    SÓ PARA IMPRIMIR AS ESTIMATIVAS DO BORDE
    *****/
    p=g0[][:limite-1];
    q=g0[][limite:];
    v=estimacion(p);

```



```

w=estimacion(q);
println("  ");
println(" Estimativa rep= ", e);
println("Estimativa de Alpha borda .D = ",v);
println("Estimativa de Alpha borda .I = ",w);
println(" ");
/*****
*****/
MÉTODO DE GAMBINI
*****/
extimer1=timer();      // tempo procedimento 1
est=zeros(COL-1,2);
for(j=1; j<=(COL-1); j=j+1)
{
    p=g0[:,j-1];
    q=g0[:,j];
    v=estimacion(p);
    w=estimacion(q);
    /*****
    Maxima verossimilhança de submatrizes
    *****/
    for(t=0; t<N1; t++)
    {
        for(i=0; i<columns(p); i++)
        {
            si+=prob(p[t][i], v);
        }
        for(i=0; i<columns(q); i++)
        {
            sf+=prob(q[t][i], w);

```

```

    }
}
est[contador][0]=j;
est[contador][1]=(si+sf);
contador=contador+1;
si=sf=0;
}
println(" ");
println("*****");
//println("maximo j= ", maxc(est));
println("VALOR FRONTERA GAMBIBI j= ", est[maxcindex(est)[0][1]][0]);
println(" TEMPO EXECUCAO: ", timespan(extimer1));
println("*****");
if(fabs(est[maxcindex(est)[0][1]][0]-limite)>erro)
{
    porc1+=1;
}
/*****
        Estatistica de teste de igualdade de variança
*****/
decl Q=0, passo;
extimer4=timer(); // tempo precedimento 3
passo=5;
Q=varia(g0, passo);
println(" ");
println("*****");
//println("maximo j= ", maxc(est));
println("VALOR FRONTERA VARIANÇA j= ", Q);
println(" TEMPO EXECUCAO: ", timespan(extimer4));
println("*****");

```

```

if(fabs(Q-limite)>erro)
{
    porc4+=1;
}

/*****/

//                                SEGUNDA PARTE

/*****/

extimer2=timer();    // tempo procedimento 2

/*****

    Procedimento para o calculo de postos o rangos

*****/

/*****/

    GO MATRIZ DE RANGOS OU POSTOS

*****/

N1=rows(gp);                //numero de filas da matrix g0
g0=postos(g0);              //g0   agora contem os postos dos dados
mediafila=meanc(g0);
mediaTrangos=meanr(mediafila); //media dos postos
COL=columns(g0);            //numero de colunas da matrix g0
contador=0;
est=zeros(COL-1, 2);
for(j=1; j<=(COL-1); j++)
{
    p=g0[][:j-1];
    q=g0[][j:];
    v=meanc(p);
    w=meanc(q);
    v=meanr(v);
    w=meanr(w);
    est[contador][0]=j;
}

```

```

        est[contador][1]=(fabs((fabs(w-v))-mediaTrangos));
        contador=contador+1;
    }
    savemat("edwin_1.txt", est);
    println(" ");
    println("***** ");
    println("VALOR FRONTERA EDWIN j= ", est[(mincindex(est[1:][0])[1])+1][0]);
    println(" TEMPO EXECUCAO: ", timespan(extimer2));
    println("***** ");
    if(fabs(est[(mincindex(est[1:][0])[1])+1][0]-limite)>erro)
    {
        porc2+=1;
    }
    /*****
        Estatistica de kruskal wallis
    *****/
    extimer3=timer(); // tempo precedimento 3
    COL=columns(g0);
    N1=sizerc(g0);
    contador=0;
    est=zeros(COL-1, 2);
    decl cta=12/(N1*(N1+1.0));
    for(j=1; j<=(COL-1); j++)
    {
        p=g0[:,j-1];
        q=g0[:,j];
        N2=sizerc(p);
        v=sumc(p);
        w=sumc(q);
        v=sumr(v);
    }

```

```

        w=sumr(w);
        est[contador][0]=j;
        est[contador][1]=(cta*(((v^2)/N2)+ ((w^2)/(N1-N2))))-(3*(N1+1.0));
        contador=contador+1;
    }
    println(" ");
    println("*****");
    //println("MAXIMO j= ", maxc(est[1][ ]));
    println("VALOR FRONTERA KRUSKAL WALLIS j= ",
        est[(maxcindex(est[ ][ ][0][1]))[0]]);
    println(" TEMPO EXECUCAO: ", timespan(extimer3));
    println("*****");
    if(fabs(est[(maxcindex(est[ ][ ][0][1]))[0]]-limite)>erro)
    {
        porc3+=1;
    }
    /*****
        Estatistica de Mann-whitney
    *****/
    extimer5=timer(); // tempo precedente 3
    COL=columns(g0);
    N1=sizerc(g0);
    contador=0;
    est=zeros(COL-1, 2);
    decl g02, R2=0;
    g02=g0.^2;
    for(j=1; j<=(COL-1); j++)
    {
        p=g0[ ][j-1];
        q=g0[ ][j];
    }

```

```

    N2=sizerc(p);
    //println(" p= ", p);
    v=sumc(p);
    w=sumc(q);
    v=sumr(v);
    w=sumr(w);
    R2=sumr(sumc(g02));
    est[contador][0]=j;
    est[contador][1]=fabs((v-(N2*(N1+1)/2))/ (( (N2*(N1-N2)/(N1*(N1-1)))*R2 -
    (N2*(N1-N2)*((N1+1)^2)/(4*(N1-1))))^0.5));
    contador=contador+1;
}
println(" ");
println("*****");
println("VALOR FRONTERA Mann-Whitney j= ",
est[(maxcindex(est[][0])[1])][0]);
println(" TEMPO EXECUCAO: ", timespan(extimer5));
println("*****");
if(fabs(est[(maxcindex(est[][0])[1])][0]-limite)>erro)
{
    porc5+=1;
}
}
println("*****");
println(" ", "alfa1= ", -alpha1, " ", " Alfa2= ", -alpha2);
println("*****");
println("*****");
println(" % ERRO GAMBINI", " ", " % ERRO EDWIN ", " ", " % ERRO KRUSKAL"
, " % ERRO VARIAN", " % ERRO MANN-WHITNEY");
println(" ", (porc1/rep)*100.0,"%", " ",

```

```
(porc2/rep)*100.0,"%", "          ", (porc3/rep)*100.0,"%"  
 , "          ", (porc4/rep)*100.0,"%" , "          "  
 (porc5/rep)*100.0,"%");  
println("***** ");  
}  
}
```

Bibliography

- Allende, H., Frery, A. C., Galbiati, J. & Pizarro, L. (2006), 'M-estimators with asymmetric influence functions: the \mathcal{G}_A^0 distribution case', *Journal of Statistical Computation and Simulation* **76**(11), 941–956.
- Beauchemin, M., Thomson, K. P. B. & Edwards, G. (1998), 'On nonparametric edge detection in multilook SAR images', *IEEE Transactions on Geoscience and Remote Sensing* **36**(5), 1826–1829.
- Bovik, A. C., Huang, T. S. & Munson, D. C. (1986), 'Nonparametric-tests for edge-detection in noise', *Pattern Recognition* **19**(3), 209–219.
- Brigger, P., Hoeg, J. & Unser, M. (2000), 'B-spline snakes: A flexible tool for parametric contour detection', *IEEE Transactions on Image Processing* **9**(9), 1484–1496.
- Bustos, O. H., Lucini, M. M. & Frery, A. C. (2002), 'M-estimators of roughness and scale for \mathcal{G}_A^0 modelled SAR imagery', *Eurasip Journal on Applied Signal Processing* **2002**(1), 105–114.
- Casella, G. & Lehman, E. L. (1998), *Theory of Point Estimation*, Springer Verlag, New York.
- Conover, W. J. (1980), *Practical Nonparametric Statistics*, John Wiley, New York.
- Cribari-Neto, F., Frery, A. C. & Silva, M. F. (2002), 'Improved estimation of clutter properties in speckled imagery', *Computational Statistics & Data Analysis* **40**(4), 801–824.
- Doornik, J. A. (2002), *Object-Oriented Matrix Programming Using Ox*, 3 edn, Timberlake Consultants Press & Oxford, London.
URL: <http://www.doornik.com>

- Fesharaki, M. N. & Hellestrand, G. R. (1994), A new edge detection algorithm based on a statistical approach, in 'International Symposium on Speech, Image Processing and Neural Networks (ISSIPNN)', Vol. 1, pp. 21–24.
- Freitas, C. C., Frery, A. C. & Correia, A. H. (2005), 'The polarimetric G distribution for SAR data analysis', *Environmetrics* **16**(1), 13–31.
- Frery, A. C., Correia, A. H. & Freitas, C. C. (2007), 'Classifying multifrequency fully polarimetric imagery with multiple sources of statistical evidence and contextual information', *IEEE Transactions on Geoscience and Remote Sensing* **45**(10), 3098–3109.
- Frery, A. C., Müller, H. J., Freitas, C. C. & Siqueira, S. J. (1997), 'A model for extremely heterogeneous clutter', *IEEE Transactions on Geoscience and Remote Sensing* **35**(3), 648–659.
- Gambini, J., Mejail, M. E., Jacobo-Berlles, J. & Frery, A. C. (2006), 'Feature extraction in speckled imagery using dynamic B-spline deformable contours under the \mathcal{G}^0 model', *International Journal of Remote Sensing* **27**(22), 5037–5059.
- Gambini, J., Mejail, M., Jacobo-Berlles, J. & Frery, A. C. (2008), 'Accuracy of edge detection methods with local information in speckled imagery', *Statistics and Computing* **18**(1), 15–26.
- Goodman, J. (1985), *Statistical Optics*, Wiley, New York.
- Gradshteyn, I. & Ryzhik, I. (1998), *Tables of Integrals, Series and Products.*, Academic Press.
- Hampel, F. R., Ronchetti, E. M., Rousseeuw, P. J. & Stahel, W. A. (1986), *Robust Statistics: The Approach Based on Influence Functions*, Wiley, New York.
- Hoon Lim, D. & Ju Jang, S. (2002), 'Comparison of two-sample tests for edge detection in noisy images', *Journal of the Royal Statistical Society: Series D (The Statistician)* **51**(1), 21–30.
- Jakeman, E. & Pusey, P. N. (1976), 'Model for non-Rayleigh sea echo', *IEEE Transactions on Antennas and Propagation* **24**(6), 806–814.
- Jao, K. (1984), 'Amplitud distribution of composite terrain radar clutter and the K distribution.', *IEEE Transactions on Antennas and Propagation* **32**, 1049 – 1061.

- Kruskal, W. H. & Wallis, W. A. (1952), 'Use of ranks in one-criterion variance analysis', *Journal of the American Statistical Association* **47**(260), 583–621.
- Lim, D. H. (2006), 'Robust edge detection in noisy images', *Computational Statistics & Data Analysis* **50**(3), 803–812.
- Manski, C. F. (1988), *Analog Estimation Methods in Econometrics*, number 39 in 'Monographs on Statistics and Applied Probability', Chapman & Hall.
URL: <http://elsa.berkeley.edu/books/analog.html>
- Mejail, M. E., Frery, A. C., Jacobo-Berlles, J. & Bustos, O. (2001), 'Approximation of distributions for SAR images: Proposal, evaluation and practical consequences', *Latin American Applied Research* **31**(2), 83–92.
- Mejail, M. E., Jacobo-Berlles, J. C., Frery, A. C. & Bustos, O. H. (2003), 'Classification of SAR images using a general and tractable multiplicative model', *International Journal of Remote Sensing* **24**(18), 3565–3582.
- Oliver, C. & Quegan, S. (1998), *Understanding Synthetic Aperture Radar Images*, Artech House, Boston.
- Picco, M., Moschetti, E., Palacio, M. G. & Frery, A. C. (2007), Evaluación de filtros map para nuevos modelos de imágenes SAR, in 'Anais XIII Simpósio Brasileiro de Sensoriamento Remoto', pp. 6043–6050.
- Pizarro, L. H. (2003), Estimación robusta de parámetros en distribuciones con datos SAR, Master's thesis, Universidad Técnica Federico Santa María. Valparaíso, Chile.
- Tur, M., Chin, K. C. & Goodman, J. W. (1982), 'When is speckle noise multiplicative', *Applied Optics* **21**(7), 1157–1159.
- Vasconcellos, K. L. P., Frery, A. C. & Silva, L. B. (2005), 'Improving estimation in speckled imagery', *Computational Statistics* **20**(3), 503–519.
- Venables, W. N. & Ripley, B. D. (2002), *Modern Applied Statistics with S*, Statistics and Computing, 4 edn, Springer, New York.
- Yanasse, C. C., Frery, A. C. & Santanna, S. (1995), Stochastic distributions and the multiplicative model: relations, properties, estimators and applications to SAR image analysis, Relatório Técnico 5630-NTC/318, INPE, São José dos Campos, SP, Brazil.

Livros Grátis

(<http://www.livrosgratis.com.br>)

Milhares de Livros para Download:

[Baixar livros de Administração](#)

[Baixar livros de Agronomia](#)

[Baixar livros de Arquitetura](#)

[Baixar livros de Artes](#)

[Baixar livros de Astronomia](#)

[Baixar livros de Biologia Geral](#)

[Baixar livros de Ciência da Computação](#)

[Baixar livros de Ciência da Informação](#)

[Baixar livros de Ciência Política](#)

[Baixar livros de Ciências da Saúde](#)

[Baixar livros de Comunicação](#)

[Baixar livros do Conselho Nacional de Educação - CNE](#)

[Baixar livros de Defesa civil](#)

[Baixar livros de Direito](#)

[Baixar livros de Direitos humanos](#)

[Baixar livros de Economia](#)

[Baixar livros de Economia Doméstica](#)

[Baixar livros de Educação](#)

[Baixar livros de Educação - Trânsito](#)

[Baixar livros de Educação Física](#)

[Baixar livros de Engenharia Aeroespacial](#)

[Baixar livros de Farmácia](#)

[Baixar livros de Filosofia](#)

[Baixar livros de Física](#)

[Baixar livros de Geociências](#)

[Baixar livros de Geografia](#)

[Baixar livros de História](#)

[Baixar livros de Línguas](#)

[Baixar livros de Literatura](#)
[Baixar livros de Literatura de Cordel](#)
[Baixar livros de Literatura Infantil](#)
[Baixar livros de Matemática](#)
[Baixar livros de Medicina](#)
[Baixar livros de Medicina Veterinária](#)
[Baixar livros de Meio Ambiente](#)
[Baixar livros de Meteorologia](#)
[Baixar Monografias e TCC](#)
[Baixar livros Multidisciplinar](#)
[Baixar livros de Música](#)
[Baixar livros de Psicologia](#)
[Baixar livros de Química](#)
[Baixar livros de Saúde Coletiva](#)
[Baixar livros de Serviço Social](#)
[Baixar livros de Sociologia](#)
[Baixar livros de Teologia](#)
[Baixar livros de Trabalho](#)
[Baixar livros de Turismo](#)